



**TURUN
YLIOPISTO**
UNIVERSITY
OF TURKU

DIFFUSION-WEIGHTED AND FUNCTIONAL MAGNETIC RESONANCE IMAGING OF THE BRAIN IN PRETERM AND TERM-BORN ADOLESCENTS

Katri Lahti



**TURUN
YLIOPISTO**
UNIVERSITY
OF TURKU

DIFFUSION-WEIGHTED AND FUNCTIONAL MAGNETIC RESONANCE IMAGING OF THE BRAIN IN PRETERM AND TERM-BORN ADOLESCENTS

Katri Lahti

University of Turku

Faculty of Medicine
Department of Clinical Medicine
Paediatric Neurology
Doctoral program in Clinical Research

Supervised by

Professor Leena Haataja
Department of Paediatric Neurology
University of Helsinki
Helsinki, Finland

Professor Riitta Parkkola
Department of Radiology
University of Turku
Turku, Finland

Reviewed by

Docent Outi Tammela
Department of Paediatrics
Tampere University
Tampere, Finland

Docent Marko Kangasniemi
Department of Radiology
University of Helsinki
Helsinki, Finland

Opponent

Docent Mervi Könönen
Diagnostic Imaging Center
Kuopio University Hospital
Department of Applied Physics
University of Eastern Finland
Kuopio, Finland

The originality of this publication has been checked in accordance with the University of Turku quality assurance system using the Turnitin OriginalityCheck service.

ISBN 978-951-29-8719-1 (PRINT)
ISBN 978-951-29-8720-7 (PDF)
ISSN 0355-9483 (Print)
ISSN 2343-3213 (Online)
Painosalama, Finland 2021

To those little girls who dream of becoming researchers

UNIVERSITY OF TURKU

Faculty of Medicine

Department of Clinical Medicine

Paediatric Neurology

KATRI LAHTI: Diffusion-weighted and functional magnetic resonance

imaging of the brain in preterm and term-born adolescents

Doctoral Dissertation, 124 pp.

Doctoral program in Clinical Research

November 2021

ABSTRACT

Magnetic resonance imaging (MRI) is widely used in clinical and research settings in the adolescent population. Technical development has allowed the use of fine-grained methods to assess both the structural and functional properties of the brain. However, the specific technical limitations and improvements are mostly studied in phantom or adult studies, which may have an impact on their reliability as research tools when studying the younger population. Very preterm (VPT) birth is associated with several neurodevelopmental impairments. The present MRI tools provide opportunities to study brain maturation in detail.

This thesis is a part of the multidisciplinary longitudinal follow-up study on the development and functioning of very low birth weight infants from infancy to school age (PIPARI). The follow-up cohort consists of infants born VPT (birth weight ≤ 1500 g and/or gestational age < 32 weeks) in Turku University Hospital in 2001–2006 and term-born controls born in 2001–2004 in the same hospital. This thesis includes only children born VPT in 2004–2006 and controls born between 2003–2004 due to an upgrade of the MRI scanner during the recruitment. In Study I, the diffusion-weighted imaging (DWI) metrics at term-equivalent age were compared to the motor outcome at 11 years of age in children born VPT. Study II assessed the effect of the susceptibility correction to the DWI metrics in a healthy adolescent population. In Study III, temporal fluctuation of the resting state brain functioning was compared between 13-year-old adolescents born VPT and at term.

The main prematurity-related findings of this thesis were that the DWI metrics of the corpus callosum, left corona radiata and right optic radiation at term are associated with later motor outcome in children born VPT and that adolescents born VPT show a decrease in active time, fluidity and range in brain activation during rest. These findings may reflect the adjustments in brain microstructure and function caused by the VPT birth. Fine-grained MRI methods are reliable tools for studying the mechanisms behind the clinical phenotypes of adolescents when technical limitations and age-appropriate analysis adjustments are considered.

KEYWORDS: Very preterm birth, motor outcome, diffusion weighted imaging, tractography, susceptibility, adolescence, resting state functional magnetic resonance imaging.

TURUN YLIOPISTO

Lääketieteellinen tiedekunta

Kliininen laitos

Lastenneurologian oppiaine

KATRI LAHTI: Diffuusiopainotteisen ja toiminnallisen aivojen

magneettikuvantamisen käyttö nuoruusiässä entisillä pikkukeskosilla ja täysiaikaisilla verrokeilla

Väitöskirja, 124 s.

Kliininen tohtorihjelma

marraskuu 2021

TIIVISTELMÄ

Magneettikuvaus (MRI) on laajassa kliinisessä ja tieteellisessä käytössä lapsia ja nuoria tutkittaessa. Tekninen kehitys mahdollistaa yhä hienojakoisempia aivojen tutkimuksia. MRI:n teknisiä korjauksia on tutkittu pääosin mallintamalla tai aikuisilla, mikä voi heikentää luotettavuutta alaikäisillä. Hyvin ennenaikaisesti syntyvillä lapsilla neurologisen kehityksen poikkeavuuksien riski on täysiaikaisena syntyviä suurempi. Poikkeavuudet voivat liittyä aivojen kehityksen muutoksiin, joita nykyisillä tekniikoilla voidaan tutkia aiempaa yksityiskohtaisemmin.

Väitöskirja on osa PIPARI-tutkimusta (Pienipainoisten riskilasten käyttäytyminen ja toimintakyky imeväisiästä kouluikään). Seurantakohortti koostuu pikkukeskosina (syntymäpaino ≤ 1500 g ja/tai raskauden kesto < 32 viikkoa) Tyksissä vuosina 2001–2006 syntyneistä lapsista sekä täysiaikaisena 2001–2004 syntyneistä verrokeista. MRI-laitteiston päivityksestä johtuen osatyöt käsittelevät pikkukeskosina vuosina 2004–2006 ja verrokkeina vuosina 2003–2004 syntyneitä. Ensimmäisessä osatyössä verrattiin aivojen diffuusiokuvantamistuloksia entisten pikkukeskosten motoriseen toimintakykyyn 11-vuotiaana. Toinen osatyö käsitteli susceptibiliteettikorjauksen vaikutusta aivojen diffuusiokuvantamisen mittaustuloksiin. Kolmannessa osatyössä vertailtiin 13-vuotiaiden entisten pikkukeskosten ja verrokkien aivojen aktiivisuuden vaihtelua lepotilassa toiminnallisen MRI-kuvauksen aikana.

Tämän väitöskirjan keskosuuteen liittyvät päätulokset olivat lasketun syntymäajan corpus callosumin, vasemman corona radiatan ja oikean optisen radaston diffuusiomittaustulosten yhteys motoriseen kehitykseen 11-vuotiaana sekä pikkukeskosina syntyneillä havaittu aivojen vähäisempi aktiivinen aika ja alentunut aktiivisuuden vaihtelun joustavuus 13-vuotiaana. Nämä löydökset saattavat olla seurausta varhaiseen syntymään liittyvistä aivojen mikrorakenteen ja toiminnan muutoksista. Hienojakoiset MRI-menetelmät vaikuttavat olevan luotettavia nuorisoikäisiä tutkittaessa, kunhan tekniset rajoitteet ja ikäsovitukset huomioidaan.

AVAINSANAT: Pikkukeskonen, motorinen kehitys, diffuusiokuvantaminen, traktografia, susceptibiliteetti, nuoruusikä, toiminnallinen magneettikuvas.

Table of Contents

| | |
|--|-----------|
| Tables | 8 |
| Figures | 10 |
| List of Original Publications | 14 |
| 1 Introduction | 15 |
| 2 Review of the Literature | 16 |
| 2.1 Preterm birth | 16 |
| 2.1.1 Vulnerability of the preterm brain | 16 |
| 2.1.2 Outcome in adolescence | 19 |
| 2.1.2.1 Motor outcome | 19 |
| 2.1.2.2 Preterm behavioral phenotype | 21 |
| 2.2 Brain magnetic resonance imaging (MRI) | 25 |
| 2.2.1 Comprehensive MRI | 25 |
| 2.2.1.1 Physical background | 25 |
| 2.2.1.2 The conventional imaging sequences | 25 |
| 2.2.1.3 Comprehensive MRI in clinical use in the VPT/VLBW population | 26 |
| 2.2.2 Diffusion-weighted imaging | 27 |
| 2.2.2.1 Physical background | 27 |
| 2.2.2.2 Methods | 28 |
| 2.2.3 Resting state functional MRI (rsfMRI) | 29 |
| 2.2.4 MRI artifacts in brain MRI | 31 |
| 2.3 MRI findings in the population of preterm infants | 32 |
| 2.3.1 Prematurity-related MRI findings in adolescence | 32 |
| 2.3.2 DWI and DCD in the VPT/EPT population at school age | 34 |
| 2.3.3 Findings using quantitative MRI approaches in the preterm behavioral phenotype at school age | 36 |
| 3 Aims | 38 |
| 4 Materials and Methods | 39 |
| 4.1 Participants | 39 |
| 4.1.1 Children born preterm (study I and III) | 39 |
| 4.1.2 Controls born at term (study II and III) | 40 |
| 4.2 Assessment of motor outcome at 11 years of age | 40 |

| | | |
|----------|--|-----------|
| 4.3 | MRI imaging at term and at 13 years of age | 41 |
| 4.3.1 | Comprehensive MRI..... | 41 |
| 4.3.2 | Diffusion-weighted imaging | 43 |
| 4.3.2.1 | Analysis at TEA | 44 |
| 4.3.2.2 | Analysis at 13 years of age | 45 |
| 4.3.3 | Resting state functional MRI at 13 years of age..... | 46 |
| 4.3.4 | Statistical methods | 51 |
| 4.3.4.1 | Study I | 51 |
| 4.3.4.2 | Study II | 51 |
| 4.3.4.3 | Study III | 51 |
| 5 | Results | 53 |
| 5.1 | Participants | 53 |
| 5.1.1 | Participants born very preterm (studies I and III) | 53 |
| 5.1.2 | Participants born at term (study II and III)..... | 54 |
| 5.2 | DTI at term and motor outcome at 11 years of age..... | 55 |
| 5.3 | Impact of susceptibility correction on DTI and tractography parameters at 13 years of age..... | 56 |
| 5.4 | Resting state fMRI in preterm children at 13 years of age | 58 |
| 6 | Discussion | 62 |
| 6.1.1 | The vulnerability of the preterm brain | 62 |
| 6.1.2 | Predicting outcome from term to adolescence based on DWI modalities | 62 |
| 6.1.2.1 | Motor outcome in children without CP..... | 63 |
| 6.1.2.2 | Preterm behavioral phenotype | 64 |
| 6.1.2.3 | Clinical utility of DWI modalities | 65 |
| 6.1.3 | The preterm brain in adolescence | 66 |
| 6.1.3.1 | Preterm behavioral phenotype | 67 |
| 6.1.3.2 | Brain maturation and the connectivity differences in the VPT/VLBW population | 68 |
| 6.2 | Clinical usability of the adolescent brain DWI | 69 |
| 6.3 | Strengths and limitations | 71 |
| 7 | Conclusions..... | 73 |
| | Acknowledgements | 74 |
| | References | 76 |
| | Original Publications | 91 |

Tables

| | | |
|-----------|---|----|
| Table 1. | The imaging parameters of the basic anatomical sequences at term-equivalent age | 43 |
| Table 2. | The imaging parameters of the basic anatomical sequences at 13 years of age. | 43 |
| Table 3. | The imaging parameters of the diffusion sequences. | 44 |
| Table 4. | The imaging parameters for rsfMRI | 46 |
| Table 5. | The background characteristics of the participants born very preterm. | 53 |
| Table 6. | The median MABC-2 scores and their range in both standard scores and percentiles. | 55 |
| Table 7. | Mean FAs (SD) at term-equivalent age for infants born preterm and univariate and the multivariate estimates and p-values for associations with MABC-2 scores at 11 years of age. The estimates are shown as change in MABC-2 standard scores when FA increases with 0.1. | 56 |
| Table 8. | Mean MDs (SD) at term (TEA) for infants born preterm and the univariate and multivariate estimates and p-values for associations with MABC-2 scores at 11 years of age. The estimates are shown as change in MABC-2 standard scores when MD increases with 0.1. | 56 |
| Table 9. | Mean diffusivity in uncorrected and corrected data, bias between the pathways, the p values of the biases, the estimates and their p values for the regression analyses. | 57 |
| Table 10. | Fractional anisotropy in uncorrected and corrected data, bias between the pathways, the p values of the biases, estimates and their p values for the regression analyses. | 57 |
| Table 11. | Bias (corrected – uncorrected) in the area under curve, the p values of the biases, estimates and their p values for the regression analyses. | 58 |
| Table 12. | State-wise mean dwell times (standard error of mean) in the whole sample of adolescents born very preterm and the term-born controls and the groups without adolescents with ADHD or cognitive impairment (VPT-E, CONTROLS-E). | 60 |
| Table 13. | State-wise mean fraction rates (standard error of mean) in the whole sample of adolescents born very preterm and term-born controls and the groups without adolescents with ADHD or cognitive impairment (VPT-E, CONTROLS-E). | 60 |

| | | |
|-----------|---|----|
| Table 14. | FDR corrected p-values for the state-wise comparisons in dwell time and fraction rate between the full sample of adolescents born VPT and at term and the sample with adolescents with ADHD or cognitive impairment excluded (VPT-E, CONTROLS-E)..... | 60 |
| Table 15. | Meta-state metrics, mean (standard error of mean) in the whole sample of adolescents born very preterm and term-born controls and the groups without adolescents with ADHD or cognitive impairment (VPT-E, CONTROLS-E)..... | 61 |
| Table 16. | The FDR corrected p-values for meta-state metrics between the full sample of adolescents born VPT and at term and the sample with adolescents with ADHD or cognitive impairment excluded (VPT-E, CONTROLS-E). | 61 |

Figures

| | | |
|------------|---|----|
| Figure 1. | The brain sulcus formation of an infant born preterm. A. 26 weeks, B. 29 weeks, and C. 36 weeks of gestation..... | 17 |
| Figure 2. | Schematic drawings with adjacent MR images of different white matter injury (WMI) types. A is representing focal cystic periventricular leukomalacia (PVL) with diffuse WMI, B focal non-cystic PVL with small scar lesions with diffuse WMI and C diffuse WMI alone | 18 |
| Figure 3. | A schematic view of the diffusion metrics in anterior corpus callosum (a, red) and left lateral ventricle (a, green). Diffusion in anterior corpus callosum is highly restricted (b) i.e., anisotropic and has got a high fractional anisotropy. Diffusion in the left lateral ventricle is unrestricted i.e., isotropic and has got a high mean diffusivity. | 28 |
| Figure 4. | First two pictures from left show the frontal effects of susceptibility artifact and correction of it. Second pictures show the same effects in temporal lobes uncorrected - corrected..... | 32 |
| Figure 5. | The three domains and scoring of MABC-2..... | 41 |
| Figure 6. | The classification of pathological brain findings in comprehensive brain MRI..... | 42 |
| Figure 7. | The regions-of-interest used at term equivalent age, marked with yellow: the colliculus inferior in the first, the anterior corpus callosum, posterior part of the capsula interna and optic radiations in the second, the posterior corpus callosum in the third and the corona radiata in the fourth picture | 44 |
| Figure 8. | The corpus callosum in sagittal, coronal, and transversal plain shown in yellow-red scale, where the central parts of corpus callosum are seen in yellow. | 46 |
| Figure 9. | An example of the spatial activation of the resting state network and their related time courses separated using independent component analysis. The last row shows the noise excluded from the analysis | 48 |
| Figure 10. | In static connectivity analysis, the measured activation is averaged over the scanning time. Dynamic connectivity is analyzed using two different methods after k-means clustering. The native-state analysis compares the clustered states and times spent in each state. The meta-state analysis assesses the transitions between the different connectivity states | 50 |
| Figure 11. | The flow chart of the participants of Study I and III..... | 54 |

| | | |
|------------|--|----|
| Figure 12. | The Bland–Altman plots and linear regression models with a significant positive association between the bias and the mean diffusivity value..... | 58 |
| Figure 13. | The native state functional network connectivity patterns in adolescents born very preterm and at term | 59 |
| Figure 14. | The meta-state metrics in adolescents born very preterm and at term. The statistically significant differences are marked with starts | 61 |

Abbreviations

| | |
|--------|--|
| AD | Axial diffusivity |
| ALIC | Anterior limb of the internal capsule |
| ADHD | Attention deficit hyperactivity disorder |
| ASD | Autism spectrum disorder |
| BW | Birth weight |
| CBCL | Child behavioral checklist |
| CC | Corpus callosum |
| CP | Cerebral palsy |
| CR | Corona radiata |
| CSD | Spherical deconvolution |
| CSF | Cerebrospinal fluid |
| CSO | Centrum semiovale |
| CST | Corticospinal tracts |
| DCD | Developmental coordination disorder |
| DFNC | Dynamic FNC |
| DWI | Diffusion weighted imaging |
| EC | External capsule |
| ELBW | Extremely low birth weight |
| EPT | Extremely preterm |
| FA | Fractional anisotropy |
| FDR | False discovery rate |
| FNC | Functional network connectivity |
| FSL | FMRIB (Functional MRI of Brain) Software Library |
| GA | Gestational ages |
| GM | Grey matter |
| HARDI | High angular diffusion imaging |
| ICA | Independent component analysis |
| ILF | Inferior longitudinal fasciculus |
| IQ | Intelligence quotient |
| IVH | Intraventricular hemorrhage |
| MABC-2 | Movement Assessment Battery for Children 2 nd edition |

| | |
|--------|--|
| MD | Mean diffusivity |
| MRI | Magnetic resonance imaging |
| MSFNC | Meta state FNC |
| NODDI | Neurite orientation dispersion and density imaging |
| NSFNC | Native space FNC |
| OR | Optic radiations |
| PLIC | Posterior limb of internal capsule |
| PVL | Periventricular leukomalacia |
| RD | Radial diffusivity |
| RSN | Resting state network |
| ROI | Region-of-interest |
| RSFNC | Resting state FNC |
| SDQ | Strengths and Difficulties Questionnaire |
| SE-EPI | Single shot echo planar imaging |
| SGA | Small for gestational age |
| SLF | Superior longitudinal fasciculus |
| TBSS | Tract-based spatial statistics |
| VBM | Voxel-based morphometry |
| VLBW | Very low birth weight |
| VPT | Very preterm |
| WFNC | Windowed FNC |
| WM | Whiter matter |
| WMI | White matter injury |
| WHO | World Health Organization |

List of Original Publications

This dissertation is based on the following original publications, which are referred to in the text by their Roman numerals:

- I Lahti K, Saunavaara V, Munck P, Uusitalo K, Parkkola R, Leena Haataja L on behalf of the PIPARI study group. Diffusion tensor imaging is associated with motor outcomes of very preterm born children at 11 years of age. *Acta Paediatrica*, 2020; 109(4): 738-745.
- II Lahti K, Parkkola R, Jääsaari P, Haataja L, Saunavaara V on behalf of the PIPARI study group. The impact of susceptibility correction on diffusion metrics in adolescents. *Pediatric radiology*, 2021; 51(8): 1471-1480.
- III Lahti K, Setänen S, Vorobyev V, Nyman A, Haataja L, Parkkola R on behalf of the PIPARI study group. Altered temporal connectivity and reduced meta-state dynamism in adolescents born very preterm. *Brain Communications*, in press.

The original publications have been reproduced with the permission of the copyright holders.

1 Introduction

A preterm birth is defined as a live birth taking place between the beginning of the 22nd week of gestation to the end of the 36th week. Nearly 5% of the infants born in Finland are born prematurely (National Institute for Health and Welfare, 2020). Despite of the improved outcomes, infants born preterm still are at a higher risk for neurodevelopmental impairments than their term-born peers (Cheong et al., 2021; Johnson et al., 2019; Tommiska et al., 2020). These neurodevelopmental impairments are associated with adversities seen in comprehensive brain magnetic resonance imaging (MRI), but especially minor impairments such as executive function deficits, minor motor impairments and neuropsychiatric disorders are often seen without brain lesions in comprehensive MRI (Setänen et al., 2016).

Brain MRI has taken enormous technical strides since its introduction. With higher field strengths and various signal detection techniques, it is possible to visualize and quantify microstructural and functional properties of the brain (Atlas, 2016; Weishaupt et al., 2006). These methods might shed light on the pathological processes behind the minor neurodevelopmental impairments seen in children and adolescents born preterm (Back, 2015; Fleiss et al., 2020; Volpe, 2019). However, many of the artifact corrections and analysis templates are created and tested in adult population or with phantoms, which may decrease their reliability in the adolescent population (Irfanoglu et al., 2019).

A preterm birth often comes as a surprise to the parents, accompanied with uncertainty and worries. To predict future outcomes, both structured follow-up during the first years of life and knowledge about the mechanisms behind different developmental adversities are needed. Encompassing longitudinal follow-up studies provide information about the prognosis, risk factors and mechanisms of these adversities, which continue to affect the life of the preterm-born even in adolescence.

2 Review of the Literature

2.1 Preterm birth

According to the World Health Organization (WHO), preterm birth is defined as a live birth between gestational ages (GA) $\geq 22+0$ and $36+6$. Preterm births can be further divided into moderate to late preterm (from GA $32+0$ to $36+6$), very preterm (VPT, from GA $28+0$ to $31+6$), and extremely preterm (EPT, GA $<28+0$) births. A birth weight (BW) of <1500 g is defined as a very low birth weight (VLBW), and a birth weight <1000 g is defined as an extremely low birth weight (ELBW). In Finland, a BW small for gestational age (SGA) is characterized as a BW below $-2SD$ of the weight appropriate for the gestational age.

In 2014, the worldwide estimate for preterm birth was 10.6% of all live births, ranging from 8.7% to 13.4% in Europe and North Africa, respectively (Chawanpaiboon et al., 2019). However, the variability between specific countries is significantly higher, for example 19.9% in Bangladesh, 9.6% in the US and 3.6% in Germany (Barfield, 2018; Chawanpaiboon et al., 2019; Vogel et al., 2018). Of all preterm births worldwide, the VPT births account for 11.3% and EPT births for 4.1% (Chawanpaiboon et al., 2019). In 2019, the rate for preterm birth in Finland was 4.9% of all live births, and VPT/VLBW infants accounted for 0.8% ($n=376$) of all live births (National Institute for Health and Welfare, 2020).

The rate of premature births has been increasing worldwide during the past 10–20 years, but the mortality of very preterm infants has decreased (Creel et al., 2017). An international register study that included the Finnish National Birth Register showed an overall survival rate of 87% for infants born in 2007–2013 with BW <1500 g. (Helenius et al., 2018)

2.1.1 Vulnerability of the preterm brain

A VPT birth occurs during an extremely rapid phase of developmental neurobiological processes, in gestational weeks 23 to 32. Neurogenesis begins with the formation and condensation of the cortical plate at GA of 8 to 12 weeks and continues up to 29 weeks of GA. After migrating to their final position, the neurons begin to form synapses. The first synapses are detectable from 19 to 23 weeks of

GA. In addition to synaptic modulation and pruning, cortical myelination continues through childhood up to adolescence. While microstructural brain development takes place during the period when VPT births occur, the secondary sulci formation only starts around 32 and tertiary around 36 weeks of GA. (Fleiss et al., 2020; Sidman et al., 1973) This can also be visualized using modern imaging techniques (Figure 1).

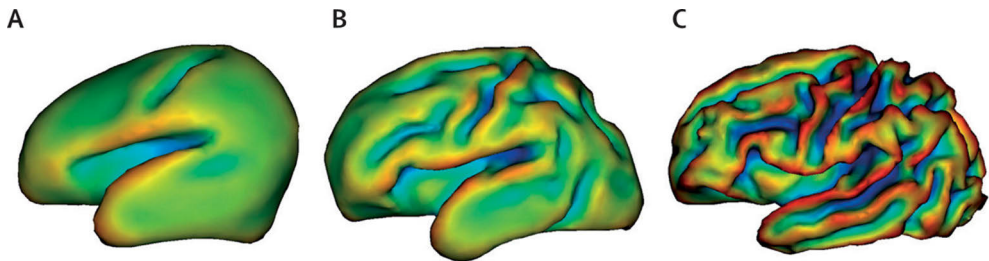


Figure 1. The brain sulcus formation of an infant born preterm. A. 26 weeks, B. 29 weeks, and C. 36 weeks of gestation. Reprinted with permission from Ment et al. 2009.

In preterm infants, the immature autoregulation and emerging cerebrovascular system make the brain vulnerable to rapid hemodynamic changes. In addition, leaving the hypoxic state in the uterus can cause a hypocarbia/hyperoxia-related reduction in cerebral blood flow in the vulnerable preterm brain. (Pandit et al., 2013)

The etiology of preterm brain injuries is multimodal. It has been described that neuroinflammation, impaired oligodendrocyte maturation, dysfunctional glial cells and axonal growth may all contribute to pathologic microscopic changes without lesions visible in the comprehensive MRI (Fleiss et al., 2020; Volpe, 2019). Injury processes are escalated by inflammation responses on the cytokine and endothelial cell level, by neuroglial interaction and imbalance with hypoxia (Fleiss et al., 2020). The glial cells play a crucial role in the formation and plasticity of the neural circuits, and they have been suggested to be of high importance in the vulnerability of the preterm brain (Reemst et al., 2016).

The total brain volume has been shown to be decreased and ventricle and cerebrospinal fluid (CSF) volumes increased in infants born preterm compared to infants born at term. The volumetric changes are associated with increasing prematurity. Furthermore, reductions in cortical grey matter (GM) and brain white matter (WM) volumes are also reported, and the volumes decrease adjacent to decreasing GA. (Makropoulos et al., 2016)

The classical and most severe type of white matter injury (WMI) of infants born VPT is periventricular leukomalacia (PVL). PVL is comprised of focal necrosis with loss of all cellular elements in deep white matter. The size of the necrotized areas varies from microscopic scars to several millimeters or even more in cystic PVL. The diffuse type of WMI is, however, more common and affects a wider volume of

the WM. It is assumed to be caused by an imbalance of different neuroglial cell types and an aberrant maturation process of myelinproducing cells. This might lead to aberrations in WM microstructure and neural circuit formation. (Reemst et al., 2016; Volpe, 2009, 2019) Diffuse WMI is seen as a spectrum, ranging from mild to severe, with mild findings present in up to 79% of the infants born VPT (Leijser et al., 2009). The cystic and most severe form of PVL is seen in less than 5% (Back, 2015). Schematic drawings with adjacent MR images of different WMI types are shown in Figure 2.

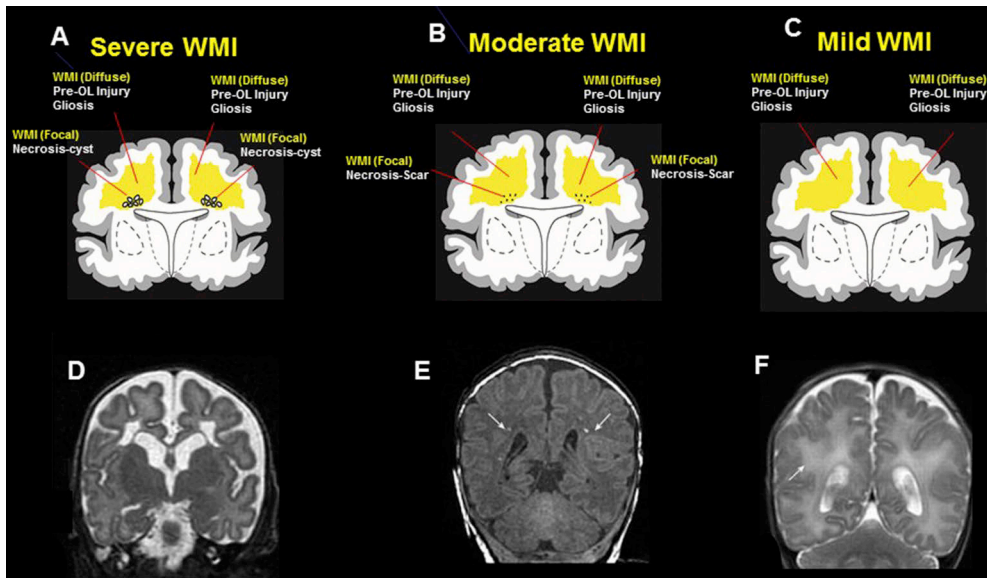


Figure 2. Schematic drawings with adjacent MR images of different white matter injury (WMI) types. A is representing focal cystic periventricular leukomalacia (PVL) with diffuse WMI, B focal non-cystic PVL with small scar lesions with diffuse WMI and C diffuse WMI alone. Reprinted with permission from Volpe 2009.

Intraventricular hemorrhage (IVH) is a typical lesion related to prematurity. While WMI is primarily diagnosed with MRI, IVHs are also seen in neonatal cranial ultrasounds. The IVH is graded from grade I to grade IV. Grade I refers to a germinal matrix hemorrhage, grade II to an intraventricular hemorrhage without ventricular dilatation, grade III to an intraventricular hemorrhage with ventricular dilatation, and grade IV to a parenchymal hemorrhage and/or hemorrhagic periventricular venous infarction (Papile et al., 1978). The risk for neurodevelopmental impairment increases with the grade. The highest developmental risks are associated with grades III and IV, with a 26% and a 53% risk respectively of an adverse neurodevelopmental outcome (Sewell et al., 2018). For grades I to IV, the prevalence of IVH in preterm

infants is 17.0%, 12.1%, 3.3% and 3.8% respectively (Chevallier et al., 2017). The prevalence of a grade IV IVH with hemorrhagic infarction in VLBW infants is approximately 5%, and it increases to up to 20–30% in infants with a BW <750 g (Volpe, 2009).

In addition to volumetric changes, there are often other GM changes associated with preterm birth. Abnormal cortical gyration, increased subarachnoid space and changes in signal intensity are GM findings occasionally associated with VPT birth. The prevalence of abnormal cortical GM findings is 27%. (Inder et al., 2003) Specifically, atypical gyration is seen in 8% of VLBW infants without chromosomal disorders or congenital anomalies (Leijser et al., 2009). The sulci of insula, superior temporal sulcus and pre- and postcentral sulci bilaterally have been shown to be fewer and shallower in VPT infants than in infants born at term (Engelhardt et al., 2015). These disruptions have been thought, to some extent, to be caused by the impaired recruitment and maturation of cortical interneurons (Panda et al., 2018). Besides cortical changes, volumetric reductions are seen also in subcortical GM, i.e., in the thalamus and basal ganglia. The findings are, however, controversial and affected by the state of WMI. (Back, 2015; Volpe, 2019)

The diffusion properties of the WM tracts have been shown to differ between infants born VPT/VLBW and at term. An increase in unrestricted diffusion and decrease in directional diffusion is seen in, for example, the corpus callosum (CC), corticospinal tracts (CST), optic radiations (OR), superior longitudinal fasciculus (SLF) and anterior and superior thalamic radiations when compared to controls at term age (Pannek et al., 2014). The subcortical changes in the thalamus have been shown to associate with the diffusivity of the thalamocortical networks (Ball et al., 2012).

At term age, functional imaging at rest has shown a similar network maturation and topology in infants born VPT/VLBW and infants born at term. The between-network interaction and inside-network connections have, however, been shown to be less integrated, i.e., functioning less efficiently in infants born VPT/VLBW than those born at term, when imaged at term. (Bouyssi-Kobar et al., 2019)

2.1.2 Outcome in adolescence

2.1.2.1 Motor outcome

During the last two to three decades, there have been two emerging trends in the motor outcomes of infants born VPT/VLBW. The severe impairments are decreasing, while the rate of minor impairments is reported to be either increasing or remaining stable. This has been associated with the development of neonatal care and the increased survival of ELBW infants. The motor problems most commonly

linked with prematurity are cerebral palsy and developmental coordination disorder (DCD). (Cheong et al., 2021; Sellier et al., 2016; Spittle et al., 2018)

Cerebral palsy

Cerebral palsy (CP) is a group of disorders with wide variations in clinical severity and clinical findings. The neurological findings are characterized by disturbances in movement, posture and their maintenance, and they are caused by a non-progressive lesion occurring during the fetal period or early infancy. (Bax et al., 2005) A review by Patel et al. (2020) reports a 1.5–3/1000 prevalence of CP in all live births (Patel et al., 2020). The prevalence of CP is decreasing both among all live births and in VPT births but stable in EPT/ELBW births (Sellier et al., 2016).

A Europe-wide register study showed a 3.6% rate of CP in infants born VPT/VLBW and a 4.6% rate in infants born EPT/ELBW in 2003 (Sellier et al., 2016). However, a recent review by Synnes et al. (2018) reports an incidence of 9.1% of CP in adults born EPT/ELBW, which is similar to the 12% reported in an Australian cohort born in 2005 and to the 9.1% reported in a Swedish cohort including only subjects with a GA of 23–25 weeks and born in 1992–1998 (Holsti et al., 2016; Spittle et al., 2018; Synnes et al., 2018).

A nationwide Finnish register study including all live births between years 1991–2008 in Finland showed a 0.22% incidence of CP in the whole population. For VPT infants, the total incidence for CP was 8.5% in 1991–2008. The incidence declined over the study period, being 13.7%, 9.5%, and 3.7% in years 1991–1995, 1996–2001, and 2002–2008, respectively. (Hirvonen et al., 2014)

Developmental coordination disorder

Developmental coordination disorder (DCD) is a term characterizing motor and coordination abilities that are below the normative level of age-appropriate motor abilities when other specific medical conditions are excluded. DCD is diagnosed based on a standardized clinical assessment and includes scores in the <5th percentile of the reference values, accompanied with significant daily problems in motor functioning. The most widely used assessment is the Movement Assessment Battery for Children (MABC-2) (Henderson et al., 2007). The literature also distinguishes a group at risk for DCD, which is defined by MABC-2 scores between the 5th and 15th percentiles in a standardized assessment. DCD may affect a person's academic achievements and daily activities. The estimation of population prevalence of DCD is 5–6%, with 2–3% experiencing major effects on daily living. (Blank et al., 2019)

A meta-analysis by Edward et al (2011), including seven studies, assessed the incidence of DCD in children born VPT/VLBW. The meta-analysis showed an odds

ratio of 6.29 (95% CI, 4.37–9.05, $p < .00001$) for DCD in VPT/VLBW born children at the age of 6.8–14.4 years (VPT/VLBW $n=819$, controls $n=813$). The odds ratio of belonging to the “at risk for DCD” group was 8.66 (95% CI, 3.40–22.07, $p < .00001$) in children born VPT/VLBW at the age of 8–13.2 years (VPT/VLBW $n=538$, controls $n=527$). (Edwards et al., 2011). Williams et al (2010) performed two meta-analyses including preterm born infants in school age included 10 studies in their meta-analysis ($n=1457$) of children “at risk for DCD” and 10 studies ($n=1928$) in their meta-analysis of children with DCD. The prevalence of “at risk for DCD” was 22.2–72.2%, with a pooled estimate of 40.5% (95% CI 32.1–48.9 /100). The prevalence of DCD was 9.5–34.0%, and the pooled estimate 19.0% (95% CI 14.2–23.8/100). (Williams et al., 2010). DCD has been shown to remain relatively stable after adolescence in the VPT/VLBW population (Husby et al., 2013).

Reported by Uusitalo et al. (2020), the rate for DCD in the PIPARI study was 11.3%. The “at risk for DCD” group included an additional 8.5% of children born VPT/VLBW in the PIPARI study when assessed at the age of 11. In the same study, children born VPT/VLBW with DCD had a lower health-related quality of life than children born VPT/VLBW who did not have DCD. The rate of DCD in EPT/ELBW children in the PIPARI study was 18%. (Uusitalo et al., 2020) In another Finnish prospective cohort study including children born EPT/ELBW in 1995–1997, the prevalence of DCD was 30% and the prevalence of “at risk for DCD” was 55% when assessed at the age of 11 years (Tommiska et al., 2020).

2.1.2.2 Preterm behavioral phenotype

The overall risk for any psychiatric disorder has been reported to be as high as 28.7% in children and adolescents born VPT/VLBW, compared to a general sample with a risk of 15.5% in the age group from 2 to 17 (Singh et al., 2013). In case control studies, the risk for any mental disorder has been 23% (more than threefold compared to controls) in an EPT/ELBW sample at 11 years of age and 28% in VPT/VLBW sample at 14 years of age (Indredavik et al., 2010; Johnson et al., 2010). The most common and clinically acknowledged psychological and behavioral phenotype of the children born preterm consists of three major traits: inattentiveness, social problems and anxiety. Together, these traits are known as the preterm behavioral phenotype. (Burnett et al., 2019; Johnson et al., 2011) This behavioral profile, containing all three features, is seen e.g. in the caregiver reports of the Strengths and Difficulties Questionnaire (SDQ) in 20% of children born ELBW/EPT, at 8 years of age (Burnett et al., 2019).

The extreme forms of these traits are also some of the core symptoms of anxiety disorders and neuropsychiatric disorders. Inattentiveness is seen in attention deficit hyperactivity disorder (ADHD) and social difficulties in autism spectrum disorder

(ASD). Both diagnoses, also together, are more frequently seen in adolescents born VPT/VLBW or EPT/ELBW. These children are also more often affected by subclinical traits that do not fulfil the diagnostic criteria but still impact daily life. (Bröring et al., 2018) The social difficulties and anxiety seen in adolescents born VPT are thought to have neurodevelopmental origins (Taylor, 2020).

Attention deficit hyperactivity disorder

ADHD is a developmental neuropsychiatric disorder characterized by inattentiveness, hyperactivity, and impulsivity that exceed the usual occurrence for age (APA, 2013). ADHD is clinically subdivided into the combined, inattentive, and hyperactive subtypes. The worldwide prevalence for ADHD in children and adolescents is estimated to be 3.4–7.2% (Polanczyk et al., 2015; Thomas et al., 2015).

A meta-analysis by Franz et al (2018) identified 12 studies (n=1787) assessing categorical ADHD diagnosis and 29 studies (n=3504) assessing ADHD symptomatology in individuals born VPT/VLBW and EPT/ELBW, regardless of their age. The odds ratio for ADHD diagnosis in the pooled VPT/VLBW and EPT/ELBW sample was 3.04 (95% CI 2.19–4.21) and separately for VPT/VLBW 2.25 (95% CI 1.56–3.26) and for EPT/ELBW 4.05 (95% CI 2.38–6.87). The meta-analysis assessing ADHD symptomatology reported that ADHD affects girls and boys more equally in the preterm population than in the whole population, where it is more likely to affect males. The studies included in the meta-analysis also suggested that the diagnostic stability of ADHD is higher in the VTP/VLBW and EPT/ELBW populations than in the general population. (Franz et al., 2018)

The prevalences shown in the meta-analysis by Franz et al. (2018) are comparable with studies focusing on adolescents. The prevalence for ADHD in adolescents born EPT/ELBW has been reported to be 11.5% compared to 2.9% in controls at the age of 11 and 15% in adolescents born EPT/ELBW compared to 7% in controls at the age of 18 (Burnett et al., 2014; Johnson et al., 2010). The results of a large Finnish register study are also comparable with the meta-analysis of Franz et al. In the Finnish population, the odds ratio for ADHD is related to the gestational age at birth being 5.77 (95% CI 1.68-19.83) at GA 25 weeks, 3.55 (95% CI 2.02–6.23) at GA 30 weeks, and 1.41 (95% CI 1.12–1.78) at GA 35 weeks. The infants' SGA-status included an odds ratio of 1.80 (95% CI 1.58–2.05) for ADHD. The odds ratios were adjusted for maternal and paternal age and psychiatric history, maternal socio-economical status, marital status, smoking during pregnancy and substance abuse, number of previous births, urbanity of child's birth place and paternal immigrant status. (Sucksdorff et al., 2015)

The meta-analysis by Fanz et al, however, revealed equally increased risk for both the inattentive and hyperactivity/impulsivity traits, which is not in line with individual studies in adolescent samples (Franz et al., 2018). At the age of 11 in the EPICure cohort, children born EPT had a 4.3-fold risk (95% CI 1.5–13.0) for ADHD. Of these 21 reported EPT children with ADHD, 13 (62%) had inattentive subtype ADHD and eight (38%) had combined subtype ADHD, while the prevalence for these subtypes in peers born at term and diagnosed with ADHD was 25% for the inattentive subtype and 75% for the combined subtype of ADHD (Johnson et al., 2010). The inattentive symptoms were significantly more frequently present in a Finnish EPT/ELBW population (n=168) than in controls at 11 years of age (Tommiska et al., 2020).

ASD, autistic traits and social cognition

ASD is a developmental neuropsychiatric disorder with impairments in reciprocal social interaction and communication, as well as restrictive and repetitive interests and behaviors (APA, 2013). The socio-economically adjusted odds ratio for ASD in the VPT/VLBW population has been reported to be 3.16 (95% CI 1.42–7.04) with a prevalence of 4.5 % compared to 1.7 % in term born children at the age of 2–17 (Singh et al., 2013).

The rate for ASD diagnosis in EPT/ELBW children in three different cohorts, at 6.5 years of age, has been reported to be 14%, and at 11 years of age 8–13% (Fevang et al., 2016; Johnson et al., 2010; Padilla et al., 2015). Additionally, at the age of 6.5, autistic traits were observed in 27.4% of the children (Padilla et al., 2015). In a large cohort study (n=889) with children born EPT/ELBW in the years 2002–2004, assessed at the age of 10, the prevalence for ASD was 7.1%. The prevalence was 15.0% for those born at a GA of 23–24 weeks and 3.4% for those born at 27 weeks of GA. Of children diagnosed with ASD, 40% also had an intellectual disability. The female-to-male 1:2 ratio differed significantly from the 1:4 ratio of the general population. (Joseph et al., 2017)

Adolescents born VPT/VLBW have been shown to have both teacher- and parent-reported increases in social problems, as well as parent-reported increases in ASD symptoms on the Social Responsiveness Scale (SRS) at the age of 13. The VPT/VLBW group has been reported to have significantly poorer social cognition and to show more traits of autistic mannerisms and impaired reciprocal social behavior. (Twilhaar et al., 2019) According to a review, the parents of adolescents born EPT/ELBW have reported their child to be more socially withdrawn, to be less likely to be involved in clubs or teams and to be victims of bullying more often than controls at 11–14 years of age (Ritchie et al., 2015).

Korzeniewski et al (2017) studied social difficulties in EPT children born in 2002–2004 (n=776). The outcome was measured at the age of 10 with the SRS, excluding children diagnosed with ASD. The prevalence for social impairment was 16% in children with a normal IQ (≥ 85) and 27% for children with an IQ < 85 , compared to the normative 4% prevalence. Children with high SRS scores were more likely to have symptoms of ADHD (especially the inattentive subtype), anxiety, depression, dysthymic disorder and/or a social phobia (Korzeniewski et al., 2017).

Anxiety

The worldwide prevalence estimation for anxiety disorder in children and adolescents varies from 5.8 to 6.5%, and the estimated prevalence for subthreshold anxiety symptoms in European countries is 32% (Polanczyk et al., 2015). The studies in adolescents born VPT/VLBW or EPT/ELBW are heterogenous in methodology, reporting both structured interviews and parent-rated questionnaires.

A meta-analysis of 6 studies (n=1519) by Sømshovd et al (2012) has reported a 2.27 odds ratio (95% CI 1.15–4.47) for 11–20-year-old adolescents born VPT/VLBW developing an anxiety disorder, with an overall prevalence of 9.9% in the adolescents born VPT/VLBW, as compared to 5.5% in the full-term controls (Sømshovd et al., 2012). However, the prevalence for anxiety disorders has been reported to be even higher, being 15% at the age of 14 in adolescents born VPT/VLBW (Indredavik et al., 2010).

The prevalence of emotional disorders (including depression and anxiety) has been reported to be 9% in EPT/ELBW children at the age of 11 compared to 2.1% in their classmates (Johnson et al., 2010). Contrastingly, in a study by Burnett et al (2011), the prevalence of anxiety disorders in adolescents born EPT/ELBW was similar to controls born at 35–42 weeks of GA, being 21% and 20% respectively (Burnett et al., 2014).

A longitudinal follow-up study from 6 to 26 years of age in VPT/VLBW-born children reported no significant difference in the occurrence of anxiety or mood disorder at the age of 6. Instead, significant differences were found at the age of 8 and 26 between the VPT/VLBW born infants and term-born controls. At 8 years of age, the odds ratio for any anxiety disorder was elevated in the VPT/VLBW group being 2.10 (95% CI 1.08–4.10), the prevalence being 11.8% in the VPT/VLBW group and 6.6% in term-born controls. At the age of 26, the odds ratio was elevated for any mood disorder, being 1.65 (95% CI 1.02–2.67) (27.5 % vs. 18.8 % in controls). However, these associations lost significance after the multiple test corrections. (Jaekel et al., 2018)

2.2 Brain magnetic resonance imaging (MRI)

2.2.1 Comprehensive MRI

2.2.1.1 Physical background

Magnetic resonance imaging is based on a physical property of hydrogen atoms, spin. Spin is an intrinsic property of all atom nuclei, and for hydrogen it is $\frac{1}{2}$. In nuclei with spin unequal to zero, the atom nucleus has an intrinsic magnetic property called magnetic moment. The hydrogen atom is also an abundant element in human body, making it the most suitable basis for the MRI technique.

When applied to an external magnetic field, the intrinsic magnetic moment of the hydrogen nuclei will align with the external field. The alignment happens either up or down the field, with a small excess with the field. This forms the net magnetization. The spins, oriented by the external magnetic field, are thereafter distracted with a radio frequency pulse. This absorption of electromagnetic energy is called excitation. It causes the net magnetization to turn to a transverse plane.

The recovery of the spin to the original orientation defined by the external magnetic field is called relaxation. The relaxation is affected by spin-lattice and spin-spin interactions, and it is a tissue-specific property. The spin-lattice relaxation process is commonly referred to as T1 relaxation and the spin-spin relaxation process is, in turn, called T2 relaxation. The echoes caused by this excitation-relaxation-process are referred to as the MR signal. In addition to the tissue's proton density, the differences in relaxation times cause the tissue contrasts in MR images.

The measured MR signal also depends on the energy transferred to the tissue in an excitation pulse, as well as the timing, order and frequency of the pulses. The localization information is derived by using magnetic field gradients. The MR signal is collected to a k-space matrix. The final 2D or 3D images are formatted using the Fourier transformation. The higher the field strength, the higher the amount of MR signal, but on the other hand, it also makes the artifacts more pronounced. (Atlas, 2016; Weishaupt et al., 2006)

2.2.1.2 The conventional imaging sequences

The contrast of the basic imaging sequences used in clinical brain MRI imaging are based on the T1 and T2 relaxation times. They are called T1- and T2-weighted images. The relaxation times are tissue specific. This makes it both possible and essential to use different weightings to assess different anatomical regions or tissues.

T1 relaxation describes the recovery of the net magnetization in the original direction caused by the external magnetic field. The faster the tissue recovers after

the excitation pulse, the brighter the tissue will be in the final image. T1-weighting can be increased by shortening the repetition time between the excitation pulses. T1-weighted images provide a good discrimination between brain GM, WM, and spaces inside the skull that contain cerebrospinal fluid (CSF) or blood. It is widely used when inspecting normal anatomy, structural anomalies and myelination in preterm infants.

T2 relaxation describes the decrease of the net magnetization in the transverse plane compared to the external magnetic field. T2-weighting is acquired by adjusting the time between the excitation and MR signal collection. This time is called echo time. With a short echo time, the decrease of the net magnetization in the transverse plane has just begun, and the measured signal is low, as is the T2-weighting. The tissue differences become more visible when the echo time is extended. This will show the tissues with a short T2 as dark, while tissues with a long T2 will still emit a stronger signal. T2-weighted images are used to assess brain tissue pathologies such as demyelination and periventricular lesions, which are common in infants born VPT. (Atlas, 2016; Weishaupt et al., 2006)

2.2.1.3 Comprehensive MRI in clinical use in the VPT/VLBW population

Comprehensive brain MRI in VPT infants at term-equivalent age is a clinical routine in many neonatal intensive care units. Besides MRI, sequential brain ultrasound (US) is also performed routinely.

The benefits of using US are the low cost and the possibility for repeated bedside imaging. It provides good visualizations of the IVHs, large cystic lesions, severe WM injuries, and ventriculomegaly (Maalouf et al., 2001). Compared to US, brain MRI is a more sensitive tool for detecting non-cystic focal injuries in the WM, diffuse WM injuries, cortical abnormalities and cerebellar lesions. Furthermore, the characterization of brain myelination and volumetric analysis are possible with new MRI techniques. (Benders et al., 2014; Maalouf et al., 2001)

The interobserver reliability of a structured MRI pathology classification has been shown to be good (intraclass correlation coefficient = 0.96; 95% CI 0.89–0.99) even though the inspection requires experience (Szakmar et al., 2021). For comparison, the interobserver reliability for US has been shown to be 68–76% (kappa 0.62) for positive agreement and 92–97% (kappa 0.68) for negative agreement for ventriculomegaly, hypoechoic lesions and IVH. The values have been shown to be lower for hyperechoic WM lesions, with 48% for positive agreement and 84% for negative agreement (kappa 0.32) (Kuban et al., 2007).

Compared to a singular US, MRI is more expensive: the costs in July 2021 in Turku University Hospital are €103 for US and €306 for MRI. MRI also necessitates transfer to the imaging unit and requires a more hemodynamically stable state of the

infant. Over the last two decades, improved MRI devices (e.g. monitoring options, ventilators, warming equipment, integrated head coil) and neonatal scanning without sedation (with simple feeding and swaddling, by using ear protection plugs and hearing protection, and by using polystyrene bead-filled “huggers”) have made early MRI imaging more feasible.

2.2.2 Diffusion-weighted imaging

2.2.2.1 Physical background

Diffusion-weighted imaging (DWI) is based on the Brownian motion of the water molecules in the tissue under examination. Without any external restrictions, diffusion occurs equally towards all directions, which is known as isotropic diffusion in comparison to the partly restricted version known as anisotropic diffusion. Natural diffusion causes a signal loss of the detected MRI signal. This creates a darker contrast where the diffusion is unrestricted and a brighter one in areas where the diffusion is restricted. When this imaging process is repeated in at least six different directions, it is possible to define the quantity of diffusion occurring towards different directions. (Basser et al., 1994; Pierpaoli et al., 1996)

The diffusion tensor model describes diffusion using a Gaussian model, with matrix driven three mutually perpendicular eigenvectors with a positive magnitude and direction in a 3D space. The white matter structures restrict the diffusion occurring perpendicular to the fiber bundle. Hence, the main eigenvector, i.e., the vector with the largest magnitude, points to the principal direction of the diffusion. This direction is similar to the fiber tract axis in brain WM tissue and can be presented as red-green-blue color maps. Besides the orientation, the tensor model also accompanies scalar values called eigenvalues. Diffusion metrics used in clinical studies are derived from these eigenvalues. (Dudink et al., 2008; Pandit et al., 2013)

The two most widely used diffusion metrics are mean diffusivity (MD) and fractional anisotropy (FA). MD measures the overall diffusion in the underlying tissue, and a decrease in MD is expected, to some extent, to measure the maturational decrease in water and increase in macromolecules and cellular components that occurs during brain development. FA measures the directionality of the diffusion of water and is mostly related to the myelination of axons. In addition to MD and FA, axial diffusivity (AD) and radial diffusivity (RD) are also measured in some studies. AD measures diffusion along the longest axis of the diffusion ellipsoid, while RD is the average of the two smaller perpendicular vectors. All of the diffusion metrics are affected by various changes in underlying tissue. The most significant factors in the context of prematurity and developmental outcomes are myelinisation, cell density,

axon size, the packing density of axons, coherence, and water content. (Pandit et al., 2013; Tamnes et al., 2017)

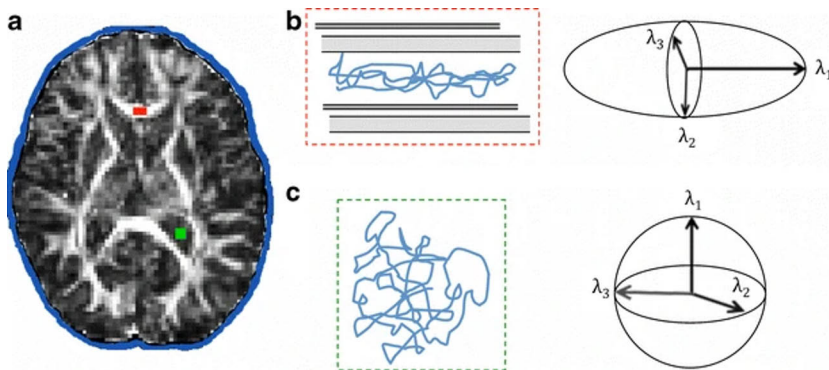


Figure 3. A schematic view of the diffusion metrics in anterior corpus callosum (a, red) and left lateral ventricle (a, green). Diffusion in anterior corpus callosum is highly restricted (b) i.e., anisotropic and has got a high fractional anisotropy. Diffusion in the left lateral ventricle is unrestricted i.e., isotropic and has got a high mean diffusivity. Reprinted with permission of Pandit et al, 2013.

2.2.2.2 Methods

The region-of-interest (ROI) method is based on small areas that are individually drawn for each patient and structure. This method takes into account the patient's anatomy as observed in the conventional MR images. The ROI method is time consuming and requires a prior hypothesis as well as neuroanatomical knowledge. The ROIs can also be selected by using anatomical templates or tractography. The reproducibility is good for both, but better for the latter (Partridge et al., 2005). The ROI method allows individual comparisons between subjects, is not affected by the multiple comparisons problem in smaller samples, and manually drawn ROIs are also usable in subjects with atypical anatomy (Pandit et al., 2013).

Tract-based spatial statistics (TBSS) allow diffusion measures for the whole WM. The FA images of the whole study group are averaged, i.e., pooled together. The WM skeleton represents the central parts of the white matter tracts that should be common to all pooled study subjects. The thresholding of these central voxels diminishes the total variation of the study subjects and allows the assessment of only the major WM tracts. Due to methodology, the acuity of the presenting voxels is excellent (Smith et al., 2006).

Like TBSS, voxel-based morphometry (VBM) also allows diffusion analysis of the whole WM. The images are spatially normalized in common space and either used with common templates or a study-specific WM template. The partial volume effect is avoided by smoothing, which is a process averaging the values of nearby

voxels. Due to the voxel-wise comparisons, the method suffers from multiple comparisons, and the results have to be corrected. VBM is an automated method allowing analysis without restricting it to an a priori hypothesis but suffers from normalization not taking into account high individual variation and is prone to artifacts and errors in the normalization process (Ashburner et al., 2001).

Diffusion tractography creates the WM tract by assessing the diffusion direction of each voxel and piecing them together to form a pathway. The tracing starts from a given seed region and ends in a target region or when encountering limiting measures, such as defined mask areas or stop criteria. The deterministic tractography method forms the tracts according to the voxels' main diffusion direction, and the streamlines terminate if the angle between two adjacent voxels exceeds a critical limit or the anisotropy is too low. With a well-defined seed ROI, the accuracy of the deterministic approach is good. Its usability is, however, limited in crossing-fiber-regions, and it only allows the analysis of one bundle per seed region. (Jones, 2008)

The probabilistic tractography method calculates a probability distribution for fiber orientation in each voxel. The use of probability that is not limited to the main diffusion direction allows the analysis of multiple tracts. The probabilistic approach also allows analysis of areas with lower FA values, including grey matter. (Behrens et al., 2007; Jones, 2008)

The tractography approach allows comparisons between individuals, and it takes into account the possible variations in a subject's anatomy. It is possible to calculate the diffusion metrics averaged over the whole tract or over a specific part. The tract volume can be derived from the spatial characteristics of the tract. (Pandit et al., 2013)

The newer DWI techniques that have not yet been frequently applied in the preterm adolescent population are high angular diffusion imaging (HARDI), neurite orientation dispersion and density imaging (NODDI) and spherical deconvolution (CSD). HARDI uses multiple b values and directions, and the imaging time has just become bearable to the pediatric and adolescent populations. NODDI and CSD might, in the future, become applicable and provide more accurate information of the intravoxel fiber organization. (Lebel et al., 2017; Pandit et al., 2013)

2.2.3 Resting state functional MRI (rsfMRI)

Functional MRI is based on blood oxygen level fluctuation in the brain GM. Functional activity increases local arterial blood flow. The detected signal is based on the different magnetic properties of deoxygenated and oxygenated hemoglobin and the increase of hydrogen atoms adjacent to the increase in blood flow. (Ogawa et al., 1990) These changes occur both as a response to a stimulus or as spontaneous intrinsic time-varying fluctuations in a resting state. This phenomenon is seen when

no task is performed and the level of spontaneous activity differs across gray matter space. This spontaneous fluctuation represents distinct functional networks. Each of them consists of areas with temporally correlated signal fluctuations that reflect their functional connections.

Independent component analysis (ICA) extracts spatially and temporally independent maps from this homogenous data. Combining the data of temporally equal fluctuation patterns, it has been possible to recognize resting state networks (RSNs). These RSNs can be assessed in terms of inside-network connectivity (inside-NC) and between-network connectivity (between-NC). Inside-NC measures connectivity between different areas inside a specific network whereas between-NC measures correlations and anti-correlations between different RSNs. When the activation is averaged over the whole scanning time, it is referred to as static functional connectivity (sFNC). sFNC assumes that the state of activation in the brain stays similar over time. (Allen et al., 2011)

The static assumption is, however, only a rough estimate of the functional complexity. This is due to constantly ongoing fluctuations of brain function during the scans. The methods used to capture these temporal fluctuations are called dynamic methods, and this type of measurements are referred to as dynamic functional network connectivity (dFNC). One of these methods is called the sliding window approach. The data is fractioned to overlapping timed windows. The variety of windowed FNC (wFNC) matrixes is reduced to a few re-occurring prototypic connectivity matrixes that most resemble the brain connectivity. (Allen et al., 2014) These connectivity states can be compared between different study groups. In addition, between-group comparisons can be made for measures of temporal occupancy of these states. These measures most often include total time spent in different native-space FNC (nsFNC) patterns (dwell time) or the dwell time distribution between the different nsFNC patterns during the scanning time (fraction rate). (de Lacy et al., 2018)

Though the nsFNC approach has proven to be fruitful, further attempts to achieve a more high-dimensional exploration of dFNC while avoiding data reduction can be made. This type of analysis technique is known as meta state dFNC (msFNC) analysis. In this approach, instead of reducing the wide variety of connectivity states to only a few ones, each windowed FNC matrix is shown as a weighted sum of a few basic connectivity patterns. Hereafter, each particular set of the weighted connectivity patterns constitutes one meta state out of a wide variety of possible meta states. (Miller et al., 2016)

The msFNC dynamism is characterized by a set of range and fluidity metrics. Fluidity is measured based on the total number of distinct meta states visited and the number of switches between meta states made by the subject during the scan. Range, in turn, is described by meta state span, i.e., the measure of maximal distance in the

L1 space between visited meta states, and by total distance, which is a sum of all distances between successively visited meta states. (Miller et al., 2016) This methodology based on nsFNC and msFNC has previously been used in studies assessing children and adolescents with ADHD or ASD (de Lacy et al., 2018; Rashid et al., 2018).

2.2.4 MRI artifacts in brain MRI

MRI is prone to various types of artifacts caused by both physical and technical issues, but also by patient-related properties. Some of the artifacts can be addressed through technical adjustments before and during scanning or through mathematical post processing, but motion, for example, can only be covered to some extent. The artifacts can cause distortions in the imaging data, which can lead to impaired measurements and even to the rejection of data with large artifacts, especially when using the quantitative MRI techniques.

Motion artifacts are widely known patient-related causes of artifacts in brain MRI scans, especially in children and adolescents. These age groups are usually sedated for the clinical image acquisition due to the fidgeting tendency. Motion artifacts tend to blur the image or cause ghosts that may overlap or confound true findings. Movement can be minimized by providing clear instructions, stabilizing the head, and using special MRI sequences and ultra-fast read-out techniques. (Taylor et al., 2016)

Some types of artifacts occur due to the physical properties of the tissues in question, especially at the interfaces of two tissues with highly different magnetic properties. Magnetic susceptibility is a fundamental feature of all matter, including tissues, and it describes the ability of the matter to become magnetized in an external magnetic field. This leads to signal loss and pile-up, i.e. darker and brighter bands at interfaces such as the bone-air interface in the paranasal sinuses or the metal-bone interface in adolescents with orthodontic appliances. Susceptibility artifacts can be assessed by using different read-out techniques, by changing phase encoding, and by using various estimates and geometrical corrections (Andersson et al., 2003; Jezzard et al., 1995; Kybic et al., 2000; Merhof et al., 2007; Wu, Chang, et al., 2008).

Susceptibility correction has been shown to cause a significant reduction in whole brain white matter FA in adults, but also in a small pediatric sample (n=6) (Carper et al., 2015; Irfanoglu et al., 2019). The anatomical location affects the quantity of distortion and the highest variation of FA values is near the interfaces where the susceptibility difference is high (Maximov et al., 2019; P. A. Taylor et al., 2016; Wu, Barnett, et al., 2008). In an adult sample, the susceptibility correction has been shown to affect the tract length and continuity, the probability of reaching

anatomically correct cortical regions, and the tract count and their spatial variance (Irfanoglu et al., 2012).

Chemical shift artifacts, in turn, are caused by the difference in electron cloud distribution around the hydrogen atoms of fat and water. This affects the behavior of hydrogen nuclei in the external magnetic field and leads to similar loss and pile-up bands as the susceptibility-affected interfaces but in different locations. Chemical shift artifacts can be minimized by increasing the bandwidth or by using fat suppression techniques. The tissue interfaces with high differences in signal intensity are also prone to an artifact called partial volume effect. This can cause misleading intermediate signal areas at these sites. (Le Bihan et al., 2006)

MR imaging as a technique also produces artifacts. The rapidly changing magnetic fields cause swirl-like electrical currents, i.e., “eddy currents” in their surroundings, which also occurs in the patient. Fast imaging sequences, for example single-shot echo-planar imaging (SE-EPI) are more prone to eddy currents because of the high switching frequency. One special type of eddy current seen especially in SE-EPI is the Nyquist ghost artifact. Diffusion-weighted imaging (DWI) uses SE-EPI and is thereby prone to this type of artifacts. These artifacts are usually dealt with using automatic image post-processing. (Le Bihan et al., 2006)

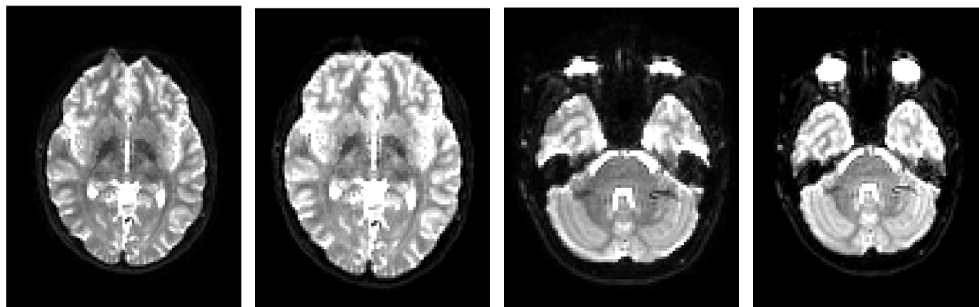


Figure 4. First two pictures from left show the frontal effects of susceptibility artifact and correction of it. Second pictures show the same effects in temporal lobes uncorrected - corrected.

2.3 MRI findings in the population of preterm infants

2.3.1 Prematurity-related MRI findings in adolescence

There are two separate MRI studies that looked at adolescents born VPT/VLBW in 1979–1980 (Stewart et al., 1999) and 1988–1993 (Nagy et al., 2009) as well as full-term controls. These studies were carried out when the subjects were at the age of 15 years. These studies show a prevalence of 23–55% for adolescents born VPT/VBLW

having a moderate to major pathological finding in comprehensive brain MRI. The prevalence for controls was 5–6%. Nagy et al (2009) reported that PVL was the only pathological finding in 41% of the abnormal scans in the VPT/VLBW group, while 65% had PVL and another pathology (Nagy et al., 2009). Stewart et al (1999) found PVL alone or combined with another finding in 90% of the cases with abnormal findings. The rates for pathologies were higher in adolescents born in 1979–80 than in adolescents born 1988–1993 (Nagy et al., 2009; Stewart et al., 1999). In a VPT/VLBW cohort born 2001–2004, the rate for major to moderate brain pathologies was reported to be 27% at TEA (Munck et al., 2010).

A meta-analysis of de Kieviet et al. (2012) reported results combining volumetric data from 15 studies that included a total of 818 adolescents born VPT/VLBW and 450 controls born at term between 1979–1995. The results showed that school-aged children born VPT/VLBW had significantly decreased whole brain, WM, GM, corpus callosum (CC), hippocampus, and cerebellum volumes compared to controls born at term. The age at which the imaging was performed (8–18 in the meta-analysis) did not have a significant effect on the volumetric differences. (de Kieviet et al., 2012) However, a recent meta-analysis by Le Zhou et al (2018), which also included adolescents born late preterm, showed that regionally, adolescents born VPT/VLBW, show both increase and decrease in WM and GM volumes (Zhou et al., 2018).

Patterns of both delayed and accelerated brain maturation in terms of GM volumetric changes have been reported in adolescents born VPT (Karolis et al., 2017). Recently, a longitudinal cohort study using MR imaging and volumetric measures at term and at 7 and 13 years of age in VPT born children showed that the overall rate of brain growth in children born VPT between term age and 7 years is reduced compared to controls when adjusting for total brain volume. There were no significant differences between the rates of brain growth in these two populations between the ages 7 to 13, but the difference in total brain volume still existed at the age of 13. (Monson et al., 2016; Thompson et al., 2020) This is partly in contrast with another longitudinal study that showed a decrease of 2–3% in cerebral GM and a 10% increase in cerebral WM between 8 and 12 years of age, compared to 9% and >26% in term-born controls, respectively (Ment, Kesler, et al., 2009). The cohort with differences was born in 1989–1992 and FMRIB (Functional MRI of Brain) Software Library (FSL) was used in the study, while the cohort without differences was born in 2001–2004, and Freesurfer was used in the study (Ment, Kesler, et al., 2009; Monson et al., 2016; Thompson et al., 2020).

Nosarti et al (2002, 2004 and 2008) reported that the adolescents born very preterm in the years 1979–80 still continued to show a 6.0% decrease in whole brain volume, a 11.8% reduction in total GM volume, a 42% increase in ventricular volumes, a 7.5% reduced surface area of the CC, and reduced subcortical GM

volumes at 15 years of age. Compared to a minor pathology or normal ultrasound finding, a major pathology in the neonatal ultrasound was associated with smaller WM and GM volumes and larger ventricle volumes. The more preterm the subject, the smaller the WM and GM volumes, but the degree of prematurity was not associated with the ventricle volumes or the size of the CC. (Nosarti et al., 2002, 2004, 2008) Deviant WM concentrations and volumes measured with VBM have been found also in absence of comprehensive MRI WM lesions in 14.5-year-old adolescents born VPT (Giménez et al., 2006).

In DTI studies focusing on 12–15-year-old adolescents born VPT/VLBW, the FA of the genu and splenium of the CC, the anterior and posterior limbs of the internal capsule (ALIC, PLIC), SLF and inferior longitudinal fasciculus (ILF), cingulum, external capsule (EC), centrum semiovale (CSO), inferior fronto-occipital fasciculus, uncinate fasciculi, and frontal and precentral subcortical WM were lower than in full-term-born controls (Constable et al., 2008; Skranes et al., 2007; Vangberg et al., 2006). However, in studies that only included adolescents born VPT/VLBW who only had normal or minor comprehensive MRI findings at the time of imaging (12–16 years), there is evidence of similar or even increased FA values compared to controls (Feldman et al., 2012; Mullen et al., 2011).

Studies related to RNSs and their inter-connectivity have been producing controversial results in adolescents born preterm when compared with controls. A longitudinal study by Rowlands et al. (2016) and Myers et al (2010) found a similar FNC pattern in children born late to extremely preterm and controls at eight years of age. At the age of 16, the activation was markedly increased in the preterm group compared to controls. (Rowlands et al., 2016) At the age of 16, an association between the cognitive scores and sFNC findings in preterm-born subjects was also present, despite not being present at the age of eight years (Myers et al., 2010). In addition, adolescents born VPT/VLBW have been shown to have increased connectivity between the sensorimotor network, salience network and central executive network at the age of 10–16. Weaker connectivity was found between the sensorimotor network, visual network, and dorsal attention network, but also within network connections in the central executive network and sensorimotor network in the same cohort. (Wehrle et al., 2018)

2.3.2 DWI and DCD in the VPT/EPT population at school age

Developmental coordination disorder (DCD) is well studied in the VPT/VLBW and EPT/ELBW populations in terms of comprehensive MRI. DCD is known to be associated with lower FA values in tracts related to motor and sensorimotor processing (Brown-Lum et al., 2020). These tracts are also known to be affected by

preterm birth (Constable et al., 2008; Ment, Hirtz, et al., 2009; Vangberg et al., 2006).

Two studies have assessed DCD and MABC-2 scores and DWI at 7 years of age in children born VPT/VLBW. In a TBSS study, a lower FA and a higher MD of the bilateral CST, CR, anterior thalamic radiation, EC, IC, cingulum and CC were found in the motor impairment group, along with other measured tracts (Dewey et al., 2019). In a CSD-based tractography assessment of global tract theory metrics, VPT/VLBW children with motor impairments tended to have decreased connection strength in a subnetwork involving the right precuneus connected to the right inferior parietal and inferior, middle and superior temporal gyri. The overall connectivity pattern was less complex in the VPT/VLBW population than controls. (Thompson et al., 2016)

Three DWI studies with MABC as the motor outcome measure has been done in VPT/VLBW and EPT/ELBW born school-aged children and adolescents. At the age of 8, children born VPT/VLBW with DCD had lower probabilistic tractography driven FA values in 14 of 18 large white matter tracts compared to children born VPT/VLBW without motor impairment. Children born VPT/VLBW without motor impairment had significantly lower FA values than controls in the forceps major, right cingulum-hippocampus tract, hippocampus, thalamus, striatum and cerebellum. (De Kieviet et al., 2014) At the age of 15, the TBSS-driven FA values of the genu of the CC, the bilateral external capsules and inferior fasciculi, right SLF and left middle fasciculus were negatively associated with manual dexterity sub scores (Skranes et al., 2007). At 18 years of age, the FA and AD values of the CST have been shown to be lower in the motor impairment group than in the group with a normal motor outcome in adolescents born EPT/ELBW (Kelly et al., 2015).

A study performed using HARDI probabilistic tractography revealed several differences in the diffusion metrics of a wide range of parceled motor tracts between 16-year-old adolescents born VPT/VLBW and term-born controls. Among a wide range of measured diffusion metrics, the researchers reported that the MD values were higher and FA values lower in the CST at the levels of the cerebral peduncles and internal capsule. In the body of the CC, a trend towards lower FA values and higher MD values without a statistical significance was identified. The CST findings for low FA remained after excluding subjects with radiological signs of a WM injury. (Groeschel et al., 2014) In further analyses of the same cohort and correlation with DWI imaging and the Zürich Neuromotor Assessment Battery, the researchers found that the quality of movement was associated with the FA values in the fibers connecting primary motor, primary sensorimotor and premotor areas to the CC. In addition, they found that the timed motor performance was significantly associated with FA values in the CC, CST and fibers connecting thalamo-cortical areas to premotor areas. (Groeschel et al., 2019)

2.3.3 Findings using quantitative MRI approaches in the preterm behavioral phenotype at school age

The core traits of the preterm behavioral phenotype are anxiety, social difficulties and inattentiveness (Burnett et al., 2019; Johnson et al., 2011). Of these, inattentiveness and social difficulties are traits also associated with ADHD and ASD. This literature review focuses on the differences observed in various quantitative imaging studies in the VPT/EPT population in terms of these two traits and disorders.

Regarding the overall psychiatric morbidity in adolescents born VPT/VLBW, smaller cerebral subcortical GM and cerebellar GM and WM volumes have been associated with developing or persisting psychiatric disorders in a longitudinal study with a follow up from 15 to 19 years of age (Botellero et al., 2016, 2017). In addition, altered connectivity of the amygdala was reported in a study by Johns et al (2019) during a rsfMRI at the age of 20 in a cohort of VPT-born young adults in subjects who scored altered behavioral markers at the age of 16 in parent reported CBCL (Johns et al., 2019).

ADHD and inattentiveness

Inattentive symptoms of ADHD have previously been associated with smaller parietal and occipital cortical GM and cerebellar WM volumes at the age of 15 and 19 and total WM and CC volumes at the age of 15 in adolescents born VLBW (Botellero et al., 2016, 2017; Indredavik et al., 2005). An association was also found between inattentive symptoms and cerebellar GM volume at the age of 15 (Botellero et al., 2016). Reductions in parietal and occipital cortical GM were associated with hyperactivity at the age of 15 when controlling for IQ (Botellero et al., 2017). The hyperactivity scores on the Rutter Parent and Teacher Scale have been negatively correlated with left caudate nucleus volume in male adolescents born VPT at the age of 15 (Nosarti et al., 2005).

In a voxel-based study with VLBW adolescents imaged at 15 years of age, the FA values of the left EC, right superior fasciculus and left middle fasciculus were associated with ADHD inattention scores based on the Kiddie Schedule for Affective Disorders and Schizophrenia (Skranes et al., 2007). In a DTI tractography study with 12.5-year-old adolescents born VPT, the tracts connecting the frontal, temporal, parietal and occipital lobes, as well as the subcortical regions and frontal cortices, had significantly lower FA values in adolescents with attentional problems. The most prevalent negative association was found to exist between attentional problems and the left precuneus – left middle temporal gyrus connection. (Tymofiyeva et al., 2018) In a task-based fMRI study, greater activation of the nearby areas, left superior-temporal and left supramarginal gyri, was also recognized also to be associated with

better performance in an attention task in 15–16-year-old adolescents born between the gestational ages of 28 and 35 weeks (Carmody et al., 2006).

ASD and autistic traits

Children with significant autistic traits born EPT/ELBW showed smaller temporal, occipital, limbic and insular cortical volumes at the age of 6.5 years. The differences disappeared after adjusting for birth weight z-score. (Padilla et al., 2015) In a DTI study in adolescents born with VLBW at the age of 15, the Autism Spectrum Screening Questionnaire scores were negatively associated with the FA values of the left VE and left superior fasciculus (Skranes et al., 2007).

Cognitive flexibility has been shown to be associated with FA values in projection fibers and long association fibers in adolescents born preterm, imaged at the age of 15 (12–18) years. The attention and processing speed scores were not significantly associated, but similar trends were found also for them. No associations were found in the controls born at term. (Vollmer et al., 2017)

Social competence

In 6-year-old children born EPT/ELBW, the FA-weighted structural connectivity of the prefronto-subcortical circuits has been associated with poorer social functioning when assessed with the SDQ (Fischi-Gómez et al., 2015). In a study by Urbain et al (2019), children born VPT were shown to have functional and volume reductions of the right angular gyrus recognized in a magnetoencephalography/MRI study at the age of 7–13. Activation in this area has previously been shown to be crucial for attention shifting after emotional stimuli. (Urbain et al., 2019)

Social functioning measured using the social adjustment scale of Cannon-Spoor has been negatively correlated with left caudate nucleus volume in male adolescents born VPT at the age of 15 (Nosarti et al., 2005). Another study in adolescents born VPT at the age of 15 showed that subjects with high social immaturity scores in the CBCL had increased GM volume in the fusiform gyrus bilaterally compared to subjects with normal scores (Healy et al., 2013).

3 Aims

The aim of this study was to investigate the usability of the various available MR imaging techniques in the adolescent population. The imaging findings were compared between adolescents born preterm and adolescents born at term age. The specific objectives of this study were:

1. To investigate, if DTI metrics at term are associated with the motor outcome at 11 years of age in children born preterm.
2. To assess whether susceptibility artifact correction has a significant effect on tractography-driven DTI metrics and tract parameters in a healthy adolescent population.
3. To examine whether the resting state dFNC of adolescents born VPT/VLBW differs from the controls born at term, and to examine whether the dFNC of the VPT/VLBW group resembles the one found in individuals with ASD or ADHD.

4 Materials and Methods

4.1 Participants

This thesis is a substudy of the PIPARI study (Development and Functioning of Very Low Birth Weight Infants from Infancy to School Age), a prospective longitudinal cohort study focusing on infants born very preterm. The study was launched in Turku University and Turku University Hospital in 2001, and the recruitment ended in 2006 for the infants born very preterm and in 2004 for the control infants born at term. The cohorts consist of 232 infants born very preterm and 246 infants born at term.

This MRI substudy only includes the preterm infants born between April 2004 and December 2006. This is due to an upgrade of the MRI scanner from 0.23T to 1.5T in April 2004, which allowed the addition of a DWI scan in the imaging protocol. This substudy includes controls born at term during 2003–2004.

The PIPARI Study protocol was approved by the Ethics Review Committee of the Hospital District of South-West Finland in 2000 and in 2012. All families provided written informed consent when recruited to the follow-up study. At the ages of 11 and 13, the adolescents and their parents provided separate consents.

4.1.1 Children born preterm (study I and III)

A total of 146 VPT/VLBW infants were born in Turku University hospital between 4/2004 and the end of 12/2006.

The inclusion criteria for the infants born preterm were:

1. GA <32+0 regardless of the BW
2. GA <37+0, if the BW was ≤ 1500 g
3. At least one of the parents spoke Finnish or Swedish with the child
4. 1.5T MRI at term-equivalent age

The exclusion criteria for the infants born preterm were:

1. Death during the neonatal period or during follow-up
2. Major congenital anomalies or recognized syndromes, including clinical suspicions
3. Living outside the hospital district
4. Refusal of the family to participate

For study I, we excluded infants born at a GA $\geq 32+0$. This was done in order to allow a better comparison with previous studies excluding the SGA children with a birth weight under 1501g. Successful DWI was also required, but we included all infants with one or more completed ROI measurements. At 11 years of age, the Touwen neurological assessment was performed to exclude neurological disorders to qualify the DCD diagnosis made with MABC-2. For study III, a successful MRI and rsfMRI were required.

4.1.2 Controls born at term (study II and III)

A total of 97 healthy infants born at term were recruited as controls for the infants born very preterm during 2003 and 2004. The controls were recruited by asking the parents of the first-born girl and the first-born boy of each week to participate. If they refused, the parents of the next boy/girl were approached.

The inclusion criteria were:

1. GA $\geq 37+0$
2. At least one of the parents spoke Finnish or Swedish with the child
3. The infant was not admitted to a neonatal intensive care unit during the first week of life.

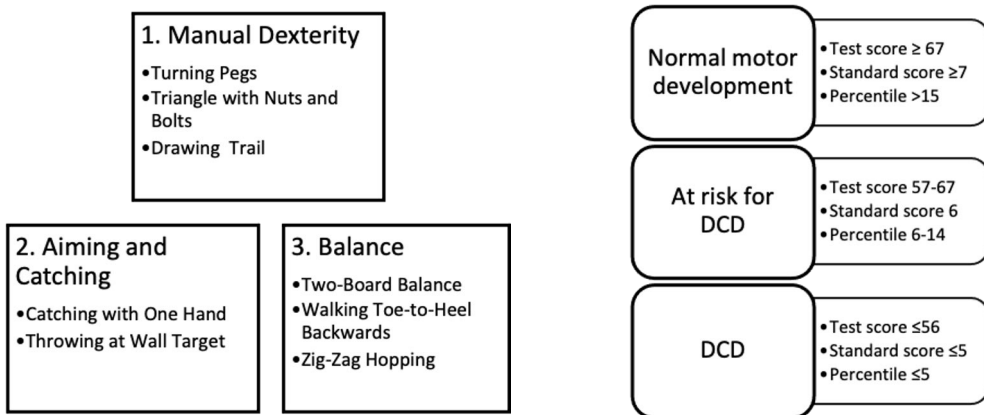
The exclusion criteria were:

1. Congenital anomalies or syndromes
2. The mother's self-reported use of illicit drugs or alcohol during pregnancy
3. Birth weight < 2.0 SD according to age and gender specific Finnish growth charts.

4.2 Assessment of motor outcome at 11 years of age

MABC-2 was used to assess the motor outcome at 11 years of age (Henderson et al., 2007). The assessment consists of three different domains, shown in Figure 5.

Together, these domains form the total score for the assessment. The scoring criteria are presented in Figure 5. MABC-2 is a widely used structured tool that is mainly used by physiotherapists. Assessment scores $\leq 5^{\text{th}}$ percentile are diagnostic for DCD when motor problems affect everyday life and cerebral palsy, neuromuscular disorders and other specific causes for motor impairment are excluded. In this study, we used the age band for 11–16-year-olds (Age band 3) according to the manual. MABC-2 and the Touwen neurological assessment were performed during the same visit by one of two PhD students, Karoliina Uusitalo (MD) or Katri Lahti (MD). Each assessment was recorded and inspected together with the supervising professor, Leena Haataja.



4.3 MRI imaging at term and at 13 years of age

4.3.1 Comprehensive MRI

The comprehensive MR imaging at TEA was performed using a 1.5T Gyroscan Intera CV Nova Dual MRI system (Philips) with a SENSE head coil. The MRI was conducted during postprandial sleep without any pharmacological sedation. Disposable ear plugs (3M, São Paulo, Brazil) and hearing protector (Wurth, Austria) were used as ear protection, and a pulse oximeter was routinely used during scans. If necessary, a physician attended the examination to monitor the infant. Only the preterm infants were imaged at term-equivalent age.

The comprehensive MR imaging at 13 years of age was performed using a 3T Philips Ingenuity TF PET/MR (Philips, Amsterdam, Netherlands) with a SENSE Head-32-channel coil. Ear protection (3M disposable ear plugs, São Paulo, Brazil) and hearing protection (Wurth, Austria) was used, and the adolescents were told to lie down with their eyes open, gazing at the fixation cross shown on an adjustable

binocular system, VisualSystem (NordicNeuroLab). Both the adolescents born VPT and the controls were imaged the year they turned 13. Fixed orthodontic appliances were removed and replaced during the scanning visit for patient security and to minimize ferromagnetism-related artifacts.

Three imaging protocols were used for the clinical assessment and pathology classification. The imaging parameters of the T1- and T2-weighted and FLAIR images are shown in Table 1 for term age and in Table 2 for 13 years of age.

An experienced neuroradiologist assessed the comprehensive MRI according to a classification shown in Figure 6. The supervising professor Riitta Parkkola assessed the images at both age points. She was blinded to the clinical status of the infant/adolescent at both age points and also to the results at term age when assessing the images at 13 years of age. The MRI imaging session (total duration 1.5–2 h) was monitored and guided through by one of two PhD students, Karoliina Uusitalo (MD, PhD student) and Katri Lahti (MD, PhD student) or a research assistant, Jere Jaakkola (BM, during years 2016 and 2017). Katri Lahti also manually corrected the Freesurfer-analysis if needed.

| | |
|--------------------------|--|
| Normal findings | Normal brain signal intensity Normal anatomy of the cortex and cortical gyration pattern, basal ganglia and thalami, posterior limb of internal capsule, WM, germinal matrix, CC, cerebellum, pons and medulla oblongata A width of extracerebral space of less than 5 mm A ventricular/brain ratio of less than 0.35 |
| Minor pathologies | The consequences of IVH of grades 1 and 2, such as minor linear T2 hyperintensities of the caudothalamic grooves or caudothalamic groove cysts smaller than 3 mm A width of the extracerebral space of 5 mm A ventricular/brain ratio of 0.35 |
| Major pathologies | The consequences of IVH of grades 3 and 4 Cystic or cystic and hemorrhagic lesions of the cortex, basal ganglia, thalamus, internal capsule, CC, cerebellum or WM Focal T1 hyperintensities of deep or periventricular WM corresponding to gliosis Increased width of extracerebral space by >5 mm A ventricular/ brain ratio of >0.35 Ventriculitis Focal infarctions |

Figure 6. The classification of pathological brain findings in comprehensive brain MRI.

Table 1. The imaging parameters of the basic anatomical sequences at term-equivalent age.

| SEQUENCE | T1 TSE | T2W TSE | FLAIR |
|-------------------------|-------------------------------|------------------|--------------|
| ORIENTATION | Axial | Axial & Sagittal | Coronal |
| FIELD OF VIEW (MM X MM) | 200 x 200 | 200 x 200 | 180 x 180 mm |
| VOXEL SIZE (MM X MM) | 0.78 x 0.78 | 0.78 x 0.78 | 0.70 x 0.70 |
| SLICE THICKNESS (MM) | 4 | 4 | 4 |
| REPETITION TIME (MS) | 494–565 | Varying | 3500 |
| ECHO TIME (MS) | 14 | 120 | 15 |
| INVERSION DELAY (MS) | - | - | 400 |
| DURATION | Total scan time 14 min 54 sec | | |

Table 2. The imaging parameters of the basic anatomical sequences at 13 years of age.

| SEQUENCE | 3D T1 TFE | T2W TSE | FLAIR |
|-------------------------|--------------|-------------|--------------|
| ORIENTATION | Sagittal | Axial | Coronal |
| FIELD OF VIEW (MM X MM) | 256 x 265 | 230 x 179.8 | 203 x 183 |
| VOXEL SIZE (MM X MM) | 1 x 1 | 0.45 x 0.45 | 0.45 x 0.45 |
| SLICE THICKNESS (MM) | 1 | 3 | 4 |
| PARALLEL FACTOR | 2 | - | - |
| REPETITION TIME (MS) | 8.1 | 3000–5000 | 10 000 |
| ECHO TIME (MS) | 3.7 | 80 | 125 |
| FLIP ANGLE | 7 degrees | - | - |
| INVERSION DELAY (MS) | - | - | 2800 |
| DURATION | 4 min 23 sec | 2 min 7 sec | 3 min 30 sec |

4.3.2 Diffusion-weighted imaging

DWI was performed at both age points. The DWI at term age was only performed on infants born VPT. At 13 years of age, both the adolescents born VPT and the controls were imaged. The data of adolescents born VPT was not used in study II. The imaging parameters for both ages are shown in Table 3.

Table 3. The imaging parameters of the diffusion sequences.

| SEQUENCE | DWI AT TEA | DWI AT 13 | DWI AT 13 (TOP UP) |
|-------------------------------|-----------------|---------------|--------------------|
| ORIENTATION | Axial | Axial | Axial |
| FAT SHIFT | | Posterior | Anterior |
| FIELD OF VIEW (MM X MM) | 200 x 200 | 256 x 256 | 256 x 256 |
| VOXEL SIZE (MM X MM) | 0.78 x 0.78 | 2 x 2 | 2 x 2 |
| SLICE THICKNESS (MM) | 5 | 2 | 2 |
| BETWEEN SLICE GAP (MM) | 1 | 0 | 0 |
| PARALLEL FACTOR | 2 | 3 | 3 |
| REPETITION TIME (MS) | 2264 | 9950 | 9950 |
| ECHO TIME (MS) | 68 | 90 | 90 |
| BAND WIDTH (HZ) | 2195 | 1786.9 | 1786.9 |
| EPI FACTOR | 47 | 45 | 45 |
| B-VALUES (S/MM ²) | 0, 600 and 1200 | 0 and 1000 | 0 and 1000 |
| DIRECTIONS | 15 | 63 | 6 |
| DURATION | 2 min 24 sec | 10 min 56 sec | 30 sec |

4.3.2.1 Analysis at TEA

The data were automatically processed using manufacturer software PRIDE V4 Fiber Tracking 4.1 beta 4 (Philips Medical Systems). The software used only b-values 0 and 600. The program performed the DTI fitting automatically, creating the finalized color-encoded fractional anisotropy maps. All ROIs were not measurable in all infants due to motion artifacts, and the size and placement of ROIs were based on the anatomical structures.

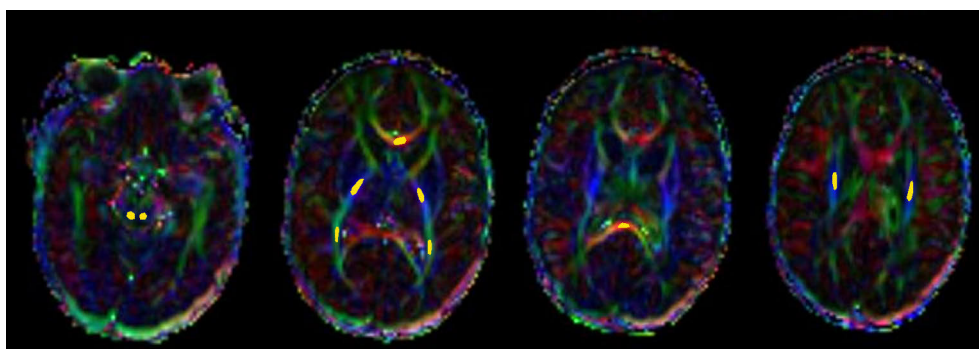


Figure 7. The regions-of-interest used at term equivalent age, marked with yellow: the colliculus inferior in the first, the anterior corpus callosum, posterior part of the capsula interna and optic radiations in the second, the posterior corpus callosum in the third and the corona radiata in the fourth picture. Modified from original publication I.

FA and MD values were measured from the genu and splenium of the CC, the posterior part of the internal capsule (PLIC), the corona radiata (CR), the optic radiation (OR) and the colliculus inferior (CI). The selected ROIs shown in Figure 7 are clearly recognizable in the anatomical images, and they have only a limited amount of crossing tracts that could interfere with the measurements. A detailed description of the ROIs and the reproducibility of the measurements in this cohort have previously been published in Lepomäki et al (Lepomäki et al., 2012).

4.3.2.2 Analysis at 13 years of age

Volumes with imaging artefacts, such as severe signal loss, were removed with DTIPrep (Oguz et al., 2014). The data were corrected for eddy current and motion artifacts. Data were accepted to the study if 30 or more volumes were of acceptable quality (Jones, 2004). Volume count varied from 39 to 62. B0-images were visually inspected for both DW sequences. After visual inspection, no data had to be removed. The susceptibility artifacts were corrected using the top-up technique of FMRIB Software Library v5.0.7 (Woolrich et al., 2009). The top-up technique requires the collection of two diffusion data sets with reversed phase encoding blips that create two oppositely distorted sets of images, from which the susceptibility can be estimated (Andersson et al., 2003; Smith et al., 2004). The FA and MD maps were calculated by fitting a tensor model to the raw diffusion data using FMRIB's Diffusion Toolbox.

The anatomical data was analyzed and visually inspected using Freesurfer version 5.3.0 (Desikan et al., 2006; Fischl, 2012). The data was manually corrected using white matter corrections, pial surface corrections and control points as needed. The FA maps were registered to the anatomical images by using Freesurfer's `tkregister2` tool (Freesurfer data to structural space) and FMRIB's Linear Image Registration tool. This allowed data transfer between Montreal Neurological Institute space of the Freesurfer parcellation and the diffusion space.

The posterior, mid posterior, central, mid anterior, and anterior areas of the CC were included in the seed regions for the CC tractography. Automatic cortical parcellation and labeling of the anatomical data was used, and tracking was restricted by using the brain stem as an avoid mask. The Desikan-Killiany Atlas (Desikan et al., 2006) was used to select seed areas for craniocaudally oriented tracts representing motor corticospinal / pyramid tracks. The brain stem was used as a seed area, and tracking was restricted using the corpus callosum and cerebellum white matter as avoid masks. Seeds for the cingulum were taken from the Desikan-Killiany-Trouville atlas (Klein et al., 2012). The rostral anterior cingulate, caudal anterior cingulate, posterior cingulate, isthmus cingulate and parahippocampal cortex were used as surface masks.

Tracking was done bilaterally using the probtrackx2 tool and its default settings (Behrens et al., 2003; Behrens et al., 2007). The fiber length distribution was calculated and saved as histogram data with 500 bins using fsf tools. The tracts were then transferred to the diffusion space, thresholded, binarized and used as masks. The FA and MD values were read. Parametric maps were calculated both for cases with and without susceptibility corrections. Both DTI analyses, at term and at 13 years of age, were performed by docent Virva Saunavaara.

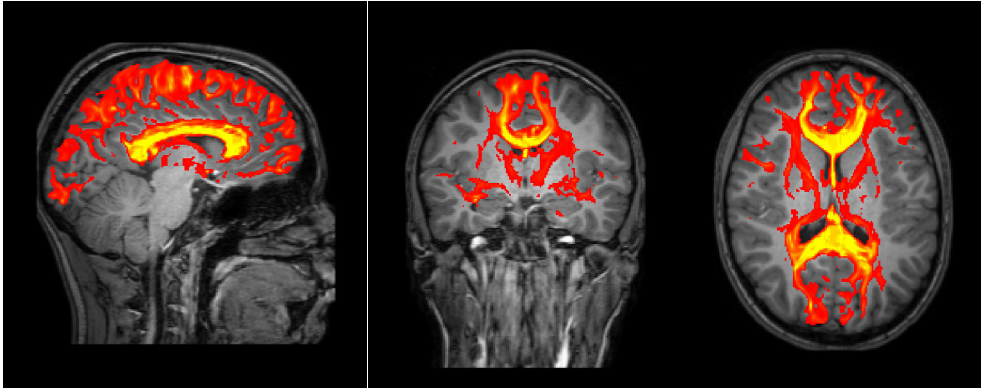


Figure 8. The corpus callosum in sagittal, coronal, and transversal plain shown in yellow-red scale, where the central parts of corpus callosum are seen in yellow.

4.3.3 Resting state functional MRI at 13 years of age

The imaging parameters for rsfMRI are shown in Table 4. Before the resting state series, the subjects were instructed to relax with their eyes closed and without thinking about anything special.

Table 4. The imaging parameters for rsfMRI.

| SEQUENCE | ORIENTATION | FIELD OF VIEW (MM X MM) | VOXEL SIZE (MM X MM) | SLICE THICKNESS (MM) | PARALLEL FACTOR | REPETITION TIME (MS) | ECHO TIME (MS) | FLIP ANGLE (DEGREES) | BAND WIDTH (HZ) | DURATION |
|------------|-------------|----------------------------|-------------------------|-------------------------|--------------------|-------------------------|----------------|-------------------------|--------------------|---------------|
| GE- EPI | Axial | 240 x 240 | 3 x 3 | 4 | 2 | 2000 | 20 | 75 | 2692.6 | 7min 48sec |

Processing of the structural and functional MRI data

The preprocessing steps were performed with Matlab-based Statistical Parametric Mapping (SPM12, Wellcome Department of Cognitive Neurology, London, UK; <http://www.fil.ion.ucl.ac.uk/spm>) (Tzourio-Mazoyer et al., 2002). Structural images were segmented and spatially normalized using a customized sample-specific template providing individual normalized gray matter, white matter, and cerebrospinal fluid images in the Montreal Neurological Institute coordinate space, as well as a set of individual deformation fields.

Six starting volumes were rejected to allow T1 equilibration and subject state stabilization, resulting in 228 volumes. The fMRI data of each subject were corrected for slice-timing difference and head motion. Subjects exceeding 0.2 mm translational or 0.2-degree rotational mean between-scan motion were rejected.

Additional denoising steps were performed in order to clean the data from artefacts.

1. The voxel time series were despiked after masking out non-brain voxels. (A. X. Patel et al., 2014)
2. Linear trends, motion-related signals and its first-order derivatives and regressors for outlier scans (>4 SD in global signal, between volume motion > 3 mm in translation or 1 degree rotation) were rejected. (Conn toolbox) (Whitfield-Gabrieli et al., 2012).
3. The principal components of the WM and CSF signals were extracted and regressed out (CompCor approach) (Behzadi et al., 2007).
4. The time series were band-pass (0.01 – 0.1 Hz) filtered.

Independent component analysis and static FNC analysis

The mean intensity over time was removed for each voxel within the brain mask. Spatial ICA was then performed on the preprocessed and denoised fMRI data with the Group ICA for fMRI Toolbox (GIFT v3.0b; <http://trendscenter.org/software>) (Calhoun et al., 2001). A total of 25 ICs with independent spatial maps and temporal courses were extracted and thereafter reconstructed (Kiviniemi et al., 2009). After defining the main maxima for each IC, only the components with maxima in the GM, clear frequency maxima within the 0.01–0.1 Hz range, and only negligible spatial overlap with non-GM areas were accepted as parts of the known RSNs (Griffanti et al., 2017). Subject-specific mean sFNC matrices were computed and group difference was estimated at each voxel with multivariate statistics. A schematic drawing of the ICA is shown in Figure 9.

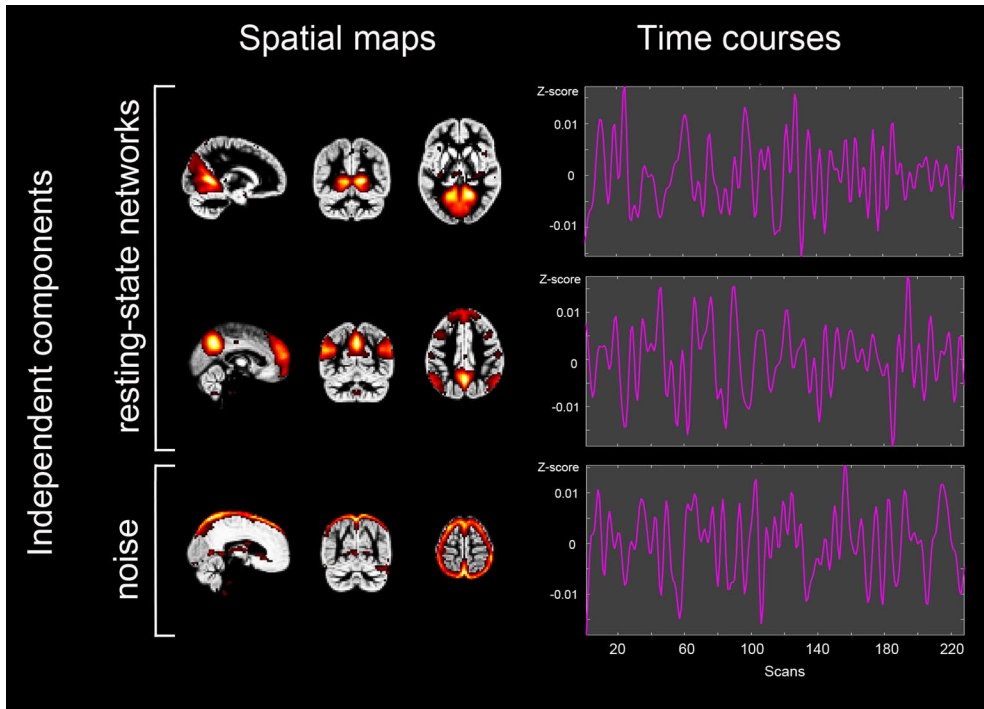


Figure 9. An example of the spatial activation of the resting state network and their related time courses separated using independent component analysis. The last row shows the noise excluded from the analysis. The figure was made by and published with the permission of Victor Vorobyev.

Dynamic FNC analysis

Dynamic connectivity was examined in two ways, using both a standard native-space approach and the meta state approaches, both incorporated in the Temporal dFNC toolbox in GIFT (Allen et al., 2014; Miller et al., 2016). As the first step, both analyses started from the extraction of wFNCs. The pair-wise correlations between the RSNs were computed using a sliding rectangular window of 30 TR (60 s) length in steps of 1 TR, yielding 198 wFNCs for each of 153 pair correlations per subject (Hindriks et al., 2016).

In the nsFNC (Allen et al., 2014), using k-means clustering, the wFNCs were replaced with four stable prototype connectivity states. First, the cluster centroids were identified on a subset of subjects with maximal FC variance. These were used as starting points to cluster each wFNC to one of the four reoccurring FNC states. The number of the FNC states was determined by the elbow criterion. A minimum threshold of 10 windows was applied for the given FNC matrixes. To analyze the temporal fluctuation in the nsFNC, a dwell time and fraction rate were calculated. Dwell time was characterized as the average continuous time period spent by the

subjects in each of the states. The fraction rate is a percentage of the total scan time that a subject spent in a particular state.

The second approach was msFNC (Miller et al., 2016). In this approach, each wFNC was replaced by a set of relatively independent connectivity patterns which are shared across the subjects' prototype connectivity patterns. The connectivity patterns are weighted according to their contribution to each wFNC. We used k-means clustering to create a vector of five distinct connectivity patterns thus obtained a 5-dimensional characterization of each subject's 153-dimensional (number of pair combinations for 18 IC time courses) structure in each of 198 windows. Each discretized vector of connectivity pattern weights forms a meta-state. Meta-state dynamism was characterized by calculating four metrics expressing fluidity and range. Thus, fluidity was measured as the total number of distinct meta states visited by a subject and as the number of times the subject switched between meta-states during the scan time. Range, in turn, was described by meta state span, i.e., a measure of maximal distance in the L1-space between visited meta-states, and by total distance, a sum of all distances between successively visited meta states.

Additional native-space and meta-state analyses were performed using different window sizes and numbers of connectivity patterns to check the consistency of the results. The additional window lengths were 44 s and 50 s (Allen et al., 2014; Hindriks et al., 2016; Miller et al., 2016). The four connectivity states were used for all three window lengths. Meta state FNC was additionally tested with 4 and 6 connectivity patterns while keeping the window equal to 60 s. The schematic drawing of the main dFNC analysis is shown in Figure 10.

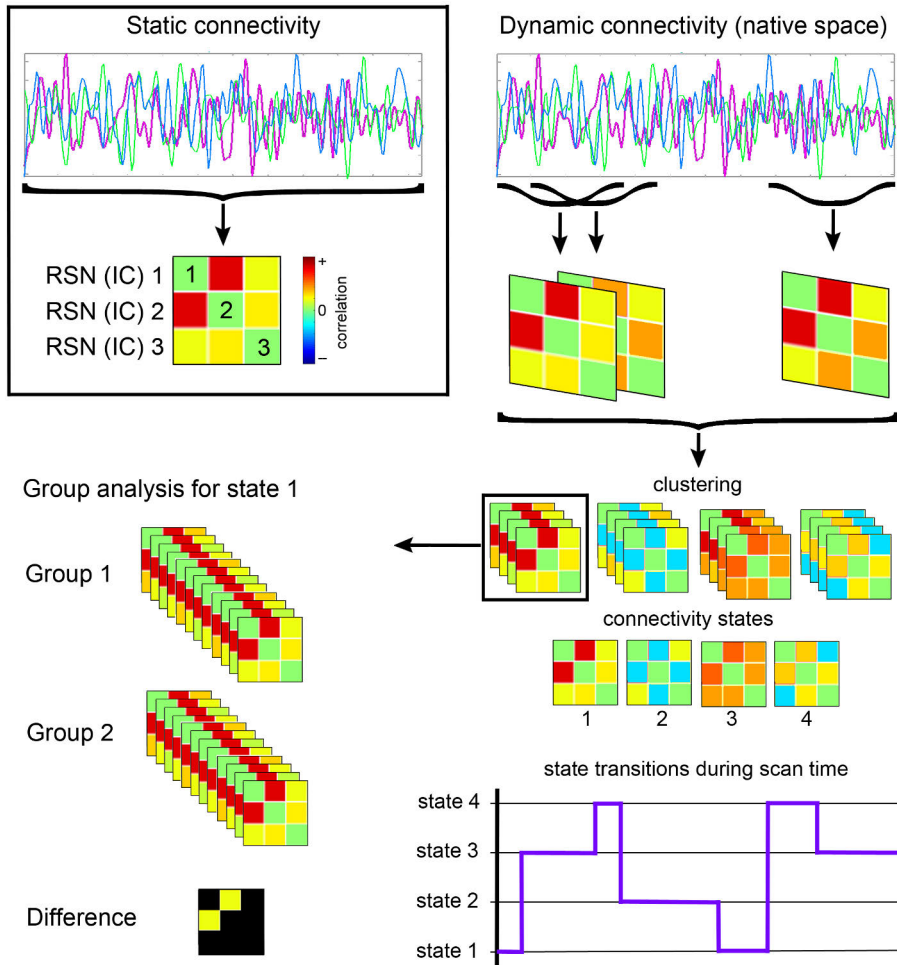


Figure 10. In static connectivity analysis, the measured activation is averaged over the scanning time. Dynamic connectivity is analyzed using two different methods after k-means clustering. The native-state analysis compares the clustered states and times spent in each state. The meta-state analysis assesses the transitions between the different connectivity states. The figure is made by and published with the permission of Victor Vorobyev.

4.3.4 Statistical methods

4.3.4.1 Study I

The MABC-2 scores, DTI metrics and gestational age were used as continuous variables characterized by means or medians and their minimums and maximums. Regardless of this, the mean values were completed with standard deviations. The MRI findings and SGA status were used as categorical variables and characterized using frequencies. Regression analysis was used to study univariate associations between the DTI metrics and MABC-2 standard scores.

The associations between the DTI metrics and MABC-2 standard scores were further studied using multiple regression analysis while controlling for gestational age, SGA status and findings in the comprehensive brain MRI. The statistical analyses were performed by a biostatistician. SAS (SAS Institute Inc) version 9.4 for Windows was used for the analyses. Statistical significance was defined as a P-value < 0.05.

4.3.4.2 Study II

The statistical analyses were performed by a physicist using R studio 3.5.1. Both the DTI metrics and histogram data were used as continuous variables. The tractography parameters were assessed using the non-compartmental analysis. The total length of the tract was defined using a probability density function of the found tracts shown by area under curve (AUC).

The agreement of the two analysis pipelines was checked using Bland–Altman plots (BlandAltmanLeh package). The differences between the methods were evaluated using the bias i.e. mean difference and 1.96 standard deviations above and below the bias. The normality of the bias distribution was tested with the Shapiro–Wilk test. The paired t-test and Wilcoxon signed rank test were used for normally and non-normally distributed data, respectively, to further evaluate the statistical significance of the bias between the full and partial analyses. To analyze whether the bias depended on the mean value of the measured parameter, a linear regression model was adjusted between the parameter means and the bias.

4.3.4.3 Study III

In the third study, the statistical analyses were linked to the different methodological approaches. The significance threshold was set at $p < 0.05$ and in the dynamic analyses, a false discovery rate (FDR) correction was used. The statistical analyses were performed by the physicist responsible for the imaging analyses.

- sFNC: Subject-specific mean sFNC matrices were computed and estimated at each voxel with multivariate analysis using the MANCOVAN toolbox. (Allen et al., 2011)
- nsFNC: Two-sample t-tests on the group medians of correlation were performed within each state to investigate group differences. A two-sample t-test was also used when assessing dwell time and fraction rate.
- msFNC: Two-sample t-tests were performed for all four meta-state metrics: 1. the number of switches from one meta-state to another 2. the number of distinct meta-states subjects occupied during scan time 3. the largest span (distance) between the occupied meta-states 4. the overall distance travelled by the subject through state space (the sum of all distances between successive meta-states). In all FNC analyses, the significance threshold was set at $p < 0.05$ and a false discovery rate (FDR) correction was used. The statistical analyses were performed by a brain image analyst.

5 Results

5.1 Participants

5.1.1 Participants born very preterm (studies I and III)

A total of 146 infants born very preterm fulfilling the inclusion and exclusion criteria of this study were born in the catchment area of Turku University Hospital during April 2004–2006. All infants born after a gestational age of ≥ 32 weeks were excluded from study I to allow comparison with previous studies. The flow chart of Studies I and III is shown in Figure 11. Table 5 presents the neonatal characteristics of the children and adolescents born very preterm.

Table 5. The background characteristics of the participants born very preterm.

| | STUDY I | STUDY III |
|---|------------------------|------------------------|
| STUDY GROUP | N=37 (27 boys) | N=24 (14 boys) |
| Gestational age, mean, [range] | 29+4, [24+5, 31+6] | 28+5 [24+0, 33+0] |
| Birth weight, median, [range] | 1370 g [620 g, 2120 g] | 1165 g [730 g, 1940 g] |
| BACKGROUND | (YES/NO/MISSING) | (YES/NO/MISSING) |
| SGA status (BW <-2 SD) | 9 / 28 / 0 | 8 / 16 / 0 |
| Antenatal steroids | 36 / 1 / 0 | 23 / 1 / 0 |
| Cesarean section | 24 / 13 / 0 | 16 / 8 / 0 |
| Multiples | 14 / 23 / 0 | 9 / 15 / 0 |
| NEC¹ | 2 / 33 / 2 | 0 / 23 / 1 |
| Sepsis or meningitis² | 4 / 33 / 0 | 1 / 23 / 0 |
| BPD³ | 3 / 34 / 0 | 2 / 22 / 0 |
| PARENTAL EDUCATION ($\leq 12 / > 12$Y) | ($\leq 12 / > 12$ Y) | ($\leq 12 / > 12$ Y) |
| Fathers | 23 / 12 / 2 | 12 / 10 / 2 |
| Mothers | 11 / 26 / 0 | 8 / 16 / 0 |
| FSIQ AT 11 YEARS | | |
| Median (SD) | 88.5 (15.0) | 92.0 (15.6) |
| FSIQ<70 | 33 / 4 / 0 | 2 / 21 / 1 |

¹Necrotizing enterocolitis (NEC), surgical treatment

²Cerebrospinal fluid or blood culture positive

³Bronchopulmonary dysplasia (BPD) requiring additional oxygen at 36 weeks postmenstrual age

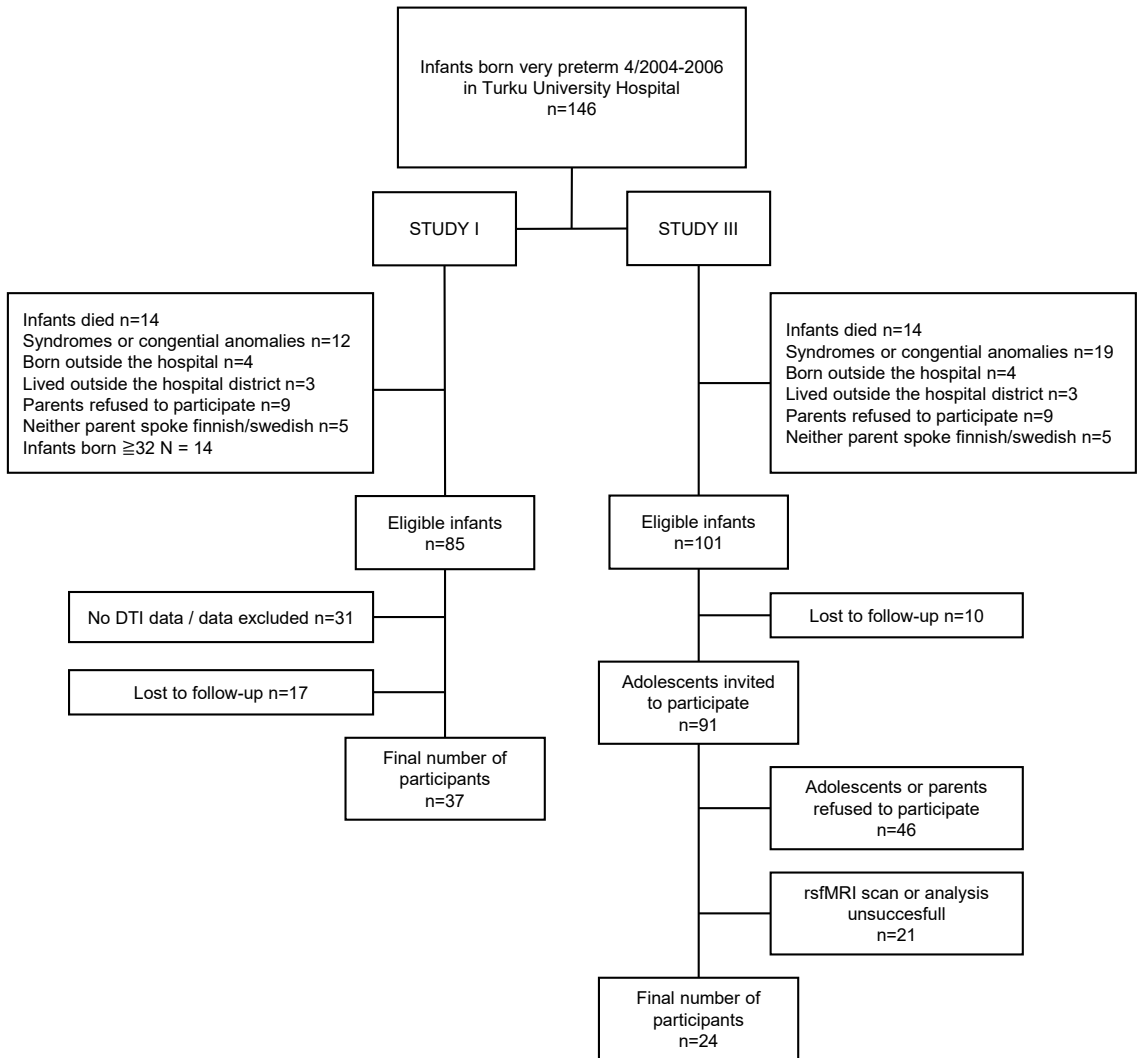


Figure 11. The flow chart of the participants of Study I and III.

5.1.2 Participants born at term (study II and III)

Of the original 97 controls recruited at the maternity ward during 2003–2004, 15 were lost during follow-up. Of the remaining 82 adolescents, 52 did not participate due to the adolescent’s refusal to participate at the age of 13 years or due to the parents withdrawing from the study in an earlier phase of this follow-up study. The controls did not differ from the preterm adolescents in terms of gender distribution or parental education.

Only the controls were included in Study II, which assessed the effect of susceptibility correction. Thirty controls attended the MRI imaging the year they

turned 13. Two of the adolescents were excluded due to failure in DWI and one due to incidental findings in frontal white matter. The mean age of the successfully imaged adolescents (18 boys) was 12.7 years (SD 0.27). None of the participants were diagnosed with neurological or psychiatric disorders at the time of scanning.

5.2 DTI at term and motor outcome at 11 years of age

A total of 37 children had both DWI successfully acquired at term and a MABC-2 assessment completed at 11 years of age. One of these children was unable to complete the balance section of the assessment due to post-surgical state. The MABC-2 scores are shown in Table 6. Eight children (22.2%) scored five or less in standard scores equaling fifth percentile or below and were diagnosed with DCD. Six children (16.7%) were considered to be at risk for motor deficits, scoring six in standard scores equaling percentiles 6–14. Twenty-two children (61.1%) reached a standard score above 7, equaling >15th percentile, which is considered as normal motor development.

Table 6. The median MABC-2 scores and their range in both standard scores and percentiles.

| DOMAIN | STANDARD SCORE | PERCENTILE |
|---------------------|----------------|-------------|
| Manual dexterity | 8.0 [4-12] | 25 [2-75] |
| Aiming and catching | 9.0 [3-15] | 37 [1-95] |
| Balance | 9.0 [2-14] | 37 [0.5-91] |
| Total | 8.5 [2-12] | 31 [0.5-75] |

A statistically significant association between FA and MABC-2 scores was found in univariate analysis in the CC splenium, left CR and right OR. The association remained significant for the left CR and right OR after controlling for confounding factors (MRI classification, SGA status and GA). An association between MD and MABC-2 scores was found in the genu of the CC. The association remained significant when controlling for confounding factors. The association between MD and MABC-2 scores in the left CR became significant in the multivariate model. The associations were positive for FA and negative for MD values. The DTI metrics and their univariate and multivariate correlations with the MABC-2 total scores are shown for FA in Table 7 and for MD in Table 8.

Table 7. Mean FAs (SD) at term-equivalent age for infants born preterm and univariate and the multivariate estimates and *p-values* for associations with MABC-2 scores at 11 years of age. The estimates are shown as change in MABC-2 standard scores when FA increases with 0.1. The significant ones **bolded**.

| REGION-OF-INTEREST | FRACTIONAL ANISOTROPY | | ASSOCIATION BETWEEN FA AND MABC-2 TOTAL SCORE | | | |
|--------------------|-----------------------|--------------|---|--------------|--------------|--------------|
| | All | DCD | Univariate | | Multivariate | |
| CC, GENU | 0.45, (0.08) | 0.43, (0.13) | 0.494 | <i>0.433</i> | 0.705 | <i>0.347</i> |
| CC, SPLENIUM | 0.52, (0.10) | 0.46, (0.15) | 0.921 | 0.049 | 0.883 | <i>0.076</i> |
| PLIC, RIGHT | 0.47, (0.06) | 0.48, (0.03) | 0.419 | <i>0.651</i> | 0.405 | <i>0.688</i> |
| PLIC, LEFT | 0.50, (0.06) | 0.52, (0.04) | 0.233 | <i>0.803</i> | 0.139 | <i>0.889</i> |
| CI, RIGHT | 0.38, (0.05) | 0.37, (0.06) | 0.896 | <i>0.379</i> | 0.805 | <i>0.459</i> |
| CI, LEFT | 0.39, (0.05) | 0.37, (0.07) | 1.162 | <i>0.260</i> | 0.970 | <i>0.381</i> |
| CR, RIGHT | 0.41, (0.08) | 0.40, (0.08) | 0.787 | <i>0.258</i> | 1.080 | <i>0.130</i> |
| CR, LEFT | 0.40, (0.08) | 0.36, (0.06) | 1.382 | 0.035 | 1.655 | 0.014 |
| OR, RIGHT | 0.37, (0.05) | 0.33, (0.06) | 2.388 | 0.017 | 3.023 | 0.006 |
| OR, LEFT | 0.37, (0.05) | 0.35, (0.06) | 1.067 | <i>0.243</i> | 1.657 | <i>0.098</i> |

Table 8. Mean MDs (SD) at term (TEA) for infants born preterm and the univariate and multivariate estimates and *p-values* for associations with MABC-2 scores at 11 years of age. The estimates are shown as change in MABC-2 standard scores when MD increases with 0.1. The significant ones **bolded**.

| REGION-OF-INTEREST | MEAN DIFFUSIVITY (x10 ⁻³ MM ² S ⁻¹) | | ASSOCIATION BETWEEN MD AND MABC-2 TOTAL SCORE | | | |
|--------------------|---|--------------|---|--------------|---------------|--------------|
| | All | DCD | Univariate | | Multivariate | |
| CC, GENU | 1.41, (0.13) | 1.48, (0.13) | -1.029 | 0.005 | -1.217 | 0.002 |
| CC, SPLENIUM | 1.44, (0.35) | 1.56, (0.48) | -0.154 | <i>0.274</i> | -0.109 | <i>0.491</i> |
| PLIC, RIGHT | 1.02, (0.07) | 1.02, (0.06) | -0.630 | <i>0.407</i> | -0.698 | <i>0.369</i> |
| PLIC, LEFT | 1.03, (0.07) | 1.02, (0.07) | -0.998 | <i>0.147</i> | -1.078 | <i>0.126</i> |
| CI, RIGHT | 1.03, (0.08) | 1.01, (0.08) | 0.006 | <i>0.993</i> | -0.222 | <i>0.738</i> |
| CI, LEFT | 1.01, (0.08) | 0.97, (0.05) | 0.459 | <i>0.458</i> | 0.401 | <i>0.539</i> |
| CR, RIGHT | 1.09, (0.10) | 1.10, (0.08) | -0.667 | <i>0.231</i> | -0.962 | <i>0.094</i> |
| CR, LEFT | 1.11, (0.12) | 1.13, (0.08) | -0.843 | <i>0.068</i> | -1.003 | 0.030 |
| OR, RIGHT | 1.36, (0.23) | 1.38, (0.32) | -0.880 | <i>0.681</i> | -0.059 | <i>0.804</i> |
| OR, LEFT | 1.34, (0.22) | 1.34, (0.23) | -1.459 | <i>0.512</i> | -0.079 | <i>0.733</i> |

5.3 Impact of susceptibility correction on DTI and tractography parameters at 13 years of age

Study II shows that there is a significant difference between the susceptibility-corrected and uncorrected measures in both diffusion metrics (FA and MD) and tract lengths. The findings are systematically present in all the measured tracts. The *p*

values for the CC, CST, right cingulum, and left cingulum are ≤ 0.001 for both diffusion metrics. The mean values for both corrected and uncorrected data, biases between the pathways and estimated MD and FA of the tracts, both for corrected and uncorrected data, are shown in Table 9 and Table 10.

The bias between the pathways is higher in conjunction with higher MD values. This is seen when the linear regression model is adjusted. The Bland—Altman plots and linear regression models in Figure 12 show a significant positive association between the bias and the mean MD value in the CC ($p=0.02$, $\text{adj.R}^2=0.1665$), right cingulum ($p=0.007$, $\text{adj.R}^2=0.2267$) and left cingulum ($p=0.02$, $\text{adj.R}^2=0.1760$). None of the FA measurements show a similar association, meaning that the bias is not related to the mean FA value.

In tractography measurements, the AUC represents the length distribution of the tracts. The tracts appeared longer in the corrected analysis. The bias between the pathways is statistically significant in the CC ($p=0.004$) and CST ($p=0.007$) and the bias of tract length is associated with the mean tract length in both, with p values of $p=0.011$ ($\text{adj.R}^2=0.1997$) and $p=0.014$ ($\text{adj.R}^2=0.1889$), respectively. All biases (corrected – uncorrected) between the pathways, the p values of the biases, and the p values and estimates for all regression analyses are shown in Table 11.

Table 9. Mean diffusivity in uncorrected and corrected data, bias between the pathways, the p values of the biases, the estimates and their p values for the regression analyses.

| MD | UNCOR MEAN (SD) | COR MEAN (SD) | BIAS (COR-UNCOR) MEAN [RANGE] | DIFF P | EST | REGR P |
|-----|-----------------|---------------|-------------------------------|----------|--------------|---------------|
| CC | 1.00, (0.03) | 0.97, (0.03) | 0.012 [0.006, 0.02] | < 0.0001 | $5.25e^{-2}$ | 0.0198 |
| CST | 1.05, (0.05) | 1.07, (0.05) | 0.026 [-0.0001, 0.05] | < 0.0001 | $3.78e^{-2}$ | 0.498 |
| RC | 0.94, (0.03) | 0.95, (0.03) | 0.015 [0.002, 0.03] | < 0.0001 | $10.3e^{-2}$ | 0.007 |
| LC | 0.95, (0.04) | 0.97, (0.04) | 0.0133 [0.003, 0.02] | < 0.0001 | $5.78e^{-2}$ | 0.0169 |

Table 10. Fractional anisotropy in uncorrected and corrected data, bias between the pathways, the p values of the biases, estimates and their p values for the regression analyses.

| FA | UNCOR MEAN (SD) | COR MEAN (SD) | BIAS (COR-UNCOR) MEAN [RANGE] | DIFF P | EST | REGR P |
|-----|-----------------|---------------|-------------------------------|---------------|--------|--------|
| CC | 0.34, (0.01) | 0.339, (0.01) | -0.0018 [-0.007, 0.003] | 0.0006 | -0.026 | 0.947 |
| CST | 0.35, (0.01) | 0.344, (0.01) | -0.0015 [-0.006, 0.003] | 0.0014 | 0.391 | 0.258 |
| RC | 0.27, (0.01) | 0.267, (0.01) | -0.0050 [-0.01, 0.004] | < 0.0001 | -0.916 | 0.286 |
| LC | 0.27, (0.01) | 0.339, (0.01) | -0.0034 [-0.01, 0.005] | 0.0002 | -0.107 | 0.868 |

Table 11. Bias (corrected – uncorrected) in the area under curve, the p values of the biases, estimates and their p values for the regression analyses.

| AUC | BIAS (COR-UNCOR) | DIFF P | ESTIMATE | REGR P |
|---------------------|-----------------------|---------------|----------|---------------|
| CORPUS CALLOSUM | 17700 [-39800, 72500] | 0.0043 | 0.117 | 0.0113 |
| CORTICOSPINAL TRACT | 18300 [-45300, 82000] | 0.0069 | 0.126 | 0.0136 |
| RIGHT CINGULUM | 2240 [-48400, 52900] | 0.6617 | 0.0084 | 0.845 |
| LEFT CINGULUM | 2730 [-59700, 65200] | 0.8593 | 0.090 | 0.0674 |

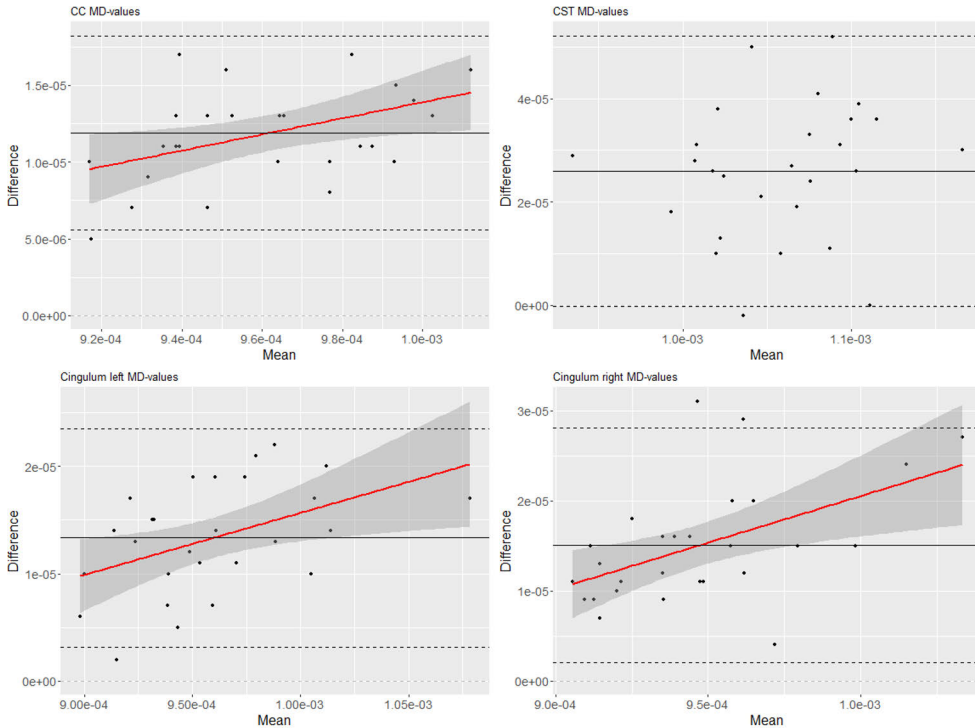


Figure 12. The Bland–Altman plots and linear regression models with a significant positive association between the bias and the mean diffusivity value. From Original publication II.

5.4 Resting state fMRI in preterm children at 13 years of age

In Study III, the nsFNC activation patterns were equal in the adolescents born preterm and the controls. The temporal dynamics, however, differed statistically significantly in both the nsFNC and msFNC approaches. The findings were similar in the whole samples of the adolescents born VPT and the controls, as well as in

control analyses where adolescents with ADHD (1 VPT, 1 control) and cognitive impairment (2 VPT) were excluded.

Adolescents born VPT spent a significantly longer proportion of the total scan time in the least active nsFNC pattern ($p=0.0220$) than the term-born controls. The fraction rates were 60.0% and 40.2% for the VPT and control groups, respectively. The findings were similar in terms of dwell time, but after FDR correction they did not reach statistical significance ($p=0.065$). The nsFNC patterns of both groups are shown in Figure 13.

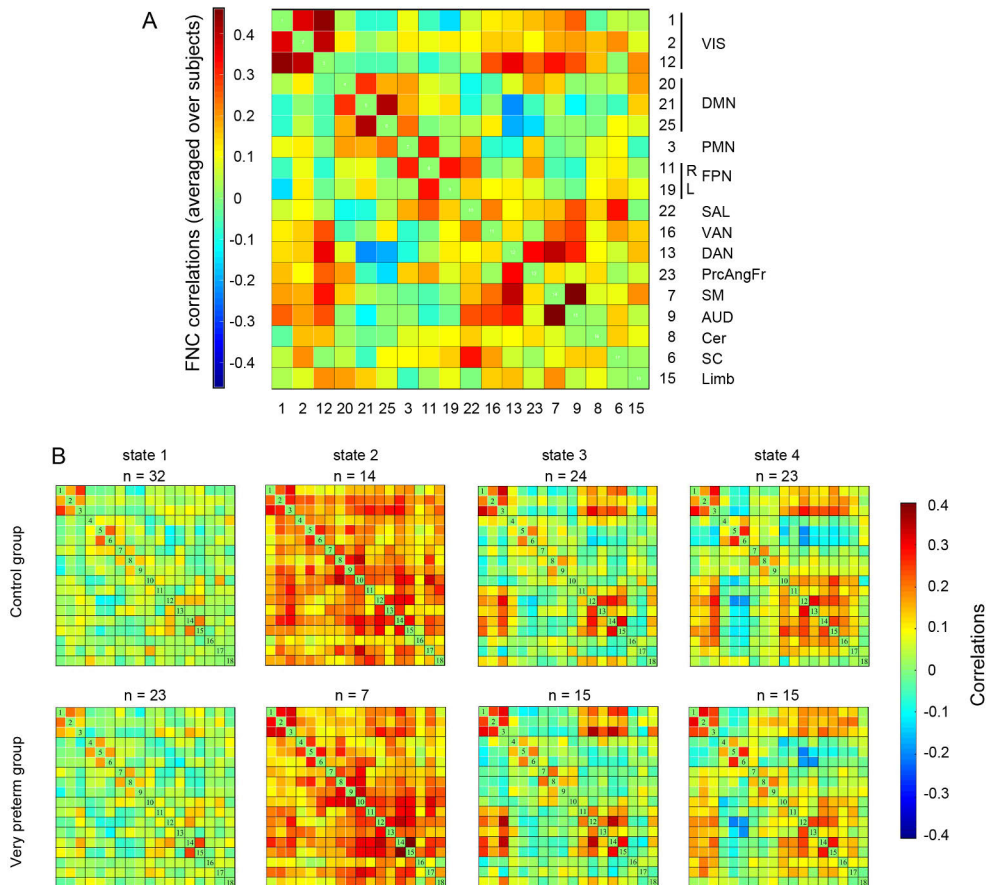


Figure 13. The native state functional network connectivity patterns in adolescents born very preterm and at term. From Original publication III.

The dwell times and fraction rates of both whole sample groups and exclusion groups are shown in Table 12 and Table 13. The state-wise p-values between both samples are shown in Table 14.

Table 12. State-wise mean dwell times (standard error of mean) in the whole sample of adolescents born very preterm and the term-born controls and the groups without adolescents with ADHD or cognitive impairment (VPT-E, CONTROLS-E).

| DWELL TIME | VPT | CONTROLS | VPT-E | CONTROLS-E |
|------------|--------------|--------------|--------------|--------------|
| State 1 | 59.4, (12.3) | 30.3, (4.35) | 57.2, (12.0) | 30.6, (4.49) |
| State 2 | 8.20, (3.87) | 9.71, (2.04) | 9.38, (4.37) | 9.92, (2.10) |
| State 3 | 12.3, (2.27) | 23.0, (4.91) | 14.9, (2.58) | 22.8, (5.07) |
| State 4 | 13.3, (2.81) | 19.2, (3.02) | 11.0, (2.21) | 18.8, (2.21) |

Table 13. State-wise mean fraction rates (standard error of mean) in the whole sample of adolescents born very preterm and term-born controls and the groups without adolescents with ADHD or cognitive impairment (VPT-E, CONTROLS-E).

| FRACTION RATE, % | VPT | CONTROLS | VPT-E | CONTROLS-E |
|------------------|--------------|--------------|--------------|--------------|
| State 1 | 60.0, (5.69) | 40.2, (4.14) | 61.3, (5.72) | 41.3, (4.20) |
| State 2 | 7.60, (3.90) | 7.59, (2.07) | 8.68, (4.42) | 7.77, (2.11) |
| State 3 | 15.6, (3.88) | 26.2, (4.21) | 17.7, (4.19) | 26.1, (4.34) |
| State 4 | 16.8, (4.20) | 26.0, (4.35) | 12.3, (2.44) | 24.9, (4.36) |

Table 14. FDR corrected p-values for the state-wise comparisons in dwell time and fraction rate between the full sample of adolescents born VPT and at term and the sample with adolescents with ADHD or cognitive impairment excluded (VPT-E, CONTROLS-E).

| | DWELL TIME P-VALUES | | FRACTION RATE P-VALUES | |
|---------|---------------------|---------------------|------------------------|---------------------|
| | VPT vs Controls | VPT-E vs Controls-E | VPT vs Controls | VPT-E vs Controls-E |
| State 1 | 0.0648 | 0.0864 | 0.0220 | 0.0224 |
| State 2 | 0.7143 | 0.9023 | 0,9991 | 0.8384 |
| State 3 | 0.1598 | 0.3040 | 0,1554 | 0.2523 |
| State 4 | 0.2304 | 0.1366 | 0,1916 | 0.0622 |

All meta-state metrics showed a statistically significant difference between the groups. The VPT group visited fewer connectivity patterns and switched between them fewer times (count 24.0, switches 41.9) than the controls (count 29.1, switches 46.8), $p=0.0251$ for both. The mean span between the connectivity patterns and the travelled overall distance during the scan time were also lower in the VPT group (span 7.45, distance 46.5) than in the controls (span 9.28, distance 53.0), $p=0.0116$ and 0.0251 respectively. The meta-state metrics of both the whole-sample groups and exclusion groups are shown in Table 15. The meta-state metrics of the VPT group and the term-born group are shown in Figure 14. The p-values between both samples are shown in Table 16.

Table 15. Meta-state metrics, mean (standard error of mean) in the whole sample of adolescents born very preterm and term-born controls and the groups without adolescents with ADHD or cognitive impairment (VPT-E, CONTROLS-E).

| META STATE METRICS | VPT | CONTROLS | VPT-E | CONTROLS-E |
|--------------------|--------------|--------------|--------------|--------------|
| Number | 24.0, (1.86) | 29.1, (1.33) | 22.7, (1.99) | 27.6, (1.43) |
| Switches | 41.9, (1.87) | 46.8, (1.20) | 40.6, (2.16) | 46.8, (1.40) |
| Mean span | 7.54, (0.37) | 9.28, (0.39) | 7.48, (0.45) | 9.13, (0.40) |
| Distance | 46.5, (2.39) | 53.0, (1.59) | 45.0, (2.58) | 52.2, (1.81) |

Table 16. The FDR corrected p-values for meta-state metrics between the full sample of adolescents born VPT and at term and the sample with adolescents with ADHD or cognitive impairment excluded (VPT-E, CONTROLS-E).

| META STATE METRICS | P-VALUES | |
|--------------------|-----------------|---------------------|
| | VPT vs Controls | VPT-E vs Controls-E |
| Number | 0.0251 | 0.0437 |
| Switches | 0.0251 | 0.0290 |
| Mean span | 0.0116 | 0.0380 |
| Distance | 0.0251 | 0.0288 |

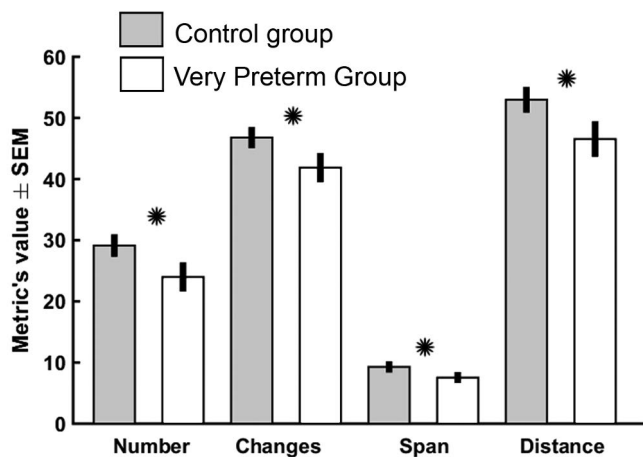


Figure 14. The meta-state metrics in adolescents born very preterm and at term. The statistically significant differences are marked with starts. From Original publication III.

6 Discussion

6.1.1 The vulnerability of the preterm brain

The prevalence of preterm birth is increasing globally (Blencowe et al., 2012). While major disabilities such as intellectual disability, cerebral palsy, blindness and deafness move towards the most extreme survivors with a GA of 23 to 25 weeks and a BW <800 g, the incidence of minor developmental deficits remains substantial (Cheong et al., 2017; Hintz et al., 2011). Infants born before 32 weeks of gestation or weighing below 1500 g are still at definite risk for developmental impairments affecting their quality of life and participation in society.

Very preterm birth has been associated with widespread alterations in the grey and white matter of the brain, which is referred to as the vulnerability of the preterm brain. The cellular-level findings include neuroinflammation, poor oligodendrocyte maturation, decreased axonal density and pruning and interneuron functional deficits. These cellular changes and their effects are, to some extent, measurable with the quantitative MRI approaches. Infants born VPT/VLBW show alterations in GM and WM volumes, global and tract specific diffusion metrics and differences in structural and functional connectivity. The same brain areas known to be affected in the preterm infants are reported to be associated with DCD, ADHD, ASD and social difficulties in the population as a whole.

This thesis studied associations between brain imaging and motor and behavioral outcomes in a regional longitudinal cohort of children and adolescents born VPT/VLBW in 2004 to 2006 in Turku University Hospital. In addition, the reliability and technical aspects of brain imaging in adolescence were assessed.

6.1.2 Predicting outcome from term to adolescence based on DWI modalities

Diffusion metrics are thought to reflect the maturation of the brain white matter, i.e., the integrity of the white matter (O'Donnell et al., 2011). Myelination mainly occurs after the period in which very preterm births occur, and it has been found to be altered in many conditions compromising adolescents born very preterm (Pandit et al., 2013).

6.1.2.1 Motor outcome in children without CP

This thesis showed an association between the diffusion metrics obtained at term age and the motor outcome at 11 years of age in pre-adolescents born with a VLBW. The FA of the left CR and right OR as well as the MD of the genu of the CC were associated with the MABC-2 scores after controlling for confounding factors. Better motor performance was seen in association with a higher FA and a lower MD.

The finding is in line with previous studies regarding the associations of FA values with later motor outcomes with a follow up of 18–24 months (De Bruïne et al., 2013; Duerden et al., 2015; Pannek et al., 2020; Rose et al., 2009, 2015). In addition, the left precuneus, right superior occipital gyrus, and right hippocampus have been suggested to predict motor development at 18–24 months in infants born with a VLBW (Schadl et al., 2018). Contrary to the results presented now, the FA of the PLIC has previously been associated with gait testing results in children born VPT/VLBW at the age of four (Rose et al., 2007).

Our results are also in line with the associations found in other cross-sectional designs in children and adolescents born VPT/VLBW or EPT/ELBW (Dewey et al., 2019; Groeschel et al., 2014, 2019; Kelly et al., 2015). The similarity of the associations found between diffusion metrics at term and the longitudinal outcome and the cross-sectional studies in childhood and adolescence indicates that the diffusion metrics capture adversities in the underlying white matter structures.

The FA value of the OR has not previously been associated with motor development in children or adolescent born VPT/VLBW or EPT/ELBW. A similar association has, however, been reported with visuo-motor performance. A lower FA of the OR was associated with poorer scores of copying tasks in the Beery-Buktenica Developmental Test of Visual-Motor Integration-V (Sripada et al., 2015). This could reflect the role of the visual dimension in accomplishing motor tasks, especially fine manipulation tasks (Henderson et al., 2007).

The previous literature regarding DWI metrics and motor outcome mainly shows associations between FA values and motor functioning. MD values have only been presented in a few previous studies. In addition to our finding of possible associations between MD values and motor outcome, a similar finding has been made by Pannek et al (2020). They assessed CSD-HARDI-based diffusion metrics at term and motor outcome with Bayley Scales of Infant and Toddler Development -III at two years of corrected age. The areas of the associations were, however, different. The MD in the bilateral posterior thalamic radiations, left retrolenticular part of the IC and left tapetum was negatively associated with the motor score. (Pannek et al., 2020) The MD values of the CC and CST, among many other large WM tracts, were also associated with the motor outcome in a TBSS study by Dewey et al (2019) in children born VPT/VLBW at the age of seven, assessed with MABC-2 (Dewey et al., 2019). Groeschel et al (2014) did not, however, find any differences

in the MD values of the CC between adolescents born VPT/VLBW and the controls, so they decided not to assess the MD values and their associations with motor outcome (Groschel et al., 2014). Interestingly, in a TBSS study on children with DCD (n=30) and controls (n=31), excluding VPT/VLBW, they did not find any associations between DCD and MD values (Brown-Lum et al., 2020).

Besides diffusion metrics, many other tools have been used to predict later motor outcome in research settings. Motor outcome has been shown to be associated with comprehensive MRI findings at term and the negative predictive value (NPV) can even be improved when combined to a structured clinical assessment also done at term (Setänen et al., 2014). The various clinical assessments have also been shown to predict motor outcome when used as the sole method, and there is a wide range of information available related to the background and family characteristics related to the predictive associations (Caesar et al., 2020; Legros et al., 2020; Patra et al., 2016). Technical development has also made it possible to use newer methods, such as rsfMRI, CSD-HARDI axonal data, genetic variance, early inflammatory measures and MRI utilizing artificial intelligence approaches, as stand-alone methods or in combination with DWI, to predict later motor outcome (Janjic et al., 2020; Moeskops et al., 2017; Nist et al., 2020; Pannek et al., 2020; Saha et al., 2020; Toulmin et al., 2021; Worley et al., 2020).

6.1.2.2 Preterm behavioral phenotype

The preterm behavioral phenotype has not been as widely studied using DWI as motor development in children and adolescents born VPT/VLBW and EPT/ELBW. One previous study searched for association between the diffusion metrics of the anterior and posterior parts of dorsal cingulum at term, acquired through probabilistic tractography and the preterm behavioral phenotype at five years of age, assessed with the CBCL, SRS-2 and the Conners Rating Scale-Revised in children born VPT/VLBW. The parent-rated phenotype was associated with increased FA in the right anterior cingulum. The teacher-rated phenotype was associated with increased FA and decreased MD in the whole cingulum as well as decreased MD in the right anterior subdivision. (Brenner et al., 2020)

A ROI-utilizing DWI study at term showed an association between SDQ scores at five years of age in children born VPT/VLBW. For attention problems, the SDQ scores for hyperactivity/inattention were associated with right inferior temporal MD. Further associations were shown in SDQ peer problem scores and right orbitofrontal cortex MD, left inferior-temporal FA, SDQ prosocial behavior score and right orbitofrontal cortex MD, right superior-frontal FA, and SDQ conduct problem scores and inferior left temporal FA. A higher MD was positively associated with poorer outcome and a higher FA with better. (Rogers et al., 2012)

6.1.2.3 Clinical utility of DWI modalities

The effects of a VPT birth have been shown to be visible both in clinical settings and in imaging studies in adolescence. The predictions made in clinical settings are important for the parents, but also for the clinicians responsible for the follow-up. Making a prediction includes uncertainties and limitations that should be taken into consideration.

This thesis and the previous literature show a wide range of diffusion metrics and other brain-MRI-derived metrics predictive of motor and behavioral outcomes. It is, however, noteworthy that the brain areas and findings associated with cognitive, motor and behavioral outcomes are relatively similar through all outcome measures and ages. This might be a reflection of the overall immaturity and aberrant development following a preterm birth. The development of various clinically significant outcomes is also affected by other aspects, such as genetic and environmental factors.

Comprehensive brain MRI is a routine practice in neonatal intensive care units in the Finnish university hospitals. In this thesis, we applied ROI-based DTI analysis at term age on infants born VPT. Due to the limited population size, no predictive values could be calculated. DTI measurements have been shown to improve the positive predictive value. However, DTI metrics are not comparable between scanners, which makes reference values difficult to obtain and it also makes an individual's metrics change over time due to, for instance, brain growth during childhood (Tamnes et al., 2017). DTI is not recommended in Finland as a diagnostic tool for adult brain injury (Current Care Guidelines, 2017). Even though minor injuries show reductions on a group level in the FA-values, the individual variability in the metrics is high even in adults and decreased values after brain injury can be mediated by other factors, such as post-injury depression or anxiety (Alhilali et al., 2015). These considerations should also be taken into account in child and adolescent studies as well as in the predictive context.

Including DTI in the imaging protocol extends the total scan time. It should be carefully considered whether this additional stress to the subject is worth the information acquired. Similar limitations also apply to other quantitative MRI methods, but there are ongoing attempts searching for machine learning algorithms that could overcome technical limitations (Smyser et al., 2016). Even without clinical use, technical development appears relevant due to the high potential of DTI in research settings.

In the context of the results of this thesis and the previous findings of the PIPARI study, predicting developmental outcomes after a VPT birth is possible up to early adolescence. Setänen et al. have previously shown an excellent negative predictive value in the absence of major brain pathology combined with a structured clinical neurological examination (Setänen et al., 2016). The clinical follow-up should be

structured and well-reasoned, and the imaging results should be combined with the clinical data. The quantitative MRI methods provide insight to the pathological processes associated with a VPT birth, but the usability in prediction is still poor due to technical limitations.

6.1.3 The preterm brain in adolescence

The brain differences between VPT/VLBW and term-born infants are still visible in adolescence in the rates of pathologies, volumetric measures, DTI metrics and FNCs, and these differences have been shown to be associated with neurocognitive development (Rogers et al., 2018). In this thesis, in Study III, adolescents born VPT and controls were assessed in terms of nsFNC and msFNC, which describe the dynamic nature of brain activation during rest.

Differences were found in the temporal nsFNC metrics and msFNC metrics, while the nsFNC configuration remained similar. Adolescents born VPT/VLBW showed a longer fraction rate in the least active state, occupied fewer states during the scan, switched between states fewer times, and their measured overall and mean switch distances between the connectivity patterns were shorter.

To our knowledge, there are no previous nsFNC and msFNC studies in adolescents born VPT. The previous studies, which used sFNC methods, have identified differences between 13-year-old adolescents born preterm and at term in both inside network connectivity and RSN anticorrelation despite the resemblance of the spatial RSN orientation between the groups (Degnan et al., n.d., 2015). Both studies were done using the same study population consisting of late-preterm-born, low to moderate income twins. In addition to the methodological differences, this makes it even harder to compare the results.

A longitudinal sFNC study with one scan at eight years of age and a second scan at 16 years of age showed a similar sFNC between the groups at the first scan, but detected differences at the age of 16. The adolescents born VPT showed an increased sFNC activation at the time of the second scan. This study also included adolescents born LPT, besides assessing sFNC. (Rowlands et al., 2016) One previous sFNC study has been carried out in the VPT/VLBW population and controls where the mean age was comparable to our study. This study showed both increased and decreased connectivity patterns. In particular, the differences were detected in the networks involved in higher-order cognitive functions. The wide age range, from 10 to 16, might affect the sFNC analysis performed using a seed-based approach. (Wehrle et al., 2018)

Our results remained similar even after excluding adolescents with minor cognitive impairments or neuropsychiatric diagnoses. Neither of the groups included adolescents with major lesions, and the minor lesions were only seen in three

adolescents born VPT and one control. Based on these results, it could be possible to hypothesize that even without brain pathologies or a diagnosis, adolescents born preterm differ from controls in the resting state fluctuation of the brain. As a whole, their brains seem to be less flexible in switching from one mode to another and less interconnected between the regions.

This hypothesis has been previously suggested by White et al (2014), who studied three large attention networks in adults born VPT/VLBW. Their results showed that, compared to term born controls, the between-network connectivity was of a lower strength, and the activation pattern was less predictive and less temporally correlated in adults born VPT/VLBW. This might visualize the same phenomenon as our results and describe the deviant brain function behind the clinically observed attentional lapses of the preterm behavioral phenotype. (White et al., 2014)

6.1.3.1 Preterm behavioral phenotype

Both ADHD and ASD have been studied previously with nsFNC and msFNC methods in term-born populations. Even though we excluded the adolescents diagnosed with ADHD and none of the subjects were diagnosed with ASD, the preterm population has previously been shown to have subclinical traits of these neuropsychiatric conditions. This interpretation is supported by previous EEG studies in adults, where the EEG at rest was shown to be similarly altered in both adults with ADHD born at term and adults born VPT without an ADHD diagnosis (Rommel et al., 2017).

Children and adolescents diagnosed with ADHD have been shown to have an increased meta-state span, which is opposite to what we found (de Lacy et al., 2018). However, adolescents born VPT have, in some studies, been shown to have excessive traits of inattentiveness. It is possible that the inattentive subtype of ADHD could differ in fluidity and range from the combined or hyperactive subtypes. This hypothesis is supported by a previous study distinguishing the inattentive and combined subtypes of ADHD by regional brain network organization (Saad et al., 2017).

Adolescents diagnosed with ASD have been shown to have a significant decrease in all msFNC metrics (Fu et al., 2019). Similar findings have been made in other age groups. Children with ASD as well as children with milder social competence adversities have been shown to have a longer dwell time in the least connected state, and adults with ASD have been shown to have a significant decrease in the number of switches between connectivity patterns (de Lacy et al., 2017; Rashid et al., 2018). Deviances in msFNC metrics have also been detected in psychiatric disorders, such as schizophrenia. The phenomena captured in the results of this thesis might also be seen as neurological vulnerability for psychiatric disorders making adolescents born

VPT/VLBW less resilient. If so, this highlights the importance of adequate support even years after the preterm birth.

6.1.3.2 Brain maturation and the connectivity differences in the VPT/VLBW population

Adolescents born VPT/VLBW have been shown to undergo delayed brain maturation compared to term-born controls. This might also be one explanation for the differences between adolescents born VPT/VLBW and controls seen in study III.

Brain maturation has been shown to affect the nsFNC and msFNC metrics with increasing fluidity and range of brain function at rest between ages nine and 32 (Hutchison et al., 2015). In a study using a fully automated framework (BrainAGE) for comprehensive MRI-based estimation of developmental brain age, adolescents at the age of 14.5, born before a GA of 27 weeks, have been shown to undergo significantly delayed brain maturation compared to those born at a GA of 29–33 weeks and imaged at the same age. The mean delay was 1.96 (SD 0.68) years for the group with a GA <27 weeks and 0.4 (1.50) years for those born at a GA of 29–33 weeks (Franke et al., 2012).

In adult populations, gender differences have also been shown to occur, with males having greater fluidity and range (de Lacy et al., 2019). The adolescents in Study III were imaged during the year they turned 13. It is possible that the later onset of puberty in boys could have influenced our results, as boys show the maturational peak later than girls (Lenroot et al., 2010). There was no statistically significant difference in gender distribution between the groups, but the control group included more girls (18/32) than the the VPT group (10/24).

The onset of puberty in adolescents born VPT has, in a large meta-analysis, been shown to be comparable to term-born peers (James et al., 2018). A large gap between the onset of hormonal puberty and brain maturation has been shown to be a risk factor for internalizing psychiatric disorders, such as generalized or social anxiety disorder and depression, especially in girls. The delayed brain maturation, together with rigid brain processing, inattentiveness and simultaneous hormonal puberty may increase the risk for anxiety in VPT-born girls. (Kaczurkin et al., 2020)

Besides prematurity, delayed maturation of cortical and subcortical GM structures and between-RSN connectivity is seen in ADHD (Shaw et al., 2007; Sripada et al., 2014). These areas show volumetric changes that resemble the changes seen in adolescents born VPT/VLBW. On the other hand, ASD studies have showed abnormal early maturation, indicating changes in cell apoptosis and synaptic pruning, and similar findings have been seen in the encephalopathy of prematurity (Marsh et al., 2008; Volpe, 2019). Even children and adolescents with DCD have been shown to have brain alterations of a very similar kind (Zwicker et al., 2009).

Compared to ASD and DCD, the majority of subjects with ADHD catch up to controls at their own pace (Shaw et al., 2007).

6.2 Clinical usability of the adolescent brain DWI

Normal brain development has been shown to include widespread increases in FA and decreases in MD values in white matter tracts. In adolescence, the differences are visible even at short intervals of one to two years. (Tamnes et al., 2017) The rapid physiological changes timed by the individual onset of puberty challenge the clinical use of the FA/MD ratio for purposes such as diagnostic use. Besides the timing of puberty, gender and leisure activities such as sport training and even playing computer games also influence the DTI metrics (Galván et al., 2012; Herting et al., 2014; Pohl et al., 2016; Sagi et al., 2012). The changes can be seen as soon as after two hours of training, but the duration of the changes after training is finished is not well known (Sagi et al., 2012).

DWI-based MRI studies are commonly used in younger populations. The sequences are fast and provide information about water diffusion, which is considered to reflect the maturation and integrity of the underlying tissue. The scanner, imaging parameters, pre- and post-processing and the chosen analysis techniques affect the quantitative measurements. These are especially important in large multicenter studies and require different approaches of harmonizing (Pohl et al., 2016).

The clinical use of DWI imaging also includes various methodological aspects that differ from the use in research purposes. Both the ROI method used in Study I and the tractography method used in Study II allow analysis of individual patients and take into account the individual variation in the brain structure. Of these, the more automated tractography method might be preferable in clinical use, but different seeding, mask and thresholding choices do result in slightly different diffusion measures and tract lengths (Pandit et al., 2013).

In Study II, the actual measured diffusion metrics were shown to differ from previously published values of healthy controls used in various case-control-studies. Our study showed lower FA values and higher MD values. The previous studies, conducted by Carper et al. and Epstein et al., were based on a combined sample of children and adolescents, which might affect the metrics (Carper et al., 2015; Epstein et al., 2014). The subjects of Rocca et al. were of a similar age as our participants, but different seeding for the CST and a stricter thresholding for the CC were used (Rocca et al., 2016). Neither did all of these studies use susceptibility correction or mention it in their methods. Also, the tractography method and the scanner used differed from the ones used in this study.

Accordingly, there are many difficulties in comparing values directly between studies. The actual measured diffusion metrics are, besides corrections, affected by the tractography method and the scanner used. During the analysis, variations in the seeding of a tract, the use of alternative masks and stricter thresholding can affect the measured values. The widely used research methods, TBSS and VBM, only allow between-group comparisons and use normalization and averaging. They might thereby not be appropriate for clinical use. The metrics derived from large population studies might not be suitable for reference values derived using other methods.

This thesis showed a statistically significant difference in diffusion metrics and tract lengths between the susceptibility corrected and uncorrected data. The difference was seen in three large, differently oriented tracts – the corpus callosum, cingulum and corticospinal tract. The results are in line with previous studies and reflect the importance of study design and methodological knowledge in large multicenter studies, but also when comparing the results of different studies (Irfanoglu et al., 2012, 2019; P. A. Taylor et al., 2016).

The FA values were lower after the susceptibility correction than before the correction was applied. This is in line with a previous study in adolescent population showing a lower FA distribution than before the correction in a study with six participants (Taylor et al., 2016). The MD values tended to be higher after the susceptibility correction when compared to the uncorrected data. This is in line with the previous knowledge of MD's usually opposite behavior compared to FA.

The difference between the corrected and uncorrected data was shown to be small in relation to the measured diffusion metrics. The range of limits of agreements of the biases was comparable with the SDs of the diffusion metrics. A similar observation was made in comparison with the previously published diffusion metrics in clinical adolescent studies and their healthy controls (Carper et al., 2015; Epstein et al., 2014; Rocca et al., 2016; Vulser et al., 2018).

Besides the diffusion metrics, a significant difference was found in tract lengths between the corrected and uncorrected pathways. The tracts appeared to be longer in the corrected analysis. A statistically significant difference was seen in tracts originating from the CST and CC. The difference was not present in either of the cingulums. In previous studies with FA, the effect of a susceptibility correction has been the most prominent in the peripheral areas of the brain, while the cingulum is centrally located (Maximov et al., 2019; P. A. Taylor et al., 2016; Wu, Barnett, et al., 2008). A pilot study by Embleton et al. showed that the effect of susceptibility correction on tractography measures is the most prominent in temporal areas, near the third and fourth ventricle (Embleton et al., 2010). Our results implicate that the effect is also visible and significant in other lobes, not only in the locations of the highest distortions.

Study II also showed that the difference between the corrected and uncorrected analyses was positively associated with the measured MD values in the CC and cingulum bilaterally. A similar finding was made for the tract lengths in the CC and CST. The association was not present for FA values in any of the assessed tracts. The bias of the MD values was systematic, and thereby we assume that it is unlikely to be coincidental. The associations were relatively minor and not as systematic in the tract lengths, which make the association more likely to be explained by the increase in the mean value. Children also have higher MD values than adults, which highlights the importance of the correction in this age group (Lebel et al., 2017).

6.3 Strengths and limitations

The main strength of this thesis is the longitudinal follow-up with a regionally representative cohort of adolescents born VPT. The neonatal characteristics were well documented from the beginning, and participation in the multidisciplinary follow up has been good. The DCD diagnosis was carried out using a structured and validated test, and both the diagnosis and the quality of the neurological examination were reviewed by the supervising professor. The control population has also been followed from birth as a part of the same follow-up study, and the background characteristics and cognitive profile at preschool-age as well as executive function profiles and school performance at 11 years of age are known (Lind et al., 2011; Munck et al., 2010; Nyman, Korhonen, et al., 2019; Nyman, Munck, et al., 2019).

The technical strengths of this thesis are mostly related to choices in the MRI analyses. The decision to use ROIs for the term-equivalent age DTI analysis was based on a hypothesis of the future use of DTI metrics as a clinical tool. The manual ROI technique allows individual values for each infant and is not template- or atlas-based. This makes it possible to acquire the metrics even when an infant has major brain injuries. The intra- and inter-rater variabilities in the ROI measurements have been previously shown to be good (Lepomäki et al., 2012).

ICA was used in the rsfMRI study, allowing an analysis without a prior hypothesis. Another one of the main strengths of the study was that the findings remained similar after the exclusion of the adolescents with neurodevelopmental impairments. The previous literature has shown that differences in temporal measures can be visible without differences in sFNC (Hutchison et al., 2015). The scanning time in a rsfMRI scan has been shown to be long enough to retrieve good quality data, and the instructions were given and presented in an age-appropriate manner (Van Dijk et al., 2010). The limitations, especially regarding the age of the subjects, was that no information of their pubertal status was gathered. The rsfMRI was the last imaging sequence in the 1.5 h imaging session, which on the other hand might make it possible for the subjects to rest relaxed in the scanner, but might also

be seen as a potential source of strain, causing changes in the measurements (Bernas et al., 2018; Galván et al., 2012).

The main limitation was the small sample size. This thesis is part of a multidisciplinary follow-up study including all eligible VPT/VLBW infants born in Turku University Hospital between 2001 and 2006. Because of the widespread field of research topics since the beginning of the follow up, no power analyses were made, but the cohort size is comparable with other VPT/VLBW cohorts and was estimated to be large enough to meet the planned hypotheses.

The MRI scanner was updated in 2004 from 0.23T to 1.5T, and the DTI data was available only from the period after the update. It was not possible to calculate predictive values for motor development at 11 years of age from the DTI metrics acquired at term-equivalent age due to the limited sample size. At 13 years of age, only the adolescents born VPT/VLBW imaged with the 1.5T scanner were invited to the imaging follow up, and quite many of the adolescents refused to participate. At this age point, a wide set of research questions from various scientific fields were also planned.

The major technical considerations of all three studies were related to the motion artifacts, which were the most common reasons for data exclusion in all three studies. The motion corrections were applicable at 13 years of age, but not at term age. This limitation is an unavoidable side effect of the long follow-up. Not all of the modern pre-processing steps were standardly used in early 2000's when the study cohort was recruited. At term-equivalent age, the MRI scanning was performed during post-prandial sleep, which minimized the motion artifacts. At 13 years of age, the imaging, which included comprehensive MRI, DTI, and both task and rsfMRI scans, was 1.5 h long. The long scanning time may have increased the amount of motion during the last imaging sequences.

7 Conclusions

In this thesis, two advanced MRI-based imaging techniques (DTI and rsfMRI) were employed to discover the vulnerability of the very preterm. In addition, technical aspects relating to artifact corrections and comparability between studies were assessed in healthy adolescents.

This thesis showed that:

1. The DTI metrics of the corpus callosum, corona radiata and optic radiation at term-equivalent age are associated with motor development at 11 years of age in children born VPT.
2. Susceptibility correction affects the DTI metrics and tract lengths derived from the brain imaging data of healthy adolescents.
3. The temporal fluctuation of the resting state activation of the brain is significantly different in adolescents born VPT/VLBW and term-born controls.
4. The temporal fluctuation of the resting state activation of the brain in adolescents born VPT/VLBW resembles the activation changes seen in ADHD and ASD, the traits of which are commonly seen in the preterm behavioral phenotype.

Based on the results of this thesis and the pre-existing knowledge of the technical limitations, the novel MRI techniques may not serve as diagnostic or prognostic clinical tools. They provide, however, utterly important knowledge of the pathogenesis and neuroanatomical background of clinically acknowledged conditions. These findings increase the general understanding of the support needed in adolescence after very preterm birth. Future research is needed to further assess both structural and functional connectomics and their relation to the neurodevelopmental problems and behavioral phenotype in this vulnerable population.

Acknowledgements

This thesis is a part of a longitudinal follow up-study, PIPARI. I utterly appreciate the dedication of the families and especially the children, adolescents – and now even adults – who have committedly participated in the follow-up visits. I have been a part of this study group from 2013, you have been in this project for your whole life. I also want to thank all the professionals in Turku University Hospital for participating in the care and follow up of both the very preterm and term-born adolescents.

I am deeply grateful to my supervisors Professor Leena Haataja and Professor Riitta Parkkola. I admire your warmth, wisdom and humor. Thank you for your patient guidance throughout this project and the appreciation you have given me since our first meeting. Thank you, Sirkku, for introducing me to this research group and all the advice you have given. Karoliina, I want to thank you for sharing this journey with me. Virva, it has been a privilege to work with you, I have enjoyed our endless theories, and ideas, it was you who got me to understand physics. Thank you, Anna, for sharing your expertise in neuropsychology and Victor, for introducing me to the methodology of fMRI and the analyses you have performed, I admire your work. Susanna, Tuomo, Jere, Päivi J and Annika, the clinical data collection would not have been possible without you. I also want to express my gratitude to the other members of the PIPARI study group.

I would like to thank you, Docent Outi Tammela and Docent Marko Kangasniemi, for carefully reviewing the thesis and providing constructive comments and academic understanding. Thank you, Docent Tuire Lähdesmäki and Docent Kimmo Mattila, for being in the follow-up committee and linguist Henna Raudaskoski for reviewing the language of this thesis and the individual studies. I am honored to have Docent Mervi Könönen as my opponent and Professor Liisa Lehtonen as our custos.

This thesis has been supported by the Foundation for Paediatric Research, Arvo and Lea Ylppö foundation, The Foundation for Neonatal Research of Southwest Finland, Turku University Hospital Foundation, and State Research Funding of the Southwest Finland. I am grateful for the support. In particular, I want to thank the Turku University Hospital Foundation for providing me with an office for the writing

periods. The discussions at “Tutkari” have offered me valuable insights into research – along with a lot of handy advice on how to avoid the bumps along the way while writing my thesis. Thank you, Professor Olli Ruuskanen and PhD Minna Lukkarinen, as the heads of the foundation, and Antti, Kjell, Anselm, Mira H, Milla, Heidi, Mari and all the others. The Turku PET center has provided the facilities for the imaging studies; what a wonderful personnel and fine equipment. Thank you also to the Department of Pediatrics and Department of Pediatric Neurology for access to the clinical equipment and other facilities and especially Satu, Timo and Mira M for helping in the study arrangements.

I have been writing my thesis alternating with the clinical residency. I have been lucky to have you enabling this, Kim Kronström and Marika Östman, as Heads of Department at Adolescent Psychiatry in Turku University Hospital and Associate Professor Max Karukivi as the Head of Department in Satasairaala. I am very thankful for the support I have received from also the other colleagues and co-workers. During the writing of the literature review, the attitude of all co-workers at Nuote 2020–2021 and ward J1 2021 has meant a lot. I am especially grateful to Juuso, Noora, Kalle, Anu R and Johanna P-E, who have believed in me and found the words to encourage me. In addition, I want to thank you for your flexibility Henry, Joanna, Elina K, Mereta and Christina.

I owe my gratitude to those who have taken care of the PhD student during the long work hours and shared the joys and sorrows. The crew of s/y Tituu; Vilja, Ville, Anna, Lauri, and boys, I wish us smooth sailing in the future, as well. Thank you families Mäkelä and Sormunen for taking me on wonderful outings. I have been blessed also with many other supportive friends, thank you Paula, Erika, Marjo, Olli J, Hannele, Jenni, Pyry, Lassi sr, Ina, Lara, and Linnea, among the others. Kim and Max, thank you for all the caring and encouragement, thank you for listening to my joyful bursts of ideas and deepest and darkest thoughts. Your existence means so much for me. I’m standing on the shoulders of giants.

My family, thank you for supporting me since I was a small girl. Mum, it was you who first introduced me to pediatrics. Dad, your example made me curious about the natural sciences. I wouldn’t be here without your encouragement. Antti, I’ve learned so much from you and with you, you are best of brothers. I’m lucky to have you, Auli, Leena, Pentti, Juhani & co and Hanna & co, especially Leevi, with me today. Anni, thank you all the laughter we’ve shared.

And finally, the one who does not even understand the meaning of all this, Morgan, my thesis retriever, you made me take the last steps. I love you.

November 2021

Katri Lahti

References

- Alhilali, L. M., Delic, J. A., Gumus, S., & Fakhran, S. 2015. Evaluation of white matter injury patterns underlying neuropsychiatric symptoms after mild traumatic brain injury. *Radiology*, *277*(3), p. 793–800. <https://doi.org/10.1148/radiol.2015142974>
- Allen, E. A., Damaraju, E., Plis, S. M., Erhardt, E. B., Eichele, T., & Calhoun, V. D. 2014. Tracking whole-brain connectivity dynamics in the resting state. *Cerebral Cortex*, *24*(3), p. 663–676. <https://doi.org/10.1093/cercor/bhs352>
- Allen, E. A., Erhardt, E. B., Damaraju, E., Gruner, W., Segall, J. M., Silva, R. F., Havlicek, M., Rachakonda, S., Fries, J., Kalyanam, R., Michael, A. M., Caprihan, A., Turner, J. A., Eichele, T., Adelsheim, S., Bryan, A. D., Bustillo, J., Clark, V. P., Ewing, S. W. F., ... Calhoun, V. D. 2011. A baseline for the multivariate comparison of resting-state networks. *Frontiers in Systems Neuroscience*, *5*(FEBRUARY 2011), p. 1–23. <https://doi.org/10.3389/fnsys.2011.00002>
- Andersson, J. L. R., Skare, S., & Ashburner, J. 2003. How to correct susceptibility distortions in spin-echo echo-planar images: Application to diffusion tensor imaging. *NeuroImage*, *20*(2), p. 870–888. [https://doi.org/10.1016/S1053-8119\(03\)00336-7](https://doi.org/10.1016/S1053-8119(03)00336-7)
- APA. 2013. American Psychiatric Association, 2013. Diagnostic and statistical manual of mental disorders (5th ed.). In *American Journal of Psychiatry*.
- Ashburner, J., & Friston, K. J. 2001. Why Voxel-based morphometry should be used. *NeuroImage*, *14*(6), p. 1238–1243. <https://doi.org/10.1006/nimg.2001.0961>
- Atlas, S. W. 2016. *Magnetic Resonance Imaging of the Brain and Spine* (S. W. Atlas (ed.); 5th ed.). Wolters Kluwer.
- Back, S. A. 2015. Brain injury in the preterm infant: New horizons for pathogenesis and prevention. *Pediatric Neurology*, *53*(3), p. 185–192. <https://doi.org/10.1016/j.pediatrneurol.2015.04.006>
- Ball, G., Boardman, J. P., Rueckert, D., Aljabar, P., Arichi, T., Merchant, N., Gousias, I. S., Edwards, A. D., & Counsell, S. J. 2012. The effect of preterm birth on thalamic and cortical development. *Cerebral Cortex*, *22*(5), p. 1016–1024. <https://doi.org/10.1093/cercor/bhr176>
- Barfield, W. D. 2018. Public Health Implications of Very Preterm Birth. *Clinics in Perinatology*, *45*(3), p. 565–577. <https://doi.org/10.1016/j.clp.2018.05.007>
- Basser, P. J., Mattiello, J., & LeBihan, D. 1994. Estimation of the effective self-diffusion tensor from the NMR spin echo. In *Journal of Magnetic Resonance* (p. 8).
- Bax, M., Goldstein, M., Rosenbaun, P., Leviton, A., Paneth, N., Dan, B., Jacobsson, B., & Damiano, D. 2005. Proposed definition and classification of cerebral palsy, April 2005. *Developmental Medicine and Child Neurology*, *47*(8), p. 571. <https://doi.org/10.1017/S001216220500112X>
- Behrens, T. E. J., Berg, H. J., Jbabdi, S., Rushworth, M. F. S. F. S., & Woolrich, M. W. W. 2007. Probabilistic diffusion tractography with multiple fibre orientations: What can we gain? *NeuroImage*, *34*(1), p. 144–155. <https://doi.org/10.1016/j.neuroimage.2006.09.018>
- Behrens, T. E. J., Woolrich, M. W., Jenkinson, M., Johansen-Berg, H., Nunes, R. G., Clare, S., Matthews, P. M., Brady, J. M., & Smith, S. M. 2003. Characterization and Propagation of Uncertainty in Diffusion-Weighted MR Imaging. *Magnetic Resonance in Medicine*, *50*(5), p. 1077–1088. <https://doi.org/10.1002/mrm.10609>

- Behzadi, Y., Restom, K., Liao, J., & Liu, T. T. 2007. A component based noise correction method (CompCor) for BOLD and perfusion based fMRI. *NeuroImage*, 37(1). <https://doi.org/10.1016/j.neuroimage.2007.04.042>
- Benders, M. J. N. L., Kersbergen, K. J., & de Vries, L. S. 2014. Neuroimaging of White Matter Injury, Intraventricular and Cerebellar Hemorrhage. *Clinics in Perinatology*, 41(1), p. 69–82. <https://doi.org/10.1016/j.clp.2013.09.005>
- Bernas, A., Barendse, E. M., Aldenkamp, A. P., Backes, W. H., Hofman, P. A. M., Hendriks, M. P. H., Kessels, R. P. C., Willems, F. M. J., de With, P. H. N., Zinger, S., & Jansen, J. F. A. 2018. Brain resting-state networks in adolescents with high-functioning autism: Analysis of spatial connectivity and temporal neurodynamics. *Brain and Behavior*, 8(2), p. 1–10. <https://doi.org/10.1002/brb3.878>
- Blank, R., Barnett, A. L., Cairney, J., Green, D., Kirby, A., Polatajko, H., Rosenblum, S., Smits-Engelsman, B., Sugden, D., Wilson, P., & Vinçon, S. 2019. International clinical practice recommendations on the definition, diagnosis, assessment, intervention, and psychosocial aspects of developmental coordination disorder. *Developmental Medicine and Child Neurology*, 61(3), p. 242–285. <https://doi.org/10.1111/dmcn.14132>
- Blencowe, H., Cousens, S., Oestergaard, M. Z., Chou, D., Moller, A. B., Narwal, R., Adler, A., Vera Garcia, C., Rohde, S., Say, L., & Lawn, J. E. 2012. National, regional, and worldwide estimates of preterm birth rates in the year 2010 with time trends since 1990 for selected countries: A systematic analysis and implications. *The Lancet*, 379(9832), p. 2162–2172. [https://doi.org/10.1016/S0140-6736\(12\)60820-4](https://doi.org/10.1016/S0140-6736(12)60820-4)
- Botellero, V. L., Skranes, J., Bjuland, K. J., Håberg, A. K., Lydersen, S., Brubakk, A. M., Indredavik, M. S., & Martinussen, M. 2017. A longitudinal study of associations between psychiatric symptoms and disorders and cerebral gray matter volumes in adolescents born very preterm. *BMC Pediatrics*, 17(1), p. 1–17. <https://doi.org/10.1186/s12887-017-0793-0>
- Botellero, V. L., Skranes, J., Bjuland, K. J., Løhaugen, G. C., Håberg, A. K., Lydersen, S., Brubakk, A. M., Indredavik, M. S., & Martinussen, M. 2016. Mental health and cerebellar volume during adolescence in very-low-birth-weight infants: A longitudinal study. *Child and Adolescent Psychiatry and Mental Health*, 10(1), p. 1–15. <https://doi.org/10.1186/s13034-016-0093-8>
- Bouyssi-Kobar, M., De Asis-Cruz, J., Murnick, J., Chang, T., & Limperopoulos, C. 2019. Altered Functional Brain Network Integration, Segregation, and Modularity in Infants Born Very Preterm at Term-Equivalent Age. *Journal of Pediatrics*, 213, p. 13–21.e1. <https://doi.org/10.1016/j.jpeds.2019.06.030>
- Brenner, R. G., Smyser, C. D., Lean, R. E., Kenley, J. K., Smyser, T. A., Cyr, P. E. P., Shimony, J. S., Barch, D. M., & Rogers, C. E. 2020. Microstructure of the Dorsal Anterior Cingulum Bundle in Very Preterm Neonates Predicts the Preterm Behavioral Phenotype at 5 Years of Age. *Biological Psychiatry*, 16, p. 1–10. <https://doi.org/10.1016/j.biopsych.2020.06.015>
- Bröring, T., Oostrom, K. J., van Dijk-Lokkart, E. M., Lafeber, H. N., Brugman, A., & Oosterlaan, J. 2018. Attention deficit hyperactivity disorder and autism spectrum disorder symptoms in school-age children born very preterm. *Research in Developmental Disabilities*, 74(February), p. 103–112. <https://doi.org/10.1016/j.ridd.2018.01.001>
- Brown-Lum, M., Izadi-Najafabadi, S., Oberlander, T. F., Rauscher, A., & Zwicker, J. G. 2020. Differences in White Matter Microstructure Among Children With Developmental Coordination Disorder. *JAMA Network Open*, 3(3), p. e201184. <https://doi.org/10.1001/jamanetworkopen.2020.1184>
- Burnett, A., Davey, C. G., Wood, S. J., Wilson-Ching, M., Molloy, C., Cheong, J. L. Y., Doyle, L. W., Anderson, P. J., Callanan, C., Carse, E., Charlton, M. P., Davis, N., De Luca, C. R., Duff, J., Hayes, M., Hutchinson, E., Kelly, E., McDonald, M., Opie, G., ... Woods, H. 2014. Extremely preterm birth and adolescent mental health in a geographical cohort born in the 1990s. *Psychological Medicine*, 44(7), p. 1533–1544. <https://doi.org/10.1017/S0033291713002158>

- Burnett, A., Youssef, G., Anderson, P., Duff, J., Doyle, L., & Cheong, J. 2019. Exploring the “Preterm Behavioral Phenotype” in Children Born Extremely Preterm. *Journal of Developmental & Behavioral Pediatrics*, 40(3), p. 200–207. <https://doi.org/10.1097/DBP.0000000000000646>
- Caesar, R., Colditz, P. B., Cioni, G., & Boyd, R. N. 2020. Clinical tools used in young infants born very preterm to predict motor and cognitive delay (not cerebral palsy): a systematic review. *Developmental Medicine and Child Neurology*, p. 1–9. <https://doi.org/10.1111/dmcn.14730>
- Calhoun, V. D., Adali, T., Pearlson, G. D., & Pekar, J. J. 2001. A method for making group inferences from functional MRI data using independent component analysis. *Human Brain Mapping*. <https://doi.org/10.1002/hbm.1048>
- Carmody, D. P., Bendersky, M., DeMarco, J. K., Hiatt, M., Dunn, S. M., Hegyi, T., & Lewis, M. 2006. Early risk, attention, and brain activation in adolescents born preterm. *Child Development*, 77(2), p. 384–394. <https://doi.org/10.1111/j.1467-8624.2006.00877.x>
- Carper, R. A., Solders, S., Treiber, J. M., Fishman, I., & Müller, R.-A. 2015. Corticospinal Tract Anatomy and Functional Connectivity of Primary Motor Cortex in Autism. *Journal of the American Academy of Child & Adolescent Psychiatry*, 54(10), p. 859–867. <https://doi.org/10.1016/j.jaac.2015.07.007>
- Chawanpaiboon, S., Vogel, J. P., Moller, A. B., Lumbiganon, P., Petzold, M., Hogan, D., Landoulsi, S., Jampathong, N., Kongwattanakul, K., Laopaiboon, M., Lewis, C., Rattanakanokchai, S., Teng, D. N., Thinkhamrop, J., Watananirun, K., Zhang, J., Zhou, W., & Gülmezoglu, A. M. 2019. Global, regional, and national estimates of levels of preterm birth in 2014: a systematic review and modelling analysis. *The Lancet Global Health*, 7(1), p. e37–e46. [https://doi.org/10.1016/S2214-109X\(18\)30451-0](https://doi.org/10.1016/S2214-109X(18)30451-0)
- Cheong, J. L. Y., Anderson, P. J., Burnett, A. C., Roberts, G., Davis, N., Hickey, L., Carse, E., & Doyle, L. W. 2017. Changing Neurodevelopment at 8 Years in Children Born Extremely Preterm Since the 1990s. *Pediatrics*, 139(6), p. e20164086. <https://doi.org/10.1542/peds.2016-4086>
- Cheong, J. L. Y., Olsen, J. E., Lee, K. J., Spittle, A. J., Opie, G. F., Clark, M., Boland, R. A., Roberts, G., Josev, E. K., Davis, N., Hickey, L. M., Anderson, P. J., Doyle, L. W., Cheong, J., Anderson, P., Bear, M., Boland, R., Burnett, A., Charlton, M., ... Turner, A.-M. 2021. Temporal Trends in Neurodevelopmental Outcomes to 2 Years After Extremely Preterm Birth. *JAMA Pediatrics*, p. 1–8. <https://doi.org/10.1001/jamapediatrics.2021.2052>
- Chevallier, M., Debillon, T., Pierrat, V., Delorme, P., Kayem, G., Durox, M., Goffinet, F., Marret, S., Ancel, P. Y., Arnaud, C., Baud, O., Bednarek, N., Claris, O., Flamant, C., Gire, C., Saliba, E., Brissaud, O., Charkaluk, M. L., Favrais, G., & Bodeau-Livinec, F. 2017. Leading causes of preterm delivery as risk factors for intraventricular hemorrhage in very preterm infants: results of the EPIPAGE 2 cohort study. *American Journal of Obstetrics and Gynecology*, 216(5), p. 518.e1–518.e12. <https://doi.org/10.1016/j.ajog.2017.01.002>
- Constable, R. T., Ment, L. R., Vohr, B. R., Kesler, S. R., Fulbright, R. K., Lacadie, C., Delancy, S., Katz, K. H., Schneider, K. C., Schafer, R. J., Makuch, R. W., & Reiss, A. R. 2008. Prematurely born children demonstrate white matter microstructural differences at 12 years of age, relative to term control subjects: An investigation of group and gender effects. *Pediatrics*, 121(2), p. 306–316. <https://doi.org/10.1542/peds.2007-0414>
- Creel, L. M., Gregory, S., McNeal, C. J., Beeram, M. R., & Krauss, D. R. 2017. Multicenter neonatal databases: Trends in research uses. *BMC Research Notes*, 10(1), p. 1–8. <https://doi.org/10.1186/s13104-016-2336-4>
- Current Care Guidelines. 2017. *Brain injury* (A. of F. I. M. D. Working group appointed by the Finnish Medical Society Duodecim, The Finnish Society of Anaesthesiologists, Division of Neuroanesthesia, Societas Medicinae Physicalis et Rehabilitationis Fenniae, Finnish Neurosurgical Society, Finnish Neurological Society (ed.)). Duodecim.
- De Bruïne, F. T., Van Wezel-Meijler, G., Leijser, L. M., Steggerda, S. J., Van Den Berg-Huysmans, A. A., Rijken, M., Van Buchem, M. A., & Van Der Grond, J. 2013. Tractography of white-matter

- tracts in very preterm infants: A 2-year follow-up study. *Developmental Medicine and Child Neurology*, 55(5), p. 427–433. <https://doi.org/10.1111/dmcn.12099>
- De Kieviet, J. F., Pouwels, P. J. W., Lafeber, H. N., Vermeulen, R. J., Van Elburg, R. M., & Oosterlaan, J. 2014. A crucial role of altered fractional anisotropy in motor problems of very preterm children. *European Journal of Paediatric Neurology*, 18(2), p. 126–133. <https://doi.org/10.1016/j.ejpn.2013.09.004>
- de Kieviet, J. F., Zoetebier, L., van Elburg, R. M., Vermeulen, R. J., & Oosterlaan, J. 2012. Brain development of very preterm and very low-birthweight children in childhood and adolescence: a meta-analysis. *Developmental Medicine and Child Neurology*, 54(4), p. 313–323. <https://doi.org/10.1111/j.1469-8749.2011.04216.x>
- de Lacy, N., & Calhoun, V. D. 2018. Dynamic connectivity and the effects of maturation in youth with attention deficit hyperactivity disorder. *Network Neuroscience*. https://doi.org/10.1162/netn_a_00063
- de Lacy, N., Doherty, D., King, B. H., Rachakonda, S., & Calhoun, V. D. 2017. Disruption to control network function correlates with altered dynamic connectivity in the wider autism spectrum. *NeuroImage: Clinical*, 15(January), p. 513–524. <https://doi.org/10.1016/j.nicl.2017.05.024>
- de Lacy, N., McCauley, E., Kutz, J. N., & Calhoun, V. D. 2019. Sex-related differences in intrinsic brain dynamism and their neurocognitive correlates. *NeuroImage*, 202, p. 116116. <https://doi.org/10.1016/j.neuroimage.2019.116116>
- Degnan, A. J., Wisnowski, J. L., Choi, S., Ceschin, R., Bhushan, C., Leahy, R. M., Corby, P., & Schmithorst, V. J. 2015. *Altered Structural and Functional Connectivity in Late Preterm Preadolescence: An Anatomic Seed-Based Study of Resting State Networks Related to the Posteromedial and Lateral Parietal Cortex*. p. 1–21. <https://doi.org/10.1371/journal.pone.0130686>
- Degnan, A. J., Wisnowski, J. L., Choi, S., Ceschin, R., Bhushan, C., Leahy, R. M., Corby, P., Schmithorst, V. J., & Panigrahy, A. n.d. *Alterations of resting state networks and structural connectivity in relation to the prefrontal and anterior cingulate cortices in late prematurity*. p. 22–26. <https://doi.org/10.1097/WNR.0000000000000296>
- Desikan, R. S., Ségonne, F., Fischl, B., Quinn, B. T., Dickerson, B. C., Blacker, D., Buckner, R. L., Dale, A. M., Maguire, R. P., Hyman, B. T., Albert, M. S., & Killiany, R. J. 2006. An automated labeling system for subdividing the human cerebral cortex on MRI scans into gyral based regions of interest. *NeuroImage*. <https://doi.org/10.1016/j.neuroimage.2006.01.021>
- Dewey, D., Thompson, D. K., Kelly, C. E., Spittle, A. J., Cheong, J. L. Y., Doyle, L. W., & Anderson, P. J. 2019. Very preterm children at risk for developmental coordination disorder have brain alterations in motor areas. *Acta Paediatrica, International Journal of Paediatrics*, 108(9), p. 1649–1660. <https://doi.org/10.1111/apa.14786>
- Dudink, J., Kerr, J. L., Paterson, K., & Counsell, S. J. 2008. Connecting the developing preterm brain. *Early Human Development*, 84(12), p. 777–782. <https://doi.org/10.1016/j.earlhumdev.2008.09.004>
- Duerden, E. G., Foong, J., Chau, V., Branson, H., Poskitt, K. J., Grunau, R. E., Synnes, A., Zwicker, J. G., & Miller, S. P. 2015. Tract-based spatial statistics in preterm-born neonates predicts cognitive and motor outcomes at 18 months. *American Journal of Neuroradiology*, 36(8), p. 1565–1571. <https://doi.org/10.3174/ajnr.A4312>
- Edwards, J., Berube, M., Erlandson, K., Haug, S., Johnstone, H., Meagher, M., Sarkodee-Adoo, S., & Zwicker, J. G. 2011. Developmental coordination disorder in school-aged children born very preterm and/or at very low birth weight: A systematic review. *Journal of Developmental and Behavioral Pediatrics*, 32(9), p. 678–687. <https://doi.org/10.1097/DBP.0b013e31822a396a>
- Embleton, K. V., Haroon, H. A., Morris, D. M., Ralph, M. A. L., & Parker, G. J. M. 2010. Distortion correction for diffusion-weighted MRI tractography and fMRI in the temporal lobes. *Human Brain Mapping*, 31(10), p. 1570–1587. <https://doi.org/10.1002/hbm.20959>
- Engelhardt, E., Inder, T. E., Alexopoulos, D., Dierker, D. L., Hill, J., Van Essen, D., & Neil, J. J. 2015. Regional impairments of cortical folding in premature infants. *Annals of Neurology*, 77(1), p. 154–162. <https://doi.org/10.1002/ana.24313>

- Epstein, K. A., Cullen, K. R., Mueller, B. A., Robinson, P., Lee, S., & Kumra, S. 2014. White matter abnormalities and cognitive impairment in early-onset schizophrenia-spectrum disorders. *Journal of the American Academy of Child and Adolescent Psychiatry*, 53(3), p. 362- 372.e2. <https://doi.org/10.1016/j.jaac.2013.12.007>
- Feldman, H. M., Lee, E. S., Loe, I. M., Yeom, K. W., Grill-Spector, K., & Luna, B. 2012. White matter microstructure on diffusion tensor imaging is associated with conventional magnetic resonance imaging findings and cognitive function in adolescents born preterm. *Developmental Medicine and Child Neurology*, 54(9), p. 809–814. <https://doi.org/10.1111/j.1469-8749.2012.04378.x>
- Fevang, S. K. E., Hysing, M., Markestad, T., & Sommerfelt, K. 2016. Mental health in children born extremely preterm without severe neurodevelopmental disabilities. *Pediatrics*, 137(4). <https://doi.org/10.1542/peds.2015-3002>
- Fischi-Gómez, E., Vasung, L., Meskaldji, D. E., Lazeyras, F., Borradori-Tolsa, C., Hagmann, P., Barisnikov, K., Thiran, J. P., & Hüppi, P. S. 2015. Structural brain connectivity in school-age preterm infants provides evidence for impaired networks relevant for higher order cognitive skills and social cognition. *Cerebral Cortex*, 25(9), p. 2793–2805. <https://doi.org/10.1093/cercor/bhu073>
- Fischl, B. 2012. FreeSurfer. In *NeuroImage*. <https://doi.org/10.1016/j.neuroimage.2012.01.021>
- Fleiss, B., Gressens, P., & Stolp, H. B. 2020. Cortical Gray Matter Injury in Encephalopathy of Prematurity: Link to Neurodevelopmental Disorders. *Frontiers in Neurology*, 11(July). <https://doi.org/10.3389/fneur.2020.00575>
- Franke, K., Luders, E., May, A., Wilke, M., & Gaser, C. 2012. Brain maturation: Predicting individual BrainAGE in children and adolescents using structural MRI. *NeuroImage*, 63(3), p. 1305–1312. <https://doi.org/10.1016/j.neuroimage.2012.08.001>
- Franz, A. P., Bolat, G. U., Bolat, H., Matijasevich, A., Santos, I. S., Silveira, R. C., Procianoy, R. S., Rohde, L. A., & Moreira-Maia, C. R. 2018. Attention-Deficit/Hyperactivity Disorder and Very Preterm/Very Low Birth Weight: A Meta-analysis. *Pediatrics*, 141(1), p. e20171645. <https://doi.org/10.1542/peds.2017-1645>
- Fu, Z., Tu, Y., Di, X., Du, Y., Sui, J., Biswal, B. B., Zhang, Z., de Lacy, N., & Calhoun, V. D. 2019. Transient increased thalamic-sensory connectivity and decreased whole-brain dynamism in autism. *NeuroImage*, 190(May 2018), p. 191–204. <https://doi.org/10.1016/j.neuroimage.2018.06.003>
- Galván, A., Van Leijenhorst, L., & McGlennen, K. M. 2012. Considerations for imaging the adolescent brain. *Developmental Cognitive Neuroscience*, 2(3), p. 293–302. <https://doi.org/10.1016/j.dcn.2012.02.002>
- Giménez, M., Junqué, C., Narberhaus, A., Bargalló, N., Botet, F., & Mercader, J. M. 2006. White matter volume and concentration reductions in adolescents with history of very preterm birth: A voxel-based morphometry study. *NeuroImage*, 32(4), p. 1485–1498. <https://doi.org/10.1016/j.neuroimage.2006.05.013>
- Griffanti, L., Douaud, G., Bijsterbosch, J., Evangelisti, S., Alfaro-Almagro, F., Glasser, M. F., Duff, E. P., Fitzgibbon, S., Westphal, R., Carone, D., Beckmann, C. F., & Smith, S. M. 2017. Hand classification of fMRI ICA noise components. *NeuroImage*, 154. <https://doi.org/10.1016/j.neuroimage.2016.12.036>
- Groeschel, S., Holmström, L., Northam, G., Tournier, J. D., Baldeweg, T., Latal, B., Caflisch, J., & Vollmer, B. 2019. Motor Abilities in Adolescents Born Preterm Are Associated With Microstructure of the Corpus Callosum. *Frontiers in Neurology*, 10(April), p. 1–10. <https://doi.org/10.3389/fneur.2019.00367>
- Groeschel, S., Tournier, J. D., Northam, G. B., Baldeweg, T., Wyatt, J., Vollmer, B., & Connelly, A. 2014. Identification and interpretation of microstructural abnormalities in motor pathways in adolescents born preterm. *NeuroImage*, 87, p. 209–219. <https://doi.org/10.1016/j.neuroimage.2013.10.034>
- Healy, E., Reichenberg, A., Nam, K. W., Allin, M. P. G., Walshe, M., Rifkin, L., Murray, S. R. M., & Nosarti, C. 2013. Preterm birth and adolescent social functioning-alterations in emotion-processing brain areas. *Journal of Pediatrics*, 163(6), p. 1596–1604. <https://doi.org/10.1016/j.jpeds.2013.08.011>
- Helenius, K., Sjörs, G., Shah, P. S., Modi, N., Reichman, B., Morisaki, N., Kusuda, S., Lui, K., Darlow, B. A., Bassler, D., Hakansson, S., Adams, M., Vento, M., Rusconi, F., Isayama, T., Lee, S. K., &

- Lehtonen, L. 2018. Survival in very preterm infants: An international comparison of 10 national neonatal networks. *Obstetrical and Gynecological Survey*, 73(4), p. 187–189. <https://doi.org/10.1097/OGX.0000000000000553>
- Henderson, S. E., Sugden, D. A., & Barnett, A. L. 2007. *Movement assessment battery for children (examiner's manual)* (2nd edn). Pearson Assessment.
- Herting, M. M., Colby, J. B., Sowell, E. R., & Nagel, B. J. 2014. White matter connectivity and aerobic fitness in male adolescents. *Developmental Cognitive Neuroscience*, 7, p. 65–75. <https://doi.org/10.1016/j.dcn.2013.11.003>
- Hindriks, R., Adhikari, M. H., Murayama, Y., Ganzetti, M., Mantini, D., Logothetis, N. K., & Deco, G. 2016. Can sliding-window correlations reveal dynamic functional connectivity in resting-state fMRI? *NeuroImage*, 127. <https://doi.org/10.1016/j.neuroimage.2015.11.055>
- Hintz, S. R., Kendrick, D. E., Wilson-Costello, D. E., Das, A., Bell, E. F., Vohr, B. R., & Higgins, R. D. 2011. Early-Childhood Neurodevelopmental Outcomes Are Not Improving for Infants Born at <25 Weeks' Gestational Age. *PEDIATRICS*, 127(1), p. 62–70. <https://doi.org/10.1542/peds.2010-1150>
- Hirvonen, M., Ojala, R., Korhonen, P., Haataja, P., Eriksson, K., Gissler, M., Luukkaala, T., & Tammela, O. 2014. Cerebral palsy among children born moderately and late preterm. *Pediatrics*, 134(6), p. e1584–e1593. <https://doi.org/10.1542/peds.2014-0945>
- Holsti, A., Adamsson, M., Serenius, F., Hägglöf, B., & Farooqi, A. 2016. Two-thirds of adolescents who received active perinatal care after extremely preterm birth had mild or no disabilities. *Acta Paediatrica, International Journal of Paediatrics*, 105(11), p. 1288–1297. <https://doi.org/10.1111/apa.13499>
- Husby, I. M., Skranes, J., Olsen, A., Brubakk, A. M., & Evensen, K. A. I. 2013. Motor skills at 23 years of age in young adults born preterm with very low birth weight. *Early Human Development*, 89(9), p. 747–754. <https://doi.org/10.1016/j.earlhumdev.2013.05.009>
- Hutchison, R. M., & Morton, J. B. 2015. Tracking the brain's functional coupling dynamics over development. *Journal of Neuroscience*, 35(17), p. 6849–6859. <https://doi.org/10.1523/JNEUROSCI.4638-14.2015>
- Inder, T. E., Wells, S. J., Mogridge, N. B., Spencer, C., & Volpe, J. J. 2003. Defining the nature of the cerebral abnormalities in the premature infant: A qualitative magnetic resonance imaging study. *Journal of Pediatrics*, 143(2), p. 171–179. [https://doi.org/10.1067/S0022-3476\(03\)00357-3](https://doi.org/10.1067/S0022-3476(03)00357-3)
- Indredavik, M. S., Skranes, J. S., Vik, T., Heyerdahl, S., Romundstad, P., Myhr, G. E., & Brubakk, A. M. 2005. Low-birth-weight adolescents: Psychiatric symptoms and cerebral MRI abnormalities. *Pediatric Neurology*, 33(4), p. 259–266. <https://doi.org/10.1016/j.pediatrneurol.2005.05.002>
- Indredavik, M. S., Vik, T., Evensen, K. A. I., Skranes, J., Taraldsen, G., & Brubakk, A. M. 2010. Perinatal risk and psychiatric outcome in adolescents born preterm with very low birth weight or term small for gestational age. *Journal of Developmental and Behavioral Pediatrics*, 31(4), p. 286–294. <https://doi.org/10.1097/DBP.0b013e3181d7b1d3>
- Irfanoglu, M. O., Sarlls, J., Nayak, A., & Pierpaoli, C. 2019. Evaluating corrections for Eddy-currents and other EPI distortions in diffusion MRI: methodology and a dataset for benchmarking. *Magnetic Resonance in Medicine*, 81(4), p. 2774–2787. <https://doi.org/10.1002/mrm.27577>
- Irfanoglu, M. O., Walker, L., Sarlls, J., Marengo, S., & Pierpaoli, C. 2012. Effects of image distortions originating from susceptibility variations and concomitant fields on diffusion MRI tractography results. *NeuroImage*, 61(1), p. 275–288. <https://doi.org/10.1016/j.neuroimage.2012.02.054>
- Jaekel, J., Baumann, N., Bartmann, P., & Wolke, D. 2018. Mood and anxiety disorders in very preterm/very low-birth weight individuals from 6 to 26 years. *Journal of Child Psychology and Psychiatry and Allied Disciplines*, 59(1), p. 88–95. <https://doi.org/10.1111/jcpp.12787>
- James, E., Wood, C. L., Nair, H., & Williams, T. C. 2018. Preterm birth and the timing of puberty: A systematic review. *BMC Pediatrics*, 18(1), p. 1–12. <https://doi.org/10.1186/s12887-017-0976-8>
- Janjic, T., Pereverzyev, S., Hammerl, M., Neubauer, V., Lerchner, H., Wallner, V., Steiger, R., Kiechl-Kohlendorfer, U., Zimmermann, M., Buchheim, A., Grams, A. E., & Gizewski, E. R. 2020. Feed-

- forward neural networks using cerebral MR spectroscopy and DTI might predict neurodevelopmental outcome in preterm neonates. *European Radiology*, 30(12), p. 6441–6451. <https://doi.org/10.1007/s00330-020-07053-8>
- Jezzard, P., & Balaban, R. S. 1995. Correction for geometric distortion in echo planar images from B0 field variations. *Magnetic Resonance in Medicine*. <https://doi.org/10.1002/mrm.1910340111>
- Johns, C. B., Lacadie, C., Vohr, B., Ment, L. R., & Scheinost, D. 2019. NeuroImage: Clinical Amygdala functional connectivity is associated with social impairments in preterm born young adults ☆. *NeuroImage: Clinical*, 21(December 2018), p. 101626. <https://doi.org/10.1016/j.nicl.2018.101626>
- Johnson, S., Hollis, C., Kochhar, P., Hennessy, E., Wolke, D., & Marlow, N. 2010. Psychiatric Disorders in Extremely Preterm Children: Longitudinal Finding at Age 11 Years in the EPICure Study. *Journal of the American Academy of Child & Adolescent Psychiatry*, 49(5), p. 453- 463.e1. <https://doi.org/10.1016/j.jaac.2010.02.002>
- Johnson, S., & Marlow, N. 2011. Preterm birth and childhood psychiatric disorders. *Pediatric Research*, 69(5 PART 2), p. 22–28. <https://doi.org/10.1203/PDR.0b013e318212faa0>
- Johnson, S., O'Reilly, H., Ni, Y., Wolke, D., & Marlow, N. 2019. Psychiatric Symptoms and Disorders in Extremely Preterm Young Adults at 19 Years of Age and Longitudinal Findings From Middle Childhood. *Journal of the American Academy of Child & Adolescent Psychiatry*, 58(8), p. 820-826.e6. <https://doi.org/10.1016/j.jaac.2019.02.020>
- Jones, D. K. 2004. The Effect of Gradient Sampling Schemes on Measures Derived from Diffusion Tensor MRI: A Monte Carlo Study. *Magnetic Resonance in Medicine*. <https://doi.org/10.1002/mrm.20033>
- Jones, D. K. 2008. Studying connections in the living human brain with diffusion MRI. *Cortex*, 44(8), p. 936–952. <https://doi.org/10.1016/j.cortex.2008.05.002>
- Joseph, R. M., O'Shea, T. M., Allred, E. N., Heeren, T., Hirtz, D., Paneth, N., Leviton, A., & Kuban, K. C. K. 2017. Prevalence and associated features of autism spectrum disorder in extremely low gestational age newborns at age 10 years. *Autism Research*, 10(2), p. 224–232. <https://doi.org/10.1002/aur.1644>
- Kaczurkin, A. N., Sotiras, A., Baller, E. B., Barzilay, R., Calkins, M. E., Chand, G. B., Cui, Z., Erus, G., Fan, Y., Gur, R. E. R. C., Gur, R. E. R. C., Moore, T. M., Roalf, D. R., Rosen, A. F. G., Ruparel, K., Shinohara, R. T., Varol, E., Wolf, D. H., Davatzikos, C., & Satterthwaite, T. D. 2020. Neurostructural Heterogeneity in Youths With Internalizing Symptoms. *Biological Psychiatry*, 87(5), p. 473–482. <https://doi.org/10.1016/j.biopsych.2019.09.005>
- Karolis, V. R., Froudust-Walsh, S., Kroll, J., Brittain, P. J., Tseng, C. E. J., Nam, K. W., Reinders, A. A. T. S., Murray, R. M., Williams, S. C. R., Thompson, P. M., & Nosarti, C. 2017. Volumetric grey matter alterations in adolescents and adults born very preterm suggest accelerated brain maturation. *NeuroImage*, 163(May), p. 379–389. <https://doi.org/10.1016/j.neuroimage.2017.09.039>
- Kelly, C. E., Chan, L., Burnett, A. C., Lee, K. J., Connelly, A., Anderson, P. J., Doyle, L. W., Cheong, J. L. Y., & Thompson, D. K. 2015. Brain structural and microstructural alterations associated with cerebral palsy and motor impairments in adolescents born extremely preterm and/or extremely low birthweight. *Developmental Medicine and Child Neurology*, 57(12), p. 1168–1175. <https://doi.org/10.1111/dmcn.12854>
- Kiviniemi, V., Starck, T., Remes, J., Long, X., Nikkinen, J., Haapea, M., Veijola, J., Moilanen, I., Isohanni, M., Zang, Y. F., & Tervonen, O. 2009. Functional segmentation of the brain cortex using high model order group PICA. *Human Brain Mapping*, 30(12). <https://doi.org/10.1002/hbm.20813>
- Klein, A., & Tourville, J. 2012. 101 Labeled Brain Images and a Consistent Human Cortical Labeling Protocol. *Frontiers in Neuroscience*, 6(DEC), p. 1–12. <https://doi.org/10.3389/fnins.2012.00171>
- Korzeniewski, S. J., Joseph, R. M., Kim, S. H., Allred, E. N., Michael O'Shea, T., Leviton, A., & Kuban, K. C. K. 2017. Social responsiveness scale assessment of the preterm behavioral phenotype in 10-year-olds born extremely preterm. *Journal of Developmental and Behavioral Pediatrics*, 38(9), p. 697–705. <https://doi.org/10.1097/DBP.0000000000000485>

- Kuban, K., Adler, I., Allred, E. N., Batton, D., Bezinque, S., Betz, B. W., Cavenagh, E., Durfee, S., Ecklund, K., Feinstein, K., Fordham, L. A., Hampf, F., Junewick, J., Lorenzo, R., McCauley, R., Miller, C., Seibert, J., Specter, B., Wellman, J., ... Leviton, A. 2007. Observer variability assessing US scans of the preterm brain: The ELGAN study. *Pediatric Radiology*, 37(12), p. 1201–1208. <https://doi.org/10.1007/s00247-007-0605-z>
- Kybic, J., Member, S., Thévenaz, P., Nirkko, A., & Unser, M. 2000. *Unwarping of Unidirectionally Distorted EPI Images*. 19(2), p. 80–93.
- Le Bihan, D., Poupon, C., Amadon, A., & Lethimonnier, F. 2006. Artifacts and pitfalls in diffusion MRI. *Journal of Magnetic Resonance Imaging*, 24(3), p. 478–488. <https://doi.org/10.1002/jmri.20683>
- Lebel, C., Treit, S., & Beaulieu, C. 2017. A review of diffusion MRI of typical white matter development from early childhood to young adulthood. *NMR in Biomedicine*, May, p. 1–23. <https://doi.org/10.1002/nbm.3778>
- Legros, L., Zaczek, S., Vaivre-Douret, L., & Mostaert, A. 2020. Concurrent and predictive validity of the Motor Functional Development Scale for Young Children in preterm infants. *Early Human Development*, 151(October), p. 105240. <https://doi.org/10.1016/j.earlhumdev.2020.105240>
- Leijser, L. M., de Bruïne, F. T., Steggerda, S. J., van der Grond, J., Walther, F. J., & van Wezel-Meijler, G. 2009. Brain imaging findings in very preterm infants throughout the neonatal period: Part I. Incidences and evolution of lesions, comparison between ultrasound and MRI. *Early Human Development*, 85(2), p. 101–109. <https://doi.org/10.1016/j.earlhumdev.2008.11.010>
- Lenroot, R. K., & Giedd, J. N. 2010. Sex differences in the adolescent brain. *Brain and Cognition*, 72(1), p. 46–55. <https://doi.org/10.1016/j.bandc.2009.10.008>
- Lepomäki, V. K., Paavilainen, T. P., Hurme, S. A. M., Komu, M. E., & Parkkola, R. K. 2012. Fractional anisotropy and mean diffusivity parameters of the brain white matter tracts in preterm infants: reproducibility of region-of-interest measurements. *Pediatric Radiology*, 42(2), p. 175–182. <https://doi.org/10.1007/s00247-011-2234-9>
- Lind, A., Korkman, M., Lehtonen, L., Lapinleimu, H., Parkkola, R., Matomäki, J., & Haataja, L. 2011. Cognitive and neuropsychological outcomes at 5 years of age in preterm children born in the 2000s. *Developmental Medicine & Child Neurology*, 53(3), p. 256–262. <https://doi.org/10.1111/j.1469-8749.2010.03828.x>
- Maalouf, E. F., Duggan, P. J., Counsell, S. J., Rutherford, M. A., Cowan, F., Azzopardi, D., & Edwards, A. D. 2001. Comparison of findings on cranial ultrasound and magnetic resonance imaging in preterm infants. *Pediatrics*, 107(4 I), p. 719–727. <https://doi.org/10.1542/peds.107.4.719>
- Makropoulos, A., Aljabar, P., Wright, R., Hüning, B., Merchant, N., Arichi, T., Tusor, N., Hajnal, J. V., Edwards, A. D., Counsell, S. J., & Rueckert, D. 2016. Regional growth and atlas of the developing human brain. *NeuroImage*, 125, p. 456–478. <https://doi.org/10.1016/j.neuroimage.2015.10.047>
- Marsh, R., Gerber, A. J., & Peterson, B. S. 2008. Neuroimaging studies of normal brain development and their relevance for understanding childhood neuropsychiatric disorders. *Journal of the American Academy of Child and Adolescent Psychiatry*, 47(11), p. 1233–1251. <https://doi.org/10.1097/CHI.0b013e318185e703>
- Maximov, I. I., Alnæs, D., & Westlye, L. T. 2019. Towards an optimised processing pipeline for diffusion magnetic resonance imaging data: Effects of artefact corrections on diffusion metrics and their age associations in UK Biobank. *Human Brain Mapping*, January, p. hbm.24691. <https://doi.org/10.1002/hbm.24691>
- Ment, L. R., Hirtz, D., & Hüppi, P. S. 2009. Imaging biomarkers of outcome in the developing preterm brain. *The Lancet Neurology*, 8(11), p. 1042–1055. [https://doi.org/10.1016/S1474-4422\(09\)70257-1](https://doi.org/10.1016/S1474-4422(09)70257-1)
- Ment, L. R., Kesler, S., Vohr, B., Katz, K. H., Baumgartner, H., Schneider, K. C., Delancy, S., Silbereis, J., Duncan, C. C., Constable, R. T., Makuch, R. W., & Reiss, A. L. 2009. Longitudinal brain

- volume changes in preterm and term control subjects during late childhood and adolescence. *Pediatrics*, *123*(2), p. 503–511. <https://doi.org/10.1542/peds.2008-0025>
- Merhof, D., Soza, G., Stadlbauer, A., Greiner, G., & Nimsky, C. 2007. Correction of susceptibility artifacts in diffusion tensor data using non-linear registration. *Medical Image Analysis*, *11*(6), p. 588–603. <https://doi.org/10.1016/j.media.2007.05.004>
- Miller, R. L., Yaesoubi, M., Turner, J. A., Mathalon, D., Preda, A., Pearlson, G., Adali, T., & Calhoun, V. D. 2016. Higher dimensional meta-state analysis reveals reduced resting fMRI connectivity dynamism in schizophrenia patients. *PLoS ONE*, *11*(3). <https://doi.org/10.1371/journal.pone.0149849>
- Moeskops, P., Išgum, I., Keunen, K., Claessens, N. H. P., Van Haastert, I. C., Groenendaal, F., De Vries, L. S., Viergever, M. A., & Benders, M. J. N. L. 2017. Prediction of cognitive and motor outcome of preterm infants based on automatic quantitative descriptors from neonatal MR brain images. *Scientific Reports*, *7*(1), p. 1–10. <https://doi.org/10.1038/s41598-017-02307-w>
- Monson, B. B., Anderson, P. J., Matthews, L. G., Neil, J. J., Kapur, K., Cheong, J. L. Y., Doyle, L. W., Thompson, D. K., & Inder, T. E. 2016. Examination of the pattern of growth of cerebral tissue volumes from hospital discharge to early childhood in very preterm infants. *JAMA Pediatrics*, *170*(8), p. 772–779. <https://doi.org/10.1001/jamapediatrics.2016.0781>
- Mullen, K. M., Vohr, B. R., Katz, K. H., Schneider, K. C., Lacadie, C., Hampson, M., Makuch, R. W., Reiss, A. L., Constable, R. T., & Ment, L. R. 2011. Preterm birth results in alterations in neural connectivity at age 16 years. *NeuroImage*, *54*(4), p. 2563–2570. <https://doi.org/10.1016/j.neuroimage.2010.11.019>
- Munck, P., Haataja, L., Maunu, J., Parkkola, R., Rikalainen, H., Lapinleimu, H., & Lehtonen, L. 2010. Cognitive outcome at 2 years of age in Finnish infants with very low birth weight born between 2001 and 2006. *Acta Paediatrica, International Journal of Paediatrics*, *99*(3), p. 359–366. <https://doi.org/10.1111/j.1651-2227.2009.01589.x>
- Myers, E. H., Hampson, M., Vohr, B., Lacadie, C., Frost, S. J., Pugh, K. R., Katz, K. H., Schneider, K. C., Makuch, R. W., Constable, R. T., & Ment, L. R. 2010. Functional connectivity to a right hemisphere language center in prematurely born adolescents. *NeuroImage*, *51*(4), p. 1445–1452. <https://doi.org/10.1016/j.neuroimage.2010.03.049>
- Nagy, Z., & Jónsson, B. 2009. Cerebral MRI findings in a cohort of ex-preterm and control adolescents. *Acta Paediatrica, International Journal of Paediatrics*, *98*(6), p. 996–1001. <https://doi.org/10.1111/j.1651-2227.2009.01278.x>
- National Institute for Health and Welfare. 2020. *Perinatal statistics – parturients, deliveries and newborns 2019*. Perinatal Statistics – Parturients, Deliveries and Newborns 2019.
- Nist, M. D., Shoben, A. B., & Pickler, R. H. 2020. Early Inflammatory Measures and Neurodevelopmental Outcomes in Preterm Infants. *Nursing Research*, *69*(5S Suppl 1). <https://doi.org/10.1097/NNR.0000000000000448>
- Nosarti, C., Al-Asady, M. H. S., Frangou, S., Stewart, A. L., Rifkin, L., & Murray, R. M. 2002. Adolescents who were born very preterm have decreased brain volumes. *Brain*, *125*(7), p. 1616–1623. <https://doi.org/10.1093/brain/awf157>
- Nosarti, C., Allin, M. P., Frangou, S., Rifkin, L., & Murray, R. M. 2005. Hyperactivity in adolescents born very preterm is associated with decreased caudate volume. *Biological Psychiatry*, *57*(6), p. 661–666. <https://doi.org/10.1016/j.biopsych.2004.12.003>
- Nosarti, C., Giouroukou, E., Healy, E., Rifkin, L., Walshe, M., Reichenberg, A., Chitnis, X., Williams, S. C. R., & Murray, R. M. 2008. Grey and white matter distribution in very preterm adolescents mediates neurodevelopmental outcome. *Brain*, *131*(1), p. 205–217. <https://doi.org/10.1093/brain/awm282>
- Nosarti, C., Rushe, T. M., Woodruff, P. W. R., Stewart, A. L., Rifkin, L., & Murray, R. M. 2004. Corpus callosum size and very preterm birth: Relationship to neuropsychological outcome. *Brain*, *127*(9), p. 2080–2089. <https://doi.org/10.1093/brain/awh230>
- Nyman, A., Korhonen, T., Lehtonen, L., Haataja, L., Aho, K., Ahtola, A., Ekblad, M., Ekblad, S., Ekholm, E., Hagelstam, C., Huhtala, M., Juntunen, M., Kero, P., Koivisto, M., Korja, R., Korpela,

- S., Lahti, K., Lapinleimu, H., Lehtonen, T., ... Ylijoki, M. 2019. School performance is age appropriate with support services in very preterm children at 11 years of age. *Acta Paediatrica, International Journal of Paediatrics*, 108(9). <https://doi.org/10.1111/apa.14763>
- Nyman, A., Munck, P., Koivisto, M., Hagelstam, C., Korhonen, T., Lehtonen, L., & Haataja, L. 2019. Executive Function Profiles at Home and at School in 11-Year-Old Very Low Birth Weight or Very Low Gestational Age Children. *Journal of Developmental & Behavioral Pediatrics*, 40(7), p. 547–554. <https://doi.org/10.1097/DBP.0000000000000689>
- O'Donnell, L. J., & Westin, C. F. 2011. An introduction to diffusion tensor image analysis. *Neurosurgery Clinics of North America*, 22(2), p. 185–196. <https://doi.org/10.1016/j.nec.2010.12.004>
- Ogawa, S., Lee, T. M., Kay, A. R., & Tank, D. W. 1990. Brain magnetic resonance imaging with contrast dependent on blood oxygenation. *Proceedings of the National Academy of Sciences*, 87(24), p. 9868–9872. <https://doi.org/10.1073/pnas.87.24.9868>
- Oguz, I., Farzinfar, M., Matsui, J., Budin, F., Liu, Z., Gerig, G., Johnson, H. J., & Styner, M. 2014. DTIPrep: Quality control of diffusion-weighted images. *Frontiers in Neuroinformatics*. <https://doi.org/10.3389/fninf.2014.00004>
- Padilla, N., Eklöf, E., Mårtensson, G. E., Bölte, S., Lagercrantz, H., & Ådén, U. 2015. Poor Brain Growth in Extremely Preterm Neonates Long Before the Onset of Autism Spectrum Disorder Symptoms. *Cerebral Cortex*, 27(2), p. bhv300. <https://doi.org/10.1093/cercor/bhv300>
- Panda, S., Dohare, P., Jain, S., Parikh, N., Singla, P., Mehdizadeh, R., Klebe, D. W., Kleinman, G. M., Cheng, B., & Ballabh, P. 2018. Estrogen treatment reverses prematurity-induced disruption in cortical interneuron population. *Journal of Neuroscience*, 38(34), p. 7378–7391. <https://doi.org/10.1523/JNEUROSCI.0478-18.2018>
- Pandit, A. S., Ball, G., Edwards, A. D., & Counsell, S. J. 2013. Diffusion magnetic resonance imaging in preterm brain injury. *Neuroradiology*, 55(S2), p. 65–95. <https://doi.org/10.1007/s00234-013-1242-x>
- Pannek, K., George, J. M., Boyd, R. N., Colditz, P. B., Rose, S. E., & Fripp, J. 2020. Brain microstructure and morphology of very preterm-born infants at term equivalent age: Associations with motor and cognitive outcomes at 1 and 2 years. *NeuroImage*, 221(June), p. 117163. <https://doi.org/10.1016/j.neuroimage.2020.117163>
- Pannek, K., Scheck, S. M., Colditz, P. B., Boyd, R. N., & Rose, S. E. 2014. Magnetic resonance diffusion tractography of the preterm infant brain: a systematic review. *Developmental Medicine & Child Neurology*, 56(2), p. 113–124. <https://doi.org/10.1111/dmcn.12250>
- Papile, L. A., Burstein, J., Burstein, R., & Koffler, H. 1978. Incidence and evolution of subependymal and intraventricular hemorrhage: A study of infants with birth weights less than 1,500 gm. *The Journal of Pediatrics*, 92(4), p. 529–534. [https://doi.org/10.1016/S0022-3476\(78\)80282-0](https://doi.org/10.1016/S0022-3476(78)80282-0)
- Partridge, S. C., Mukherjee, P., Berman, J. I., Henry, R. G., Miller, S. P., Lu, Y., Glenn, O. A., Ferriero, D. M., Barkovich, A. J., & Vigneron, D. B. 2005. Tractography-based quantitation of diffusion tensor imaging parameters in white matter tracts of preterm newborns. *Journal of Magnetic Resonance Imaging*, 22(4). <https://doi.org/10.1002/jmri.20410>
- Patel, A. X., Kundu, P., Rubinov, M., Jones, P. S., Vértes, P. E., Ersche, K. D., Suckling, J., & Bullmore, E. T. 2014. A wavelet method for modeling and despiking motion artifacts from resting-state fMRI time series. *NeuroImage*, 95. <https://doi.org/10.1016/j.neuroimage.2014.03.012>
- Patel, D. R., Neelakantan, M., Pandher, K., & Merrick, J. 2020. Cerebral palsy in children: a clinical overview. *Translational Pediatrics*, 9(S1), p. S125–S135. <https://doi.org/10.21037/tp.2020.01.01>
- Patra, K., Greene, M., Patel, A., & Meier, P. 2016. Maternal Education Level Predicts Cognitive, Language, and Motor Outcome in Preterm Infants in the Second Year of Life. *American Journal of Perinatology*, 33(08), p. 738–744. <https://doi.org/10.1055/s-0036-1572532>
- Pierpaoli, C., Jezzard, P., Basser, P. J., Barnett, A., & Di Chiro, G. 1996. Diffusion tensor MR imaging of the human brain. *Radiology*. <https://doi.org/10.1148/radiology.201.3.8939209>

- Pohl, K. M., Sullivan, E. V., Rohlfing, T., Chu, W., Kwon, D., Nichols, B. N., Zhang, Y., Brown, S. A., Tapert, S. F., Cummins, K., Thompson, W. K., Brumback, T., Colrain, I. M., Baker, F. C., Prouty, D., De Bellis, M. D., Voyvodic, J. T., Clark, D. B., Schirda, C., ... Pfefferbaum, A. 2016. Harmonizing DTI measurements across scanners to examine the development of white matter microstructure in 803 adolescents of the NCANDA study. *NeuroImage*, 130, p. 194–213. <https://doi.org/10.1016/j.neuroimage.2016.01.061>
- Polanczyk, G. V., Salum, G. A., Sugaya, L. S., Caye, A., & Rohde, L. A. 2015. Annual research review: A meta-analysis of the worldwide prevalence of mental disorders in children and adolescents. *Journal of Child Psychology and Psychiatry and Allied Disciplines*, 56(3), p. 345–365. <https://doi.org/10.1111/jcpp.12381>
- Rashid, B., Blanken, L. M. E., Muetzel, R. L., Miller, R., Damaraju, E., Arbabshirani, M. R., Erhardt, E. B., Verhulst, F. C., van der Lugt, A., Jaddoe, V. W. V., Tiemeier, H., White, T., & Calhoun, V. 2018. Connectivity dynamics in typical development and its relationship to autistic traits and autism spectrum disorder. *Human Brain Mapping*, 39(8), p. 3127–3142. <https://doi.org/10.1002/hbm.24064>
- Reemst, K., Noctor, S. C., Lucassen, P. J., & Hol, E. M. 2016. The Indispensable Roles of Microglia and Astrocytes during Brain Development. *Frontiers in Human Neuroscience*, 10(NOV2016), p. 1–28. <https://doi.org/10.3389/fnhum.2016.00566>
- Ritchie, K., Bora, S., & Woodward, L. J. 2015. Social development of children born very preterm: A systematic review. *Developmental Medicine and Child Neurology*, 57(10), p. 899–918. <https://doi.org/10.1111/dmcn.12783>
- Rocca, M. A., Sonkin, M., Copetti, M., Pagani, E., Arnold, D. L., Narayanan, S., Sled, J. G., Banwell, B., & Filippi, M. 2016. Diffusion tensor magnetic resonance imaging in very early onset pediatric multiple sclerosis. *Multiple Sclerosis*, 22(5), p. 620–627. <https://doi.org/10.1177/1352458515596600>
- Rogers, C. E., Anderson, P. J., Thompson, D. K., Kidokoro, H., Wallendorf, M., Treyvaud, K., Roberts, G., Doyle, L. W., Neil, J. J., & Inder, T. E. 2012. Regional cerebral development at term relates to school-age social-emotional development in very preterm children. *Journal of the American Academy of Child and Adolescent Psychiatry*, 51(2), p. 181–191. <https://doi.org/10.1016/j.jaac.2011.11.009>
- Rogers, C. E., Lean, R. E., Wheelock, M. D., & Smyser, C. D. 2018. Aberrant structural and functional connectivity and neurodevelopmental impairment in preterm children. *Journal of Neurodevelopmental Disorders*, 10(1), p. 38. <https://doi.org/10.1186/s11689-018-9253-x>
- Rommel, A. S., James, S. N., McLoughlin, G., Brandeis, D., Banaschewski, T., Asherson, P., & Kuntsi, J. 2017. Altered EEG spectral power during rest and cognitive performance: a comparison of preterm-born adolescents to adolescents with ADHD. *European Child and Adolescent Psychiatry*, 26(12), p. 1511–1522. <https://doi.org/10.1007/s00787-017-1010-2>
- Rose, J., Butler, E. E., Lamont, L. E., Barnes, P. D., Atlas, S. W., & Stevenson, D. K. 2009. Neonatal brain structure on MRI and diffusion tensor imaging, sex, and neurodevelopment in very-low-birthweight preterm children. *Developmental Medicine and Child Neurology*, 51(7), p. 526–535. <https://doi.org/10.1111/j.1469-8749.2008.03231.x>
- Rose, J., Cahill-Rowley, K., Vassar, R., Yeom, K. W., Stecher, X., Stevenson, D. K., Hintz, S. R., & Barnea-Goraly, N. 2015. Neonatal brain microstructure correlates of neurodevelopment and gait in preterm children 18–22 mo of age: an MRI and DTI study. *Pediatric Research*, 78(6), p. 700–708. <https://doi.org/10.1038/pr.2015.157>
- Rose, J., Mirmiran, M., Butler, E. E., Lin, C. Y., Barnes, P. D., Kermoian, R., & Stevenson, D. K. 2007. Neonatal microstructural development of the internal capsule on diffusion tensor imaging correlates with severity of gait and motor deficits. *Developmental Medicine & Child Neurology*, 49(10), p. 745–750. <https://doi.org/10.1111/j.1469-8749.2007.00745.x>

- Rowlands, M. A., Scheinost, D., Lacadie, C., Vohr, B., Li, F., Schneider, K. C., Todd Constable, R., & Ment, L. R. 2016. Language at rest: A longitudinal study of intrinsic functional connectivity in preterm children. *NeuroImage: Clinical*, *11*, p. 149–157. <https://doi.org/10.1016/j.nicl.2016.01.016>
- Saad, J. F., Griffiths, K. R., Kohn, M. R., Clarke, S., Williams, L. M., & Korgaonkar, M. S. 2017. Regional brain network organization distinguishes the combined and inattentive subtypes of Attention Deficit Hyperactivity Disorder. *NeuroImage: Clinical*, *15*(October 2016), p. 383–390. <https://doi.org/10.1016/j.nicl.2017.05.016>
- Sagi, Y., Tavor, I., Hofstetter, S., Tzur-Moryosef, S., Blumenfeld-Katzir, T., & Assaf, Y. 2012. Learning in the Fast Lane: New Insights into Neuroplasticity. *Neuron*, *73*(6), p. 1195–1203. <https://doi.org/10.1016/j.neuron.2012.01.025>
- Saha, S., Pagnozzi, A., Bourgeat, P., George, J. M., Bradford, D., Colditz, P. B., Boyd, R. N., Rose, S. E., Fripp, J., & Pannek, K. 2020. Predicting motor outcome in preterm infants from very early brain diffusion MRI using a deep learning convolutional neural network (CNN) model. *NeuroImage*, *215*(April), p. 116807. <https://doi.org/10.1016/j.neuroimage.2020.116807>
- Schadl, K., Vassar, R., Cahill-Rowley, K., Yeom, K. W., Stevenson, D. K., & Rose, J. 2018. Prediction of cognitive and motor development in preterm children using exhaustive feature selection and cross-validation of near-term white matter microstructure. *NeuroImage: Clinical*, *17*, p. 667–679. <https://doi.org/10.1016/j.nicl.2017.11.023>
- Sellier, E., Platt, M. J., Andersen, G. L., Krägeloh-Mann, I., De La Cruz, J., & Cans, C. 2016. Decreasing prevalence in cerebral palsy: a multi-site European population-based study, 1980 to 2003. *Developmental Medicine & Child Neurology*, *58*(1), p. 85–92. <https://doi.org/10.1111/dmcn.12865>
- Setänen, S., Lahti, K., Lehtonen, L., Parkkola, R., Maunu, J., Saarinen, K., & Haataja, L. 2014. Neurological examination combined with brain MRI or cranial US improves prediction of neurological outcome in preterm infants. *Early Human Development*, *90*(12), p. 851–856. <https://doi.org/10.1016/j.earlhumdev.2014.09.007>
- Setänen, S., Lehtonen, L., Parkkola, R., Aho, K., & Haataja, L. 2016. Prediction of neuromotor outcome in infants born preterm at 11 years of age using volumetric neonatal magnetic resonance imaging and neurological examinations. *Developmental Medicine & Child Neurology*, *58*(7), p. 721–727. <https://doi.org/10.1111/dmcn.13030>
- Sewell, E. K., & Andescavage, N. N. 2018. Neuroimaging for Neurodevelopmental Prognostication in High-Risk Neonates. *Clinics in Perinatology*, *45*(3), p. 421–437. <https://doi.org/10.1016/j.clp.2018.05.004>
- Shaw, P., Eckstrand, K., Sharp, W., Blumenthal, J., Lerch, J. P., Greenstein, D., Clasen, L., Evans, A., Giedd, J., & Rapoport, J. L. 2007. Attention-deficit/hyperactivity disorder is characterized by a delay in cortical maturation. *Proceedings of the National Academy of Sciences*, *104*(49), p. 19649–19654. <https://doi.org/10.1073/pnas.0707741104>
- Sidman, R. L., & Rakic, P. 1973. Neuronal migration, with special reference to developing human brain: a review. *Brain Research*, *62*(1), p. 1–35. [https://doi.org/10.1016/0006-8993\(73\)90617-3](https://doi.org/10.1016/0006-8993(73)90617-3)
- Singh, G. K., Kenney, M. K., Ghandour, R. M., Kogan, M. D., & Lu, M. C. 2013. Mental Health Outcomes in US Children and Adolescents Born Prematurely or with Low Birthweight. *Depression Research and Treatment*, *2013*, p. 1–13. <https://doi.org/10.1155/2013/570743>
- Skranes, J., Vangberg, T. R., Kulseng, S., Indredavik, M. S., Evensen, K. a I., Martinussen, M., Dale, a M., Haraldseth, O., & Brubakk, a-M. 2007. Clinical findings and white matter abnormalities seen on diffusion tensor imaging in adolescents with very low birth weight. *Brain: A Journal of Neurology*, *130*(Pt 3), p. 654–666. <https://doi.org/10.1093/brain/awm001>
- Smith, S. M., Jenkinson, M., Johansen-Berg, H., Rueckert, D., Nichols, T. E., Mackay, C. E., Watkins, K. E., Ciccarelli, O., Cader, M. Z., Matthews, P. M., & Behrens, T. E. J. 2006. Tract-based spatial statistics: Voxelwise analysis of multi-subject diffusion data. *NeuroImage*, *31*(4), p. 1487–1505. <https://doi.org/10.1016/j.neuroimage.2006.02.024>
- Smith, S. M., Jenkinson, M., Woolrich, M. W., Beckmann, C. F., Behrens, T. E. J., Johansen-Berg, H., Bannister, P. R., De Luca, M., Drobnjak, I., Flitney, D. E., Niazy, R. K., Saunders, J., Vickers, J., Zhang, Y., De Stefano, N., Brady, J. M., & Matthews, P. M. 2004. Advances in functional and

- structural MR image analysis and implementation as FSL. *NeuroImage*, 23, p. S208–S219. <https://doi.org/10.1016/j.neuroimage.2004.07.051>
- Smyser, C. D., Dosenbach, N. U. F., Smyser, T. A., Snyder, A. Z., Rogers, C. E., Inder, T. E., Schlaggar, B. L., & Neil, J. J. 2016. Prediction of brain maturity in infants using machine-learning algorithms. *NeuroImage*, 136, p. 1–9. <https://doi.org/10.1016/j.neuroimage.2016.05.029>
- SØMHOVD, M. J., HANSEN, B. M., BROK, J., ESBJØRN, B. H., & GREISEN, G. 2012. Anxiety in adolescents born preterm or with very low birthweight: a meta-analysis of case-control studies. *Developmental Medicine & Child Neurology*, 54(11), p. 988–994. <https://doi.org/10.1111/j.1469-8749.2012.04407.x>
- Spittle, A. J., Cameron, K., Doyle, L. W., & Cheong, J. L. 2018. Motor Impairment Trends in Extremely Preterm Children: 1991–2005. *Pediatrics*, 141(4), p. e20173410. <https://doi.org/10.1542/peds.2017-3410>
- Sripada, C. S., Kessler, D., & Angstadt, M. 2014. Lag in maturation of the brain’s intrinsic functional architecture in attention-deficit/hyperactivity disorder. *Proceedings of the National Academy of Sciences*, 111(39), p. 14259–14264. <https://doi.org/10.1073/pnas.1407787111>
- Sripada, K., Løhaugen, G. C., Eikenes, L., Bjørlykke, K. M., Håberg, A. K., Skranes, J., & Rimol, L. M. 2015. Visual–motor deficits relate to altered gray and white matter in young adults born preterm with very low birth weight. *NeuroImage*, 109, p. 493–504. <https://doi.org/10.1016/j.neuroimage.2015.01.019>
- Stewart, A., Rifkin, L., Amess, P., Kirkbride, V., Townsend, J., Miller, D., Lewis, S., Kingsley, D., Moseley, I., Foster, O., & Murray, R. 1999. Brain structure and neurocognitive and behavioural function in adolescents who were born very preterm. *The Lancet*, 353(9165), p. 1653–1657. [https://doi.org/10.1016/S0140-6736\(98\)07130-X](https://doi.org/10.1016/S0140-6736(98)07130-X)
- Sucksdorff, M., Lehtonen, L., Chudal, R., Suominen, A., Joelsson, P., Gissler, M., & Sourander, A. 2015. Preterm Birth and Poor Fetal Growth as Risk Factors of Attention-Deficit/Hyperactivity Disorder. *PEDIATRICS*, 136(3), p. e599–e608. <https://doi.org/10.1542/peds.2015-1043>
- Synnes, A., & Hicks, M. 2018. Neurodevelopmental Outcomes of Preterm Children at School Age and Beyond. *Clinics in Perinatology*, 45(3), p. 393–408. <https://doi.org/10.1016/j.clp.2018.05.002>
- Szakmar, E., Meunier, H., El-Dib, M., Yang, E., & Inder, T. E. 2021. Interobserver Reliability of an MR Imaging Scoring System in Infants with Hypoxic-Ischemic Encephalopathy. *American Journal of Neuroradiology*, 42(5), p. 969–974. <https://doi.org/10.3174/ajnr.A7048>
- Tannes, C. K., Roalf, D. R., Goddings, A. L., & Lebel, C. 2017. Diffusion MRI of white matter microstructure development in childhood and adolescence: Methods, challenges and progress. *Developmental Cognitive Neuroscience*, 33(February 2017), p. 161–175. <https://doi.org/10.1016/j.dcn.2017.12.002>
- Taylor, H. G. 2020. Neurodevelopmental origins of social competence in very preterm children. *Seminars in Fetal and Neonatal Medicine*, 25(3), p. 101108. <https://doi.org/10.1016/j.siny.2020.101108>
- Taylor, P. A., Alhamud, A., van der Kouwe, A., Saleh, M. G., Laughton, B., & Meintjes, E. 2016. Assessing the performance of different DTI motion correction strategies in the presence of EPI distortion correction. *Human Brain Mapping*, 37(12), p. 4405–4424. <https://doi.org/10.1002/hbm.23318>
- Thomas, R., Sanders, S., Doust, J., Beller, E., & Glasziou, P. 2015. Prevalence of Attention-Deficit/Hyperactivity Disorder: A Systematic Review and Meta-analysis. *Pediatrics*, 135(4), p. e994–e1001. <https://doi.org/10.1542/peds.2014-3482>
- Thompson, D. K., Chen, J., Beare, R., Adamson, C. L., Ellis, R., Ahmadzai, Z. M., Kelly, C. E., Lee, K. J., Zalesky, A., Yang, J. Y. M., Hunt, R. W., Cheong, J. L. Y., Inder, T. E., Doyle, L. W., Seal, M. L., & Anderson, P. J. 2016. Structural connectivity relates to perinatal factors and functional impairment at 7 years in children born very preterm. *NeuroImage*, 134, p. 328–337. <https://doi.org/10.1016/j.neuroimage.2016.03.070>
- Thompson, D. K., Matthews, L. G., Alexander, B., Lee, K. J., Kelly, C. E., Adamson, C. L., Hunt, R. W., Cheong, J. L. Y., Spencer-Smith, M., Neil, J. J., Seal, M. L., Inder, T. E., Doyle, L. W., &

- Anderson, P. J. 2020. Tracking regional brain growth up to age 13 in children born term and very preterm. *Nature Communications*, 11(1), p. 696. <https://doi.org/10.1038/s41467-020-14334-9>
- Tommiska, V., Lano, A., Kleemola, P., Klenberg, L., Lehtonen, L., Löppönen, T., Olsen, P., Tammela, O., & Fellman, V. 2020. Analysis of neurodevelopmental outcomes of preadolescents born with extremely low weight revealed impairments in multiple developmental domains despite absence of cognitive impairment. *Health Science Reports*, 3(3), p. 1–10. <https://doi.org/10.1002/hsr2.180>
- Toulmin, H., O’Muircheartaigh, J., Counsell, S. J., Falconer, S., Chew, A., Beckmann, C. F., & Edwards, A. D. 2021. Functional thalamocortical connectivity at term equivalent age and outcome at 2 years in infants born preterm. *Cortex*, 135, p. 17–29. <https://doi.org/10.1016/j.cortex.2020.09.022>
- Twilhaar, E. S., de Kieviet, J. F., Bergwerff, C. E., Finken, M. J. J., van Elburg, R. M., & Oosterlaan, J. 2019. Social Adjustment in Adolescents Born Very Preterm: Evidence for a Cognitive Basis of Social Problems. *The Journal of Pediatrics*, 213, p. 66–73.e1. <https://doi.org/10.1016/j.jpeds.2019.06.045>
- Tymofiyeva, O., Gano, D., Trevino, R. J., Glass, H. C., Flynn, T., Lundy, S. M., McQuillen, P. S., Ferriero, D. M., Barkovich, A. J., & Xu, D. 2018. Aberrant Structural Brain Connectivity in Adolescents with Attentional Problems Who Were Born Prematurely. *American Journal of Neuroradiology*, 39(11), p. 2140–2147. <https://doi.org/10.3174/ajnr.A5834>
- Tzourio-Mazoyer, N., Landeau, B., Papathanassiou, D., Crivello, F., Etard, O., Delcroix, N., Mazoyer, B., & Joliot, M. 2002. Automated Anatomical Labeling of Activations in SPM Using a Macroscopic Anatomical Parcellation of the MNI MRI Single-Subject Brain. *NeuroImage*, 15(1), p. 273–289. <https://doi.org/10.1006/nimg.2001.0978>
- Urbain, C., Sato, J., Hammill, C., Duerden, E. G., & Taylor, M. J. 2019. Converging function, structure, and behavioural features of emotion regulation in very preterm children. *Human Brain Mapping*, 40(11), p. 3385–3397. <https://doi.org/10.1002/hbm.24604>
- Uusitalo, K., Haataja, L., Nyman, A., Ripatti, L., Huhtala, M., Rautava, P., Lehtonen, L., Parkkola, R., Lahti, K., Koivisto, M., & Setänen, S. 2020. Preterm children’s developmental coordination disorder, cognition and quality of life: a prospective cohort study. *BMJ Paediatrics Open*, 4(1), p. e000633. <https://doi.org/10.1136/bmjpo-2019-000633>
- Van Dijk, K. R. A., Hedden, T., Venkataraman, A., Evans, K. C., Lazar, S. W., & Buckner, R. L. 2010. Intrinsic functional connectivity as a tool for human connectomics: Theory, properties, and optimization. *Journal of Neurophysiology*, 103(1). <https://doi.org/10.1152/jn.00783.2009>
- Vangberg, T. R., Skranes, J., Dale, A. M., Martinussen, M., Brubakk, A.-M., & Haraldseth, O. 2006. Changes in white matter diffusion anisotropy in adolescents born prematurely. *NeuroImage*, 32(4), p. 1538–1548. <https://doi.org/10.1016/j.neuroimage.2006.04.230>
- Vogel, J. P., Chawanpaiboon, S., Moller, A.-B., Watananirun, K., Bonet, M., & Lumbiganon, P. 2018. The global epidemiology of preterm birth. *Best Practice & Research Clinical Obstetrics & Gynaecology*, 52, p. 3–12. <https://doi.org/10.1016/j.bpobgyn.2018.04.003>
- Vollmer, B., Lundequist, A., Mårtensson, G., Nagy, Z., Lagercrantz, H., Smedler, A.-C., & Forssberg, H. 2017. Correlation between white matter microstructure and executive functions suggests early developmental influence on long fibre tracts in preterm born adolescents. *PLOS ONE*, 12(6), p. e0178893. <https://doi.org/10.1371/journal.pone.0178893>
- Volpe, J. J. 2009. Brain injury in premature infants: a complex amalgam of destructive and developmental disturbances. *The Lancet Neurology*, 8(1), p. 110–124. [https://doi.org/10.1016/S1474-4422\(08\)70294-1](https://doi.org/10.1016/S1474-4422(08)70294-1)
- Volpe, J. J. 2019. Dysmaturation of Premature Brain: Importance, Cellular Mechanisms, and Potential Interventions. *Pediatric Neurology*, 95, p. 42–66. <https://doi.org/10.1016/j.pediatrneurol.2019.02.016>
- Vulser, H., Paillère Martinot, M.-L., Artiges, E., Miranda, R., Penttilä, J., Grimmer, Y., van Noort, B. M., Stringaris, A., Struve, M., Fadai, T., Kappel, V., Goodman, R., Tzavara, E., Massaad, C., Banaschewski, T., Barker, G. J., Bokde, A. L. W., Bromberg, U., Brühl, R., ... Lemaitre, H. 2018. Early Variations in White Matter Microstructure and Depression Outcome in Adolescents With

- Subthreshold Depression. *American Journal of Psychiatry*, 9, p. appi.ajp.2018.1. <https://doi.org/10.1176/appi.ajp.2018.17070825>
- Wehrle, F. M., Michels, L., Guggenberger, R., Huber, R., Latal, B., O’Gorman, R. L., & Haggmann, C. F. 2018. Altered resting-state functional connectivity in children and adolescents born very preterm short title. *NeuroImage: Clinical*, 20(August), p. 1148–1156. <https://doi.org/10.1016/j.nicl.2018.10.002>
- Weishaupt, D., Köchli, V. D., & Marincek, B. 2006. *How Does MRI Work?* Springer Berlin Heidelberg. <https://doi.org/10.1007/978-3-540-37845-7>
- White, T. P., Symington, I., Castellanos, N. P., Brittain, P. J., Froudast, S., Nam, K., Sato, J. R., Allin, M. P. G., Shergill, S. S., Murray, R. M., Williams, S. C. R., & Nosarti, C. 2014. NeuroImage: Clinical Dysconnectivity of neurocognitive networks at rest in very-preterm born adults ☆. *NeuroImage: Clinical*, 4, p. 352–365. <https://doi.org/10.1016/j.nicl.2014.01.005>
- Whitfield-Gabrieli, S., & Nieto-Castanon, A. 2012. Conn: A Functional Connectivity Toolbox for Correlated and Anticorrelated Brain Networks. *Brain Connectivity*, 2(3). <https://doi.org/10.1089/brain.2012.0073>
- Williams, J., Lee, K. J., & Anderson, P. J. 2010. Prevalence of motor-skill impairment in preterm children who do not develop cerebral palsy: a systematic review. *Developmental Medicine & Child Neurology*, 52(3), p. 232–237. <https://doi.org/10.1111/j.1469-8749.2009.03544.x>
- Woolrich, M. W., Jbabdi, S., Patenaude, B., Chappell, M., Makni, S., Behrens, T., Beckmann, C., Jenkinson, M., & Smith, S. M. 2009. Bayesian analysis of neuroimaging data in FSL. *NeuroImage*, 45(1), p. S173–S186. <https://doi.org/10.1016/j.neuroimage.2008.10.055>
- Worley, G., Erickson, S. W., Gustafson, K. E., Nikolova, Y. S., Ashley-Koch, A. E., Belsky, D. W., Goldstein, R. F., Page, G. P., Cotten, C. M., Carlo, W. A., Bell, E. F., Goldberg, R. N., Schibler, K., Higgins, R. D., Sood, B. G., Stevenson, D. K., Stoll, B. J., Van Meurs, K. P., Johnson, K. J., ... Murray, J. C. 2020. Genetic variation in dopamine neurotransmission and motor development of infants born extremely-low-birthweight. *Developmental Medicine & Child Neurology*, 62(6), p. 750–757. <https://doi.org/10.1111/dmcn.14383>
- Wu, M., Barnett, A. S., Marengo, S., Walker, L., Lemaitre, H., & Pierpaoli, C. 2008. Comparison of EPI Distortion Correction Methods in Diffusion Tensor MRI. *Isrmr*, 16, p. 4515.
- Wu, M., Chang, L.-C., Walker, L., Lemaitre, H., Barnett, A. S., Marengo, S., & Pierpaoli, C. 2008. Comparison of EPI Distortion Correction Methods in Diffusion Tensor MRI Using a Novel Framework. In *Isrmr* (Vol. 16, pp. 321–329). https://doi.org/10.1007/978-3-540-85990-1_39
- Zhou, L., Zhao, Y., Liu, X., Kuang, W., Zhu, H., Dai, J., He, M., Lui, S., Kemp, G. J., & Gong, Q. 2018. Brain gray and white matter abnormalities in preterm-born adolescents: A meta-analysis of voxel-based morphometry studies. *PLOS ONE*, 13(10), p. e0203498. <https://doi.org/10.1371/journal.pone.0203498>
- Zwicker, J. G., Missiuna, C., & Boyd, L. A. 2009. Neural Correlates of Developmental Coordination Disorder: A Review of Hypotheses. *Journal of Child Neurology*, 24(10), p. 1273–1281. <https://doi.org/10.1177/0883073809333537>



**TURUN
YLIOPISTO**
UNIVERSITY
OF TURKU

ISBN 978-951-29-8719-1 (PRINT)
ISBN 978-951-29-8720-7 (PDF)
ISSN 0355-9483 (Print)
ISSN 2343-3213 (Online)

